UNIVERSITEIT VAN PRETORIA
UNIVERSITY OF PRETORIA
YUNIBESITHI YA PRETORIA

Development of a constitutive luciferase reporter line for comparable evaluation of antiplasmodial drugs on all life cycle stages of *Plasmodium falciparum*

Dorè Joubert

Submitted in partial fulfilment of the requirements of the degree

Magister Scientiae Biotechnology

(Specialisation in Biochemistry)

Faculty of Natural and Agricultural Sciences

Department of Biochemistry, Genetics and Microbiology

Division of Biochemistry

University of Pretoria

South Africa

(Date of submission: 24/7/2020)

SUBMISSION DECLARATION

I, Dorè Joubert, declare that the dissertation, which I hereby submit for the degree *Magister Scientiae* in the Department of Biochemistry, Genetics and Microbiology at the University of Pretoria, is my own work and has not previously been submitted by me for a degree at this or any other tertiary institution.

SIGNATURE: ……  ……

DATE: ..20/7/2020…….

DECLARATION OF ORIGINALITY

UNIVERSITY OF PRETORIA

The Department of Biochemistry, Genetics and Microbiology places great emphasis upon integrity and ethical conduct in the preparation of all written work submitted for academic evaluation.

Full name of student: Dorè Joubert
Student number: 13413628
Topic of work: Dissertation

Declaration:

1. I understand what plagiarism is and am aware of the University's policy in this regard.

2. I declare that this dissertation is my own original work. Where other people's work has been used (either from a printed source, Internet or any other source), this has been properly acknowledged and referenced in accordance with departmental requirements.

3. I have not used work previously produced by another student or any other person to hand in as my own.

4. I have not allowed, and will not allow, anyone to copy my work with the intention of passing it off as his or her own work.

SIGNATURE

.....  .....

ACKNOWLEDGEMENTS

I would like to thank the following people, without whom I would not have been able to complete this research and made it through my MSc degree.

First of all, I would like to thank my supervisor, Prof. Lyn-Marie Birkholtz, for giving me guidance and feedback throughout the project. Her knowledge, support and encouragement have pushed me to deliver excellence in all my work. I would also like to thank her for giving me the opportunity to visit the Istituto Superiore di Sanita (Rome, Italy) where I gained valuable knowledge about my project from Pietro Alano and Giulia Siciliano. I am also thankful for the Malaria Parasite Molecular Laboratory (M_2PL) team for their willingness to help, especially Dr Elisha Mugo for giving advice and assistance when needed.

I appreciate my friends and family who have supported me and extra thanks to Masego and Suzan who have made this journey fun and memorable. My biggest thanks to my mother, Marina, and sister, Mareli, for all their support and encouragement, and putting up with my stresses throughout my studies. Most importantly, thank you to my husband, Thinus, for always being there and supporting me through this journey.

Finally, I want to give thanks to the Lord for giving me the talent and knowledge to pursue this degree. I was continuously encouraged by His Word to finish this long and challenging journey. When I started three years ago and while writing my dissertation, I was reminded that I was not doing this for people but for the Lord. "*Whatever you do [whatever your task may be], work from the soul [that is, put in your very best effort], as [something done] for the Lord and not for men*." Colossians 3:23 AMP

Summary

The vision of a malaria-free world is threatened by antimalarial drug resistance. For malaria elimination to be achieved, drug combinations should have dual action: cure infection and block transmission of the *Plasmodium* parasite between the human host and mosquito vector. Furthermore, such dual action drugs should lower the risk of resistance development and prolong the therapeutic lifespan of antimalarials. New antimalarial drugs need to comply to a set guideline from the Medicines for Malaria Venture with regards to the types of molecules [target candidate profiles (TCP)] and the combination of medicines being developed. Therefore, knowing a compound's activity towards a specific stage of the parasite, in other words its TCP, is important for drug development. However, due to the parasite's complex life cycle, each stage of the parasite currently requires a different biochemical platform to assay compounds for activity against that particular life cycle state. This does introduce assay readout variability and complicates standardisation of drug assays. This study, therefore, aimed to generate a constitutive luciferase-expressing *P. falciparum* line that can be used to develop a single assay platform for all life cycle stages of the parasite. By using gene expression profiling, we identified several constitutively expressed genes throughout the life cycle of *P. falciparum*. The promoters of these genes were used to generate transgenic lines in which a robust luciferase reporter is strongly expressed under control of these promoters. Two transgenic lines were successfully generated and allowed luciferase expression under control of promoters for histone H3 and nuclear assembly protein (NF54^{H3} and NF54^{nap}). Whilst NF54^{H3} could be used to effectively determine antiplasmodial activity for compounds towards the asexual stages, this line was compromised to the extent that it was not able to produce gametocytes. By contrast, NF54^{nap} produced both asexual parasites and gametocytes and was used to evaluate drug activity for both these stages on a single luciferase reporter assay platform. As a result, the line generated here enables a single platform to delineate the TCP of compounds and identify novel compounds that are active against multiple stages or that show selective activity towards a specific stage of the parasite. This data contributes to a novel avenue in antimalarial drug discovery, thereby supporting malaria elimination strategies.

Table of Contents

List of Figures

List of Tables

List of Abbreviations

ACT	Artemisinin-based combination therapy
BSA	Bovine serum albumin
CBG99	*Pyrophorus plagiophthalamus* Click beetle luciferase
CQ	Chloroquine
DHA	Dihydroartemisinin
DHFR	Dihydrofolate reductase
E8	Elimination Eight
FPKM	Fragments Per Kilobase of transcript per Million mapped reads
G6PD	Glucose-6-phosphate dehydrogenase
GFP	Green fluorescent protein
GTS	Global Technical Strategy
H3	Histone H3
HTS	High-throughput screening
IC_{50}	Half maximal (50 %) inhibitory concentration
IRS	Indoor residual spraying
ITNs	Insecticide-treated nets
LB	Luria-Bertani
MB	Methylene blue
MMV	Medicines for Malaria Venture
NAP	Nucleosome assembly protein
PBS	Phosphate-buffered saline
pLDH	Parasite lactate dehydrogenase
RLU	Relative Luminescence Unit
RNAseq	RNA sequencing
SMFA	Standard membrane feeding assay
SP	Sulfadoxine-pyrimethamine
TAE	Tris-Acetate-EDTA
TCP	Target Candidate Profiles
TPP	Target Product Profiles
UTR	Untranslated region
WHO	World Health Organization

Chapter 1: Literature review

1.1 Malaria epidemiology

Malaria remains a major global health problem and in 2018, affected ~228 million people worldwide, causing ~405 000 deaths [1]. Although the number of malaria cases and deaths have decreased since 2000, the rate of decline has slowed down and, in some regions, even reversed since 2014 [2]. Therefore, there is a need to progress faster, especially in Africa, which still accounts for 93 % of malaria cases and 94 % of global malaria deaths [1]. Malaria has a devastating impact on the health and livelihood of people worldwide. The burden of malaria is especially high in vulnerable populations, such as children and pregnant women, with ~67 % of malaria deaths occurring in children under the age of five [1].

The protozoan *Plasmodium* parasite is responsible for malaria in humans, of which *Plasmodium falciparum* causes the most deaths [1]. Four *Plasmodium* species almost exclusively utilise humans as their natural intermediate host, including *Plasmodium falciparum*, *Plasmodium vivax*, *Plasmodium ovale* and *Plasmodium malariae* [2]. *P. falciparum* and *P. vivax* are the most predominant malaria parasites [3], with *P. falciparum* responsible for the majority of malaria cases in South Africa [4]. Another malaria parasite, *P. knowlesi*, also causes malaria in humans but naturally infects macaques in Southeast Asia [2]. Malaria parasites are transmitted to human hosts by infected female *Anopheles* mosquito vectors. More than 400 species of *Anopheles* mosquitoes exist of which ~30 species are important malaria vectors [2]. The efficiency of malaria transmission by a vector is dependent on many factors, including robustness to change, climate, longevity, preference to bite humans and breeding often [3]. In South Africa, *Anopheles arabiensis* and *Anopheles funestus* are the most prevalent vectors for malaria transmission [5].

Malaria can be classified as asymptomatic, uncomplicated, or severe (complicated). The severity of the disease depends on the *Plasmodium* species involved as well as human host factors. Asymptomatic malaria occurs when no symptoms are present even though parasites are circulating in the host's blood or transmissible gametocyte stages are sequestering in tissues such as the bone marrow [6, 7]. Asymptomatic malaria usually occurs in moderate- and high-transmission settings where people develop partial immunity against the parasite [6]. Unfortunately, these asymptomatic carriers remain undetected in a population and act as reservoirs of the parasite to infect mosquitoes and thereby continue the transmission cycle [6]. Uncomplicated malaria has nonspecific symptoms, including fever, muscle aches, shaking chills, headaches, digestive symptoms and anaemia [6]. The disease can progress rapidly into severe malaria if untreated, which is caused by microvascular obstruction due to intra-erythrocytic parasites being present in

capillaries [6]. Complications of severe malaria consist of severe anaemia and multi-organ damage, including cerebral malaria [6]. Severe malaria is predominantly caused by *P. falciparum* and is linked to increased mortality rates [6].

Working towards global malaria elimination, the World Health Organization (WHO) has set out a Global Technical Strategy (GTS) that consists of achievable targets for 2030 with progress milestones set for 2020 and 2025 [4]. These targets consist of reducing malaria cases and mortality rates by 90 % as well as eliminating malaria in at least 35 countries by 2030 [4]. Elimination of malaria is becoming a reality as more countries are moving towards zero indigenous cases, with 27 countries reporting less than 100 indigenous cases in 2018 (Figure 1.1) [1]. In 2016, the WHO identified 21 countries, known as the "E-2020 countries", with the potential to have zero indigenous cases and eliminate malaria by 2020, with South Africa being one of them [4]. Although 10 of the E-2020 countries remain on track with achieving elimination, several countries reported an increase in malaria cases between 2016 and 2018 [1, 8]. Important milestones of the GTS might be missed as progress to reduce malaria cases has slowed down.

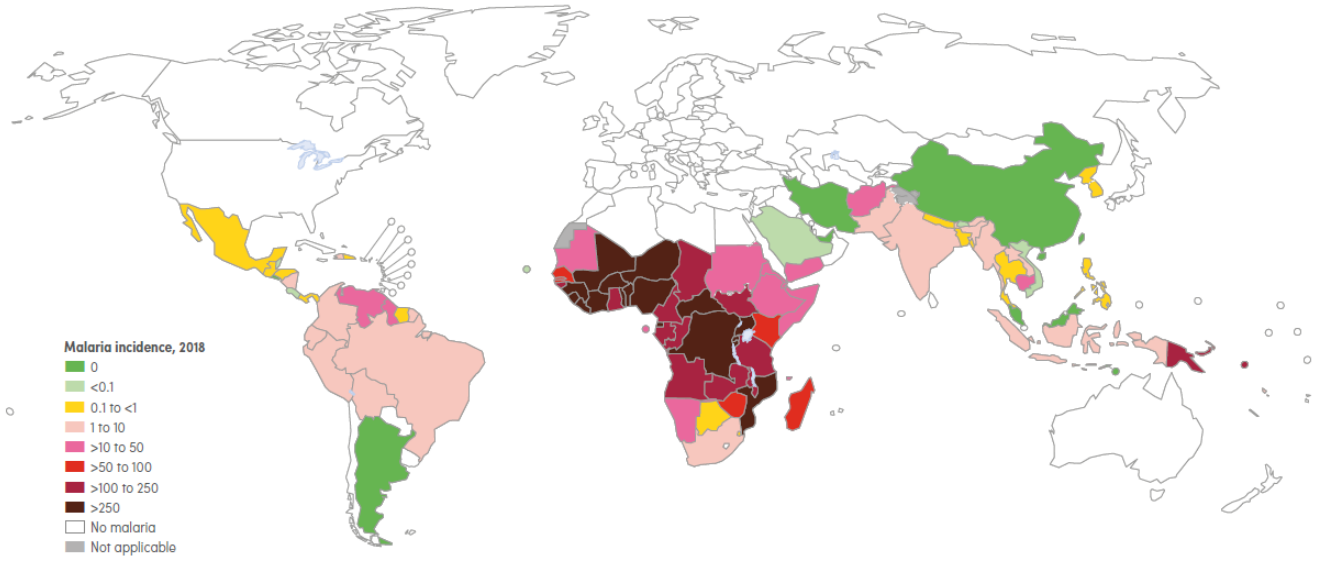

Figure 1.1: Geographical distribution of malaria incidence rate per 1000 population at risk. The 2018 malaria case incidence rate is shown by country with a scale from 0 (green), for zero indigenous cases, to >250 (plum), for more than 250 indigenous cases per 1000 population at risk. The countries coloured in white are not malaria-endemic countries and those in grey are not applicable due to insufficient data [1].

South Africa is part of the Elimination Eight (E8) regional initiative, which envisions a malaria-free southern Africa by eliminating malaria in eight African countries by 2030 [9]. South Africa has a high number of imported cases due to migrant workers and travellers from neighbouring countries, as such, a cross-border initiative was also started between Mozambique, South Africa, and Swaziland to achieve zero local transmission by 2020 [10]. Since the four frontline countries in the

E8 – South Africa, Swaziland, Botswana and Namibia – did not reach the goal of zero local transmission by 2020, the E8 ministers decided to develop a new strategic plan for the upcoming years to reach the goal of malaria elimination in southern Africa by 2030 [11]. Malaria is endemic to the low-altitude border regions of three provinces in South Africa with only 10 % of the country's population living in malaria risk areas [10]. South Africa reported a fivefold increase in the number of malaria cases between 2016 and 2017, however, a 57 % reduction in cases was seen in 2018 compared to 2017 [1]. Although South Africa has made good progress with its elimination plan, it is not on track with the GTS targets to reduce malaria incidence by at least 40 % by 2020 [1].

1.2 Malaria prevention and control

Malaria control programs use a combined intervention approach to prevent, detect and treat malaria infections and this include vector control, vaccination, chemoprevention, and chemoprophylaxis [12]. To achieve the goal of malaria eradication, certain targets need to be met and strategies must be implemented. The Malaria Eradication Research Agenda addresses the challenges for drug development and malaria eradication by providing scientific research strategies and solutions [12, 13]. This has acted as driver of progress in the scientific community and let to the development of a potential vaccine, new nonpyrethroid insecticides, the identification of resistance markers, and new approaches to screen for active compounds such as drugs and insecticides [12].

The most effective methods of vector control include insecticide-treated nets (ITNs) and indoor residual spraying (IRS) [6, 14]. ITNs not only provide a physical barrier against mosquitoes but also have lethal effects on mosquitoes due to insecticides, such as pyrethroids, present on the bed net material [15]. IRS is the application of insecticides to the inside of walls and other surfaces of houses, thereby killing mosquitoes that rest on the treated surfaces [15]. These vector control interventions rely on the repeated behaviour of a mosquito, therefore, IRS will be most effective if mosquitoes bite indoors and ITNs will be most effective while a person is asleep [15]. The most commonly used insecticides are pyrethroids as they are the only insecticide approved for treating bed nets [15]. Due to pyrethroid resistance, IRS programs have to rely on nonpyrethroids, such as organophosphates, carbamates, and the organochlorine, DDT, but resistance against these insecticides is also on the rise [16]. Although these methods are largely responsible for the decline in malaria cases, the effectiveness of mosquito nets are being challenged by misuse of nets, changes in the mosquito's behaviour as it is starting to bite during the daytime, and most importantly insecticide resistance [6, 17]. Therefore, novel vector control tools and insecticides are needed with the goal of malaria elimination in mind.

Vaccine development forms an integral part of malaria interventions as they could interrupt parasite transmission as well as reduce morbidity and mortality in children [18, 19]. The ideal vaccine should protect against multiple *Plasmodium* species and not just against *P. falciparum* [19]. Developing a vaccine for malaria is challenging since all the components of the host's immune response are involved and the parasite has a large genome, which makes the parasite very effective against immune evasion [6]. As a result, no vaccines currently exist on the market but there is a lot of ongoing research on malaria vaccine development and numerous vaccine candidates are in the pipeline [6, 14]. The most promising, leading vaccine candidate is the RTS,S/AS01 vaccine, which targets the circumsporozoite protein of *P. falciparum* that is expressed by the parasite during the exo-erythrocytic stage in the liver [18]. Even though the vaccine failed to provide long-term protection during clinical studies, it could still be used with other effective control measures in high-transmission settings to reduce malaria cases [18] or used with chemoprevention to inhibit transmission in low endemic areas [6, 14]. Consequently, vaccines that show partial efficacy can still be used since they could aid in decreasing the reservoir of the parasite and reducing parasite transmission [6, 20]. The rise in resistance development threatens malaria control, therefore, an effective vaccine is needed to complement existing interventions for malaria elimination [19].

To reduce malaria prevalence, chemoprevention has been used on large populations in high transmission settings [2]. Chemoprevention consists of seasonal malaria chemoprevention, intermittent preventive treatment in infants, intermittent preventive treatment in pregnancy and mass drug administration [2, 20]. The WHO recommends mass drug administration to increase the rate of elimination as well as decrease the malaria burden in groups with a high risk for malaria infection [2, 21]. Mass drug administration occurs when antimalarial treatment is given to every person in a defined population or geographical area at approximately the same time at repeated intervals [2, 21].

Chemoprophylaxis is the use of medicines to temporarily protect individuals going to malaria-endemic areas by taking prophylaxis and also to protect populations at risk from emergent epidemics, especially in elimination settings [2, 20]. In South Africa, the most commonly taken prophylaxis include Malarone® (atovaquone-proguanil), doxycycline and mefloquine [22], which are also the three gold standard drugs for chemoprophylaxis [6]. Chemoprophylactics are actively being investigated with a great focus on medicines that only require weekly or less frequent administration [6].

Chemotherapeutics are used exclusively to treat symptomatic patients and are therefore not currently seen as malaria control interventions. The current WHO gold-standard treatment is artemisinin-based combination therapies (ACT) [6] but development of resistance towards several

components thereof is constantly on the rise, primarily because of the unusual biology and life cycle of the parasite.

1.3 The *P. falciparum* parasite life cycle

The life cycle of the *P. falciparum* parasite (Figure 1.2) begins when an infected female *Anopheles* mosquito takes a blood meal, thereby injecting sporozoites into the human host [23]. Exo-erythrocytic replication starts with sporozoites that infect liver cells and mature asexually to hepatic schizonts that rupture to release merozoites [23]. Intra-erythrocytic development then commences when merozoites invade erythrocytes to undergo a 48 h replicative cycle progressing through the ring, trophozoite and schizont stages [24, 25]. These repeated cycles consist of invasion, intracellular growth, asexual replication, egress, and reinvasion and these intra-erythrocytic cycles give rise to the symptoms associated with malaria such as fever [24, 25].

After merozoite invasion, the initial ring-stage parasite starts to feed on haemoglobin from the erythrocyte and as the parasite matures, it rounds up to become the morphologically distinct trophozoite stage. The latter is the most metabolically active stage of the parasite [25] where the majority of haemoglobin digestion occurs. The toxic product of this process is sequestered as haemozoin crystals in a distinct pigment vacuole [24]. After the cellular growth phase, the parasite enters into schizogony where nuclear division occurs to produce 16-32 merozoites [24, 25]. Once the erythrocyte ruptures, merozoites are released into the bloodstream to invade new erythrocytes and continue the intra-erythrocytic cycle.

A small portion of asexual parasites commits to gametocytogenesis, which can be triggered by environmental and host factors [26-28]. The merozoites from a sexually committed schizont are released to develop into a homogeneous population of either male or female gametocytes [29]. Male and female *P. falciparum* gametocytes mature in approximately 10 to 12 days through five distinct morphological stages (stage I to stage V) [25, 30]. This prolonged and stage-stratified process is unique to this human malaria parasite. Stage I gametocytes are hard to differentiate from young trophozoites but from stage II onwards the gametocytes can be easily set apart with Giemsa-stained blood smears [31]. The AP2-G transcription factor (part of the apicomplexan apetala 2 family of transcription factors) was found to be a key regulator of *Plasmodium* sexual commitment and activates transcription of early gametocyte genes [32, 33].

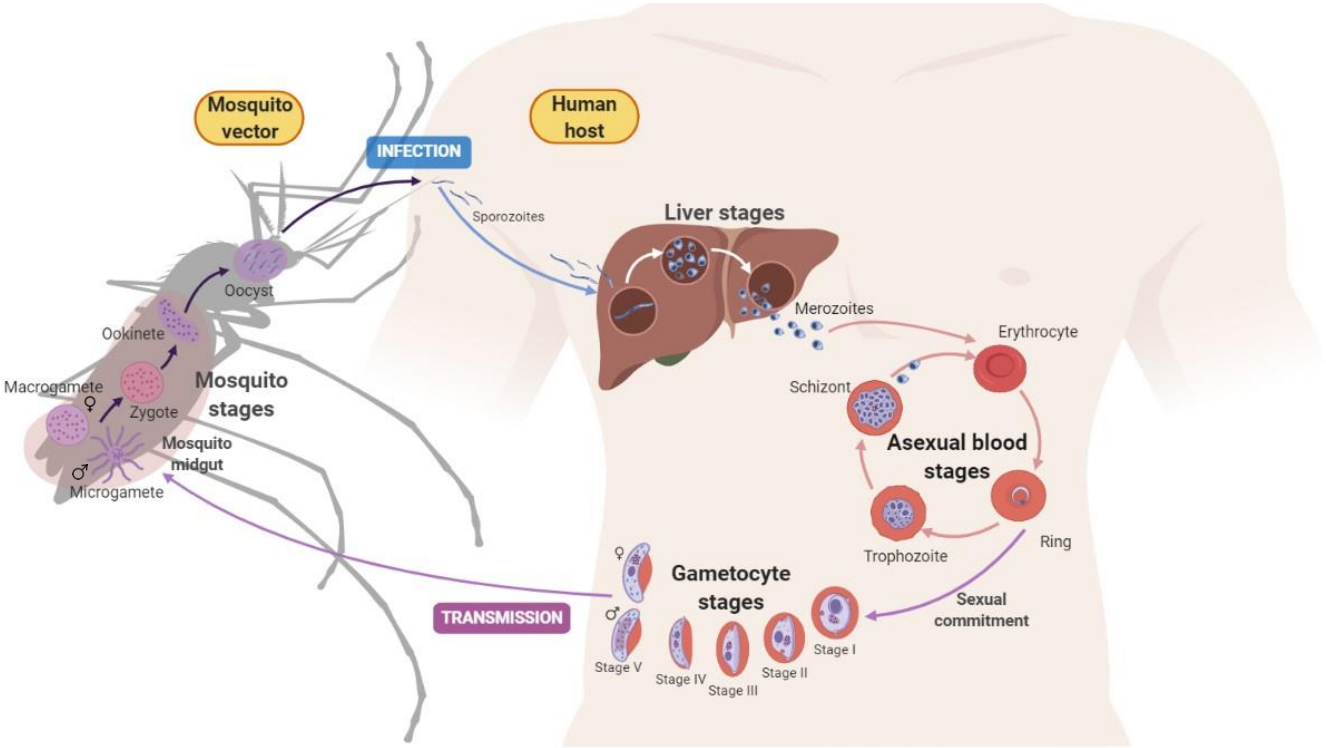

Figure 1.2: The life cycle of the *Plasmodium falciparum* parasite.
Sporozoites are transmitted to a human host when a female *Anopheles* mosquito takes a blood meal. The sporozoites develop in the liver to produce merozoites that are released into the bloodstream to initiate the asexual blood (intra-erythrocytic) stage, developing through the ring, trophozoite and schizont stages. A small portion of asexual parasites enter the sexual stage by committing to gametocytogenesis, which consists of gametocyte development from stage I to V. The mosquito stage begins once another mosquito ingests the stage V gametocytes. Male and female gametocytes differentiate into gametes that fuse to form a zygote, which develops into an ookinete and then oocyst that matures and ruptures to release sporozoites. Sporozoites migrate to the salivary glands of a mosquito from where transmission continues. Image created with BioRender.com [25].

Male and female gametocytes become distinguishable from one another from stage IV onwards, with female gametocytes having a smaller nucleus than male gametocytes [30]. Furthermore, female gametocytes have a more concentrated pigment pattern whereas in males the pigment is more spread out [31]. During the development process, gametocytes remain in the bone marrow and once mature, the stage V gametocytes re-enter the bloodstream [30]. These mature stage V gametocytes can remain dormant until ingested into the mosquito's midgut [30] but they are the only form of gametocytes that can be transmitted to the next feeding mosquito. *P. falciparum* parasites show a female-biased sex ratio of approximately one male for every four female gametocytes [34], which is balanced out as gametes are formed, since one male gametocyte develops into eight male gametes in the mosquito midgut, thereby nearly equalling the ratio of male to female gametes [27]. Therefore, during gametogenesis exflagellation occurs, which is when the male gametocyte (1n) undergoes three rounds of genome replication and mitotic cell division to release eight flagellated male (micro) gametes (8n) [35, 36]. The female gametocyte differentiates

into one immobile female (macro) gamete [35]. The process of gamete activation is dependent on environmental stimuli in the mosquito midgut [35]. These environmental stimuli comprise a temperature decrease of ~10°C from the warm-blooded human host to the mosquito vector, the presence of a mosquito-derived molecule xanthurenic acid and an increase in the pH from 7.2 to 8 [35, 37]. These stimuli result in molecular changes in the sexual stages of the parasite and activate stage-specific genes through differential gene expression to initiate reproduction (gametogenesis) and to prepare the gametes for the hostile mosquito midgut [27]. The flagellated male gamete fertilises the female gamete forming a diploid zygote in the mosquito midgut [35]. Zygotes form motile, elongated ookinetes that enter the mosquito's midgut wall to develop into oocysts [30]. Oocysts grow and rupture to release sporozoites, which move to the mosquito's salivary glands to be transmitted to the next human host and continue the malaria life cycle [26].

Throughout the intra-erythrocytic cycle, at least 60 % of the parasite's genome is transcriptionally active through a unique gene regulation cascade [38]. Furthermore, gametocytes have sexual stage-specific promoters for gene expression at the correct time of development with a few of the gametocyte-specific transcripts only being translated in the gamete stages of the parasite due to a translation repression mechanism being present in the parasite [31, 36]. As such, the unique transcriptional mechanism of the parasite can be utilised for various applications and research of the parasite to aid in drug development.

1.4 Treatment with antimalarial drugs

Chemotherapeutics are antimalarial drugs used to suppress malaria infections and alleviate symptoms by killing the parasite [14]. For effective malaria treatment, early diagnosis is essential, otherwise, severe malaria could develop. Severe malaria requires effective treatment as the mortality rate for untreated patients without immunity is close to 100 % [21]. Quick and efficient treatment along with supportive care can reduce the mortality rate to 10-20 % [21]. Also, early malaria diagnosis provides less time for the malaria parasite to circulate in the blood, thereby reducing the transmission risk [2].

For the treatment of uncomplicated malaria, oral medication is required with high efficiency and low side effects to clear parasites as quickly as possible to prevent the development of severe malaria [6, 21]. Due to *P. falciparum* resistance against first generation antimalarials including chloroquine (CQ), sulfadoxine-pyrimethamine (SP) and others, chemotherapeutics are currently wholly dependent on ACT. According to Verlinden *et al.*, numerous strategies to resist resistance from antimicrobial and anticancer research can be applied to antimalarial drug discovery [39]. These strategies, such as increasing the number of drug partners and applying polypharmacology to

drugs, are important for developing antimalarial drugs that have a long therapeutic lifespan by resisting resistance [39].

ACT consist of an artemisinin derivative such as artesunate, which is rapid-acting and decreases the parasites quickly, which is combined with a partner drug with a different pharmacokinetic and mechanism of action [40]. These can include a quinine derivative partner drug such as mefloquine, which is longer-acting and removes the remaining parasites [2, 40]. Although ACT have played an important part in malaria control, their effectiveness is threatened by resistance emerging for artemisinin and the partner drugs [2]. Artemisinin resistance is characterised by parasites being cleared slower from the blood after ACT and treatment failure occurring more frequently [41, 42]. Furthermore, artemisinin resistance has contributed to the selection of partner drug resistance as partner drugs are exposed to a larger number of parasites after the normal 3-day ACT, thereby, limiting the number of ACT that can be used in certain areas [41, 42]. Therefore, until new antimalarial drugs are available on the market, efficient management of existing drugs is of utmost importance to reduce the development of resistance. Moreover, whilst ACT are therapeutically essential, they are not useful tools in malaria elimination strategies. The latter relies on compounds that are also able to target the transmissible gametocytes stages and thereby block onwards transmission of the parasite [43].

1.5 Antimalarial drugs with transmission-blocking activity

To disrupt transmission multiple factors need to be taken into consideration. These include parasites in the mosquito vector, the parasite reservoir in asymptomatic or semi-immune carriers [20, 44], and the parasite pool in symptomatic malaria patients [43]. The premise for transmission-blocking antimalarials relies on the ability to target gametocytes, which are seen as population bottlenecks in the parasite life cycle, and the only transmissible stage between humans and mosquitoes. Delivery of drugs that target gametocytes should, therefore, be possible by dosing humans additionally, these could be highly effective as they only need to target very few circulating parasites [45]. For instance, asexual blood stage parasite numbers range from 1 to 10^6 / µL of blood in an uncontrolled infection, whereas less than 100 mature gametocytes are typically found per µL of blood [46]. The block in transmission from human to mosquito can occur by either affecting gametocytes in the human host or by affecting downstream mosquito vector stage parasites [47].

Only a few druggable targets have been described in mature gametocytes since mature gametocytes have terminally differentiated and only require household activities, such as redox maintenance while awaiting ingestion by a mosquito [48]. To exclusively target gametocytes, drugs should aim to inhibit translational repression, sperm function, and meiosis since these functions

are not important for asexual stages [49]. The only clinically approved compounds currently effective against gametocytes are methylene blue (MB) and primaquine with contrasting evidence as to the efficacy of artemisinin derivatives [43, 45, 50]. Although ACT have shown to decrease gametocyte numbers, they are mostly active against early gametocytes and unable to completely remove mature stage V gametocytes, therefore, transmission is still possible [45, 51]. Primaquine (an 8-aminoquinoline) is the only licensed drug that has been shown to successfully kill mature gametocytes [13, 40, 52]. However, malaria patients with a glucose-6-phosphate dehydrogenase (G6PD) deficiency develop intravascular haemolysis when treated with primaquine, thereby limiting its use [13, 40]. Primaquine's mechanism of action in the parasite is still poorly understood but studies have shown that primaquine may impair mitochondrial metabolism as well as cause production of reactive oxygen species [53, 54]. Another 8-aminoquinoline compound with mature gametocyte activity, tafenoquine, is currently in phase III clinical trials [55]. Although tafenoquine also causes haemolysis of G6PD-deficient patients, it has a longer half-life than primaquine making it possible to administer tafenoquine as a single dose [55]. Tafenoquine might be safer than primaquine since the patient has less exposure to the haemolysis causing drug, thereby reducing the risk of developing severe haemolysis. Therefore, derivatives of primaquine or drugs with similar modes of action that do not cause haemolysis need to be investigated as gametocytocidal drugs. Alternatively, completely new compounds that target gametocytes are being investigated [56].

Male gametes have also shown to be sensitive to inhibition since they undergo rapid development to produce eight male gametes and thereby they provide many new drug targets [48]. However, the challenge with targeting the parasite stages within the mosquito vector is that drugs need to be designed to remain effective for the entire period that the gametocytes circulate in the blood until taken up by a mosquito [20, 48, 50]. Atovaquone is one such interesting example that is active against all stages of all *Plasmodium* species by interfering with the mitochondrial membrane potential and inhibiting the transport of numerous parasite enzymes [21, 41]. However, the transmission-blocking drug compendium indeed needs to be expanded. As such, there is a need for novel drugs, especially against the transmissible gametocyte stages.

1.6 Drug discovery and development pipeline

The antimalarial drug discovery pipeline has been populated with new antimalarial candidates in various stages of clinical development over the past decade. For a new chemotherapeutic to be valuable, it must either have a novel chemotype, which the parasite has not seen before, to prevent cross-resistance or it must be able to resist resistance formation [20, 39]. Furthermore, the chemotherapeutic should target essential and novel biological processes or entities, as well as be able to function in combination with other chemical entities [39, 47]. In addition, to enable malaria

elimination, chemotherapeutics should have dual action: cure infection as well as prevent parasite transmission [20, 39].

The ideal antimalarial drug for eradication needs to eliminate the human reservoir, which can be achieved by a Single Encounter Radical Cure and Prophylaxis – SERCaP [13, 57, 58]. Nevertheless, it was seen that a single chemical entity would not be able to comply with these standards but instead, a combination of two or more compounds would be the solution [57, 58]. A single exposure to a drug would allow health workers to observe drug administration to reduce drug misuse and could decrease the risk of resistance development [58]. Furthermore, a radical cure implies the drug can remove all parasites as well as all *Plasmodium* species in a patient [13, 57]. Chemoprevention antimalarial drugs are also needed that are safe and effective to prevent infection, especially in vulnerable populations [58]. Due to resistance emerging for SP treatment [59], new chemoprotectants are needed that have activity against the parasite's liver stage [58].

Focus on eradication requires different approaches, of which transmission-blocking is the main intervention. Since only mature gametocytes are taken up by mosquitoes during a blood meal, antimalarial drugs should selectively kill the sexual stages or prevent onwards development of the parasite in the infected mosquito [58]. Furthermore, these antimalarial drugs should be safe enough to use on symptomatic as well as asymptomatic patients during mass drug administration campaigns [58].

The Medicines for Malaria Venture (MMV), a not-for-profit foundation, in collaboration with its partners have developed an antimalarial drug discovery portfolio [6]. Three approaches were used to identify promising antimalarial compounds for the drug discovery portfolio, including hypothesis-driven design, target-based screening and rational design, and phenotypic screening, which has been the most successful approach thus far [6]. MMV set out a guideline for the discovery and development of new antimalarial drugs to indicate the types of molecules [target candidate profiles (TCP)] and the combination of medicines [target product profiles (TPP)] needed [20, 57]. The TCP refers to a single candidate or molecule, whereas the TPP refers to two or more active candidates that produce a final product [20].

Two groups of TPP exist: TPP-1, medicines that can cure infected patients, and TPP-2, medicines that can protect patients from infection (Figure 1.3) [57]. According to TPP-1, to treat patients with acute uncomplicated malaria, a combination of molecules should be used that clear asexual blood-stage parasites (TCP-1 activity), target gametocytes (TCP-5 activity) and vectors to block transmission (TCP-5 activity) as well as target hypnozoites, which are mainly *P. vivax* parasites (TCP-3 activity) [20]. A TCP-5 candidate should ideally have activity against all five gametocyte

stages as well as inhibit oocyst or sporozoite formation [20]. Furthermore, patients with severe malaria require compounds with TCP-1 activity. The TPP-2 profile describes chemoprotection, which includes treatment when epidemics occur or individuals going to endemic areas [20]. These individuals should be treated with molecules that have hepatic schizont activity (TCP-4 activity) in combination with TCP-1 molecules for emerging infections [20].

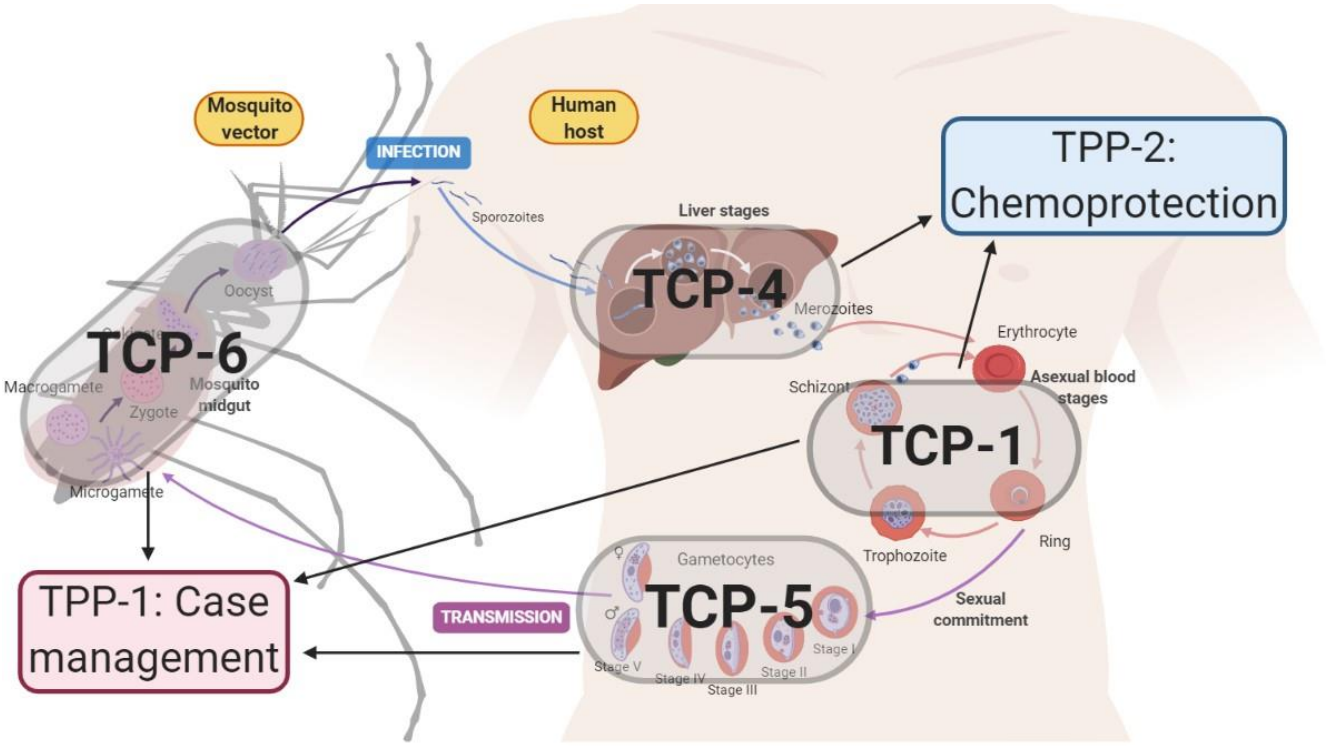

Figure 1.3: Parasite life cycle emphasising the target candidate profiles to form the target product profiles for developmental antimalarial drugs.
The target product profiles (TPP) consist of TPP-1, focussed on case management to treat infected patients and TPP-2, focussed on chemoprotection to protect patients from infection. TPP-1 comprises of molecules active against asexual blood-stage parasites (TCP-1) and drugs with transmission-blocking activity (TCP-5 and TCP-6). TPP-2 includes molecules with hepatic schizont (liver stages) activity (TCP-4) together with TCP-1 activity [20]. Image created with BioRender.com [25].

Four new compounds in clinical development at present have activity against multiple stages of the parasite's life cycle, including KAF156, DSM265, OZ439, and KAE609 [20]. Both OZ439 and KAE609 have activity against the asexual blood stages and reduce transmission [20], whereas DSM265 shows activity against the asexual blood stages and provides chemoprotection [20]. Finally, KAF156 has a TPP-1 and TPP-2 profile since it has activity against the asexual blood stages provides chemoprotection and reduces transmission [6].

Many of the antimalarial drugs that inhibit asexual blood-stage parasites have activity against immature stage I-III gametocytes [31, 43]. However, these drugs are not active against mature stage V gametocytes as they have a decreased metabolic activity and are biochemically different from asexual parasites [31, 43]. Even though the development of antimalarial drugs with

gametocyte-selective activity is possible [56], current compounds in the drug pipeline target both transmission and the asexual blood stages, albeit not at equally effective concentrations [58]. Compounds with such dual activity against asexual and sexual parasites [60], and where the same protein is targeted, have an increased risk for resistance development and transmission of the parasite [43]. Therefore, compounds with polypharmacology, meaning different modes of action in the asexual and sexual parasites, are of greater interest as they will lower the risk of developing resistance [43]. Furthermore, a combination of antimalarial drugs, one that has specific activity against transmissible gametocytes and another one with activity against asexual parasites, will also lower the risk of resistance development since the parasite would not be prone to select for resistance mutations [43]. Gametocyte-selective compounds can either be used in combination therapy to target residual transmission in low transmission settings or as targeted drug administration in high-transmission settings [43]. Therefore, there is a need to find gametocyte-selective compounds since no chemical hits exist in clinical development that are only active against gametocytes, although the first reports of gametocyte-targeted compounds have been published recently [56, 61, 62]. In the one study, they focused on identifying compounds that specifically target transmission stages of the parasite and identified 11 promising novel compounds, thereby paving the way for future investigation into transmission-blocking antimalarials [56]. Based on the information above, knowing the stage-specific activity of a compound (TCP) is very important for drug discovery. This data can help in preventing drug resistance development and aid in discovery of novel transmission-blocking compounds necessary for malaria elimination.

1.7 Variability in compound activity associated with different assay platforms

The discovery of new antimalarials through phenotypic screening is therefore dependent on the ability to accurately describe the activity of compounds against different stages of the parasite. Compounds are therefore also prioritised for further development based on these activities and this relies also on comparison of activities of compounds. However, numerous literature has highlighted discrepancies in compound activities where the same compound, assayed on two different assay readouts will result in different activities. This is mostly ascribed to be due to the differences in assay readouts, due to different assay technologies and, when the variability is across stages, metabolic pathways in the parasite is being targeted [50, 63]. Every lab has adopted the use of its assays and parameters, thereby introducing technical variables that are related to the lab such as culturing method, assay setups such as the technology used, and data analysis such as hit activity cut-off selection [63]. These variables make it difficult to compare data from different assays and to identify potential antimalarial hits. The MMV malaria box (open-access compound library) is a useful tool for this purpose and indicated large variability when antiplasmodial activity was compared across a broad range of assays and laboratories [45, 64].

Two reports by Cui *et al*. [65] and Hasenkamp *et al*. [66] also compared different asexual stage assay technologies to determine its effect on antiplasmodial activity data. They compared their asexual-specific luciferase-expressing lines with the SYBR Green I fluorescence or the [^{3}H]-hypoxanthine incorporation assay and found comparable 50% inhibition concentration (IC_{50}) results for known antimalarial drugs (Table 1.1) [65, 66]. Furthermore, Hasenkamp *et al*. showed that genetic modification to create the luciferase-expressing transgenic line (NF54^{luc}) did not have an effect on the IC_{50} values for known antimalarial drugs using the luciferase and SYBR Green I assays (Table 1.1) [66]. Even though different promoters were used to drive luciferase reporter expression between the different studies, IC_{50} values remained similar for the compounds [65-67]. Since the [^{3}H]-hypoxanthine incorporation assay is the gold standard, similar IC_{50} values between the different asexual assays (Table 1.1) indicate their suitability to replace the use of radioactive materials [65-68].

Table 1.1: Comparison of antiplasmodial activity against asexual stages of *P. falciparum* parasites using different assay technologies from different studies.
Data were obtained from previously published work. IC_{50} values are shown as mean (± standard error).

Compound name	IC_{50} (nM) values from different assay technologies					
	pLDH [69]	Luciferase		SYBR Green I Fluorescence [66]	ATP-bioluminescence [70]	[^{3}H]-hypoxanthine incorporation [68]
Methylene blue	-	30 [71]	-	-	10	-
Chloroquine	-	17.3 ± 0.5 [67]	21.0 ± 1.3 [66]	13.2 ± 2.1[a] & 26.7 ± 1.0[b]	7	11.2 ± 2.7
MMV390048	-	-	-	-	-	28 [72]
Dihydroartemisinin	3	19.58 ± 1.12 [65]	19.4 ± 1.8 [66]	14.1 ± 2.2 [a] & 7.9 ± 0.7 [b]	13	1.1 ± 0.1
OZ439	18	-	-	-	-	3.0 ± 0.5
Artesunate	-	4.1 ± 0.5 [67]	18.42 ± 1.50 [65]	-	54	3.5 ± 1.7

[a] NF54^{luc} transgenic line and [b] NF54^{attB} control line [66].

To determine whether the assay technology being used is the main driver for variability in assay outcome, three studies have directly compared gametocyte activity of compounds (including the malaria box) on different assay platforms by performing the experiments in parallel [45, 50, 69, 73]. Notable differences were seen for several compounds and varying IC_{50} values were obtained for the same compound by using the different technologies (Table 1.2) [50, 69, 73]. The report by D'Alessandro *et al*. found that the pLDH and luciferase assay showed good correlation even though they measure different biomarkers in the parasite [73]. By contrast, another report by Reader *et al*. showed that the ATP-bioluminescence and pLDH assay showed weaker gametocytocidal activity for several compounds compared to the luciferase assay [50]. Furthermore, compound activity also showed variable data for the same assay platform between the different laboratories. This highlights the need to cross-validate results from different assay technologies and different

laboratories to ensure potential hit compounds are identified from large compound libraries and to make the drug development pipeline progress faster [45].

Table 1.2 Comparison of antiplasmodial activity against stage IV/V gametocytes of *P. falciparum* parasites using different assay technologies from different studies.
Data were obtained from previously published work. IC_{50} values are shown as mean (± standard error).

Compound name	IC_{50} (nM) values from different assay technologies							
	pLDH				Luciferase assay		ATP-bioluminescence	
Methylene blue	-	800 [50]	530 [69]	-	226.1 ± 31.2 [63]	143 [50]	900 [50]	490 [70]
Chloroquine	-	-	1100 [69]	-	-	-	-	23450 [70]
MMV390048	285 [72]	-	-	-	140 [72]	-	-	-
Dihydroartemisinin	12 [72]	20 [50]	36 [69]	490.2 ± 240.0 [73]	435.3 ± 286.8 [73]	11 [50]	14900 [50]	3560 [70]
OZ439	-	-	160 [69]	-	-	-	-	-
Artesunate	-	-	50 [69]	36.2 ± 11.5 [73]	117.8 ± 13.4 [73]	-	-	10830 [70]

One of the first generation antimalarials, CQ, is known to be inactive against stage IV/V gametocytes but shows good activity towards early gametocytes and asexual stages [66]. CQ showed good correlation between the different assay platforms for asexual stages (Table 1.1) [66]. However, its inactivity towards stage IV/V gametocytes resulted in variable IC_{50} values (Table 1.2) [69, 70]. MMV390048 (2-aminopyridine) is a promising new chemical class currently in clinical trials with a new mechanism of action that inhibits *Plasmodium* phosphatidylinositol 4-kinase (PI4K) [72]. MMV390048 shows potential as a dual-active drug with low nM activity against the parasites' asexual and sexual stages (Table 1.1 and Table 1.2) [72]. Another compound currently in clinical development is OZ439 and from this data it can be seen that it also has low nM activity against asexual and sexual stages of the parasite, making it a promising transmission-blocking candidate as it shows gametocytocidal effects at clinically relevant concentrations [20, 69]. In contrast, dihydroartemisinin (DHA) and artesunate also have dual activity but the gametocytocidal activity is too low for current dosing regimens to have a significant impact on transmission blocking [69]. DHA is the active metabolite of artesunate, which explains the similarities in antiplasmodial activity between the two drugs [69]. Both show significantly higher activity towards the asexual stages with relatively similar IC_{50} data between the different technologies (Table 1.1) [66, 68-70]. However, the DHA IC_{50} values for stage IV/V gametocytes show a lot of discrepancies between the different technologies with values ranging from 11 nM to 14.9 µM (Table 1.2) [50].

Another dual active compound is MB, which shows good nM activity against asexual and gametocyte stages by potentially perturbing redox balance in the parasite [69, 70, 74]. MB has significantly lower IC_{50} values in asexual stages compared to gametocytes [70, 71]. One report could not use MB for the pLDH assay since the high MB concentration interfered with the readout [73]. Furthermore, a high variation in MB IC_{50} values for gametocyte stages are seen between the different assay technologies (Table 1.2) [45]. More significantly, is the > 5.6-fold increase in IC_{50} values for the pLDH and ATP-bioluminescence assays compared to the luciferase assay, which was run in parallel in the same lab [50]. Similar effects were seen for DHA in this study. Thereby, highlighting the variance created by different assay technologies since the same culturing methods and compound handling was applied. A single assay platform can remove the technical variances caused by different assay technologies to ensure that variation in antiplasmodial activity between the life cycle stages is only based on compound selectivity towards a specific stage of the parasite.

1.8 Drug screening assays

Phenotypic screening as a starting point in drug discovery involves screening of large numbers of chemical libraries with biochemical assays and has been the most successful approach to describe new antimalarial hits. Due to the complexity of drug effects on the parasite, these cell-based assays are more valuable for drug discovery than target-based assays since they imitate the *in vivo* environment better by exposing drug candidates to the whole-cell instead of only the target protein [63]. Phenotypic screening can identify new drug candidates with antimalarial activity as well as new mode of action [75]. However, since the parasite's life cycle stages are very different from each other, various assay platforms, with different readouts, and different parasite lines are used to determine drug efficacy for each stage evaluated (Table 1.3). Therefore, a lot of variabilities is created in drug activity data which in turn complicates TCP determination for antiplasmodial compounds.

Table 1.3: Drug screening methods for the different *Plasmodium* life cycle stages.

Life cycle stage	Target Candidate Profile [20]	*In vitro* culturing potential and screening methods for evaluation of drug efficacy
Asexual blood-stage parasites	TCP-1	Asexual blood stages are easy to maintain *in vitro* and highly amenable to HTS assays [75]. Drug efficacy is determined through parasite proliferation or viability, e.g. SYBR Green I assay.
Hepatic schizonts	TCP-4	Complete *P. falciparum* liver-stage development is possible *in vitro*, in human hepatocytes, but the infection rate is very low [76]. To determine drug efficacy in hepatocytes, murine models with luminescent sporozoites are used for whole animal-imaging of parasites, or antibody-stained parasites are screened by infrared or high-content imaging [75].
Gametocytes	TCP-5	Maintenance *in vitro* is relatively easy but obtaining high gametocytaemia is a challenge. Numerous gametocytocidal assays exist that are amenable to HTS and measure parasite viability since DNA replication has stalled. Assays include gametocyte-specific luciferase reporter assays, metabolic indicators and antibody detection of stage-specific markers [75].
Gametes	TCP-5	Gamete formation can be achieved in microplates at room temperature. Drug efficacy on gametes is determined with the dual gamete formation assay, which uses live imaging to measure male exflagellation bodies and fluorescence microscopy for female gametes [26]. Another method is the acridine orange gamete assay, which uses high-content imaging to monitor the transition of gametocytes into gametes [75, 77].
Ookinetes	TCP-5	The *P. berghei* ookinete development assay identifies compounds that affect early vector-stages by counting the ookinetes with fluorescence microscopy [26]. *In vitro* culturing conditions are possible to obtain sporulating oocysts from gametocyte cultures of a transgenic *P. berghei* line, which expresses GFP and luciferase at the mature ookinete, oocyst, and sporozoite stages [78].
Oocysts	TCP-5	The standard membrane feeding assay (SMFA) is the current gold standard to assess transmission reducing the activity of a drug by counting the number of oocysts inside mosquito midguts [75]. However, the SMFA is low-throughput and requires the use of mosquitoes [75].
Sporozoites	TCP-5	Bioluminescence measurements of luciferase-expressing *P. berghei* sporozoites can be used to determine drug efficacy [78].

The major difference in drug screening assays for asexual and gametocyte stages is the fact that proliferation can be determined in asexual parasites but not in gametocytes since gametocytes only mature and do not replicate anymore [79]. However, the same viability assays can be applied to asexual blood stage parasites and gametocytes.

The asexual blood stage of the *P. falciparum* parasite is the easiest life cycle stage to maintain *in vitro* and is also highly amenable to high-throughput screening (HTS) technologies [75]. Therefore, HTS campaigns have focused on antimalarial activity (TCP-1) against the asexual blood stage of the parasite. The gold standard assay for detecting antimalarial activity against the asexual blood

stages is considered to be the [^{3}H]-hypoxanthine incorporation assay, which is based on the incorporation of [^{3}H]-hypoxanthine into nucleic acids of the parasite [80, 81]. However, this assay requires radioactive materials. Consequently, nonradioactive materials, such as nucleic acid intercalating dyes, are cheap and simple to use [81] and includes SYBR Green I, which only stains the parasite's DNA since DNA is absent in erythrocytes, thus any fluorescent signal is an indication of parasite proliferation [75]. Numerous HTS assays have subsequently been performed against the asexual blood stage by making use of similar nucleic acid staining technologies [75]. Another fluorescence-based assay makes use of 4-6-diamidino-2-phenylindole (DAPI) DNA-binding dye for confocal imaging [80]. A drawback of these fluorescence-based assays is their low signal to background ratio and the interference of some chemical entities with the fluorescence output [80, 81]. The parasite lactate dehydrogenase (pLDH) colourimetric assay is another reliable marker of parasite viability as it plays a role in glucose metabolism [69] and can be used on any parasite strain [73] with HTS capability. Unfortunately, the assay can produce high background levels when assaying slow acting compounds [81].

A typical transmission-blocking screening cascade relies on identifying compounds with mature gametocyte activity (TCP-5) and to subsequently show that this translates into a block in gamete and oocyst formation. In all cases, once a compound has shown activity against gametocytes and gametes, the transmission-blocking activity must be confirmed through SMFA, where the inability of the parasite to transmit to *Anopheles* is assayed [43]. This assay, however, is very laborious and expensive, therefore, stringent prior filters of activity against gametocytes and gametes are required [26]. Consequently, robust HTS assays are needed as primary filters for mature stage V gametocyte activity as well as gamete formation inhibition. It has also been shown that mature male and female gametocytes respond differently to antimalarial drugs [82]. Thus, gametocyte screening assays that provide sex specificity of compounds would be advantageous but does not currently exist.

Numerous gametocytocidal assays exist for early- and late-stage gametocytes but not all are amenable to HTS. Gametocyte assays use various reagents to detect parasite viability since gametocytes only undergo maturation [83]. Current gametocyte screening assays make use of fluorescent indicators to measure metabolic activity (ATP [84], AlamarBlue and pLDH [69, 73]), fluorescence imaging (green fluorescent protein (GFP) and MitoTracker Red [60]), or viability determination of transgenic parasite lines expressing stage-specific reporter genes (GFP-luciferase reporters [71, 85-87] and dual-luciferase reporter [73, 79]). Gametocyte assays use various reagents to detect metabolic activity. For instance, AlamarBlue determines metabolic function and cellular health by monitoring the reducing environment of the parasite [88]. The AlamarBlue assay is easy to use, inexpensive and has a high sensitivity but it has a long incubation

time to produce a fluorescent signal, which increases the chance of producing artefacts [88, 89]. The activity of pLDH is also a reliable marker of gametocyte viability. However, the assay takes a long time since pLDH activity continues for 24 hours after gametocyte death and pLDH is present in asexual parasites as well as gametocytes, therefore, gametocyte samples must be pure to give accurate results [73]. Gametocyte viability can also be measured by fluorescence microscopy, which allows for the visual determination of parasite viability by detecting cells and cellular components with fluorochromes [90]. However, fluorescence microscopy has numerous limitations, including a loss of fluorescence ability of fluorophores after illumination and fluorochromes producing reactive oxygen species when illuminated [90]. MitoTracker red dye is a fluorochrome that determines mitochondrial function through the presence of mitochondrial membrane potential in viable gametocytes [91]. Another fluorescent marker is GFP, which can be visualised with fluorescence microscopy and can be used to produce fluorescently-tagged proteins that are driven by stage-specific promoters and expressed in living parasites [92]. These fluorescent proteins allow for visual quantification of parasite numbers in drug assays [60].

The ATP-bioluminescence assay measures the metabolic activity of a parasite, such as gametocytes, with the amount of intracellular ATP content present by making use of luciferase enzymes [89]. Viable parasites contain ATP but parasites that are not viable are unable to synthesise ATP and any remaining ATP is depleted by ATPases [89]. Luciferase catalyses the reaction of luciferin, a substrate added to the reaction, and ATP, a substrate found in cells, to produce photons of light (Figure 1.4) [89]. Therefore, parasite viability can be determined since nonviable parasites have less ATP and produce a smaller amount of light than viable parasites. The ATP-bioluminescence assay is sensitive and less likely to produce artefacts than other viability assays since the luminescent signal is produced in ~10 minutes [89]. However, the ATP-bioluminescence assay only measures ATP levels of the parasite and this can be contaminated by ATP contributed from the erythrocyte. To provide even greater sensitivity, luciferase activity can be assayed, which not only measures ATP levels but also luciferase expression within the parasite (relying on functional transcription and protein translation of luciferase). To provide more specificity, luciferase is used as a reporter gene that is expressed under the control of a stage-specific promoter in transgenic parasite lines [79]. A luciferase reporter line is suitable for cell-based assays as it is non-toxic to cells and does not require post-translational modification for activity [79]. A luciferase reporter line also allows for specificity and accuracy in quantitatively determining the effects of drugs on specific stages of the parasite [73]. This led us to propose that the TCP (stage specificity) of compounds can be determined with this bioluminescent assay by adding a luciferase reporter under the control of a constitutive promoter to create one assay platform where luciferase activity is measured (as a function of parasite viability) in all stages of parasite development.

Therefore, this would eliminate the variability inherent with using different assay platforms of the different parasite life cycle stages. Differences in the activity of compounds would, therefore, be a direct result of only stage differences.

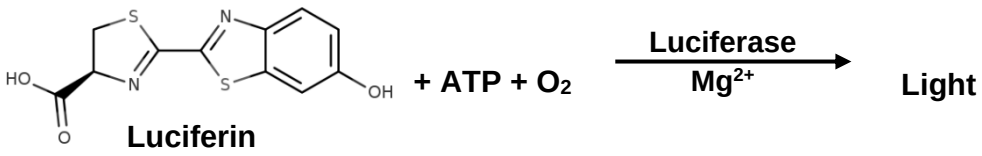

Figure 1.4: Luciferase catalyses the reaction of luciferin, ATP, and oxygen to produce light. For light (luminescence) to be produced, a luciferase enzyme requires the presence of luciferin substrate, ATP, oxygen (O_2) and the cofactor magnesium (Mg^{2+}). The luminescence signal is measured in a bioluminescence assay to indicate parasite viability [89].

Current luciferase assays (Table 1.4) are mostly used to assess compounds against gametocytes, e.g. where a GFP-luciferase fusion reporter was placed under the *pfs16* promoter, which is expressed in all five gametocyte stages [71, 73, 79, 85, 86]. Other luciferase assays exist that are specific for mature stage V gametocytes, with luciferase reporters being under the promoters' *mal8p1.16, pfs28* and *pfULG8* [71, 87]. Only, two asexual stage luciferase assays have used the *Pfhsp86* and *Pfpcna* promoters to drive luciferase expression [65, 66]. Different sources of luciferase have been explored in malaria parasites, with the *Photinus pyralis* firefly luciferase being the most common for drug assays [79].

A recent study created a transgenic *P. falciparum* line that expresses a mCherry-luciferase fusion under control of the *Pfetramp10.3* gene promoter [93]. Although the line shows constitutive luciferase expression, the levels of expression between the different stages vary a lot and are not suitable for high reporter expression in asexual and liver stages [93]. Additionally, two other transgenic lines contain a GFP-luciferase fusion reporter under the control of the constitutive *Pfhsp70* [94] or the *Pfef1α* promoter [67]. The constitutive *Pfhsp70* promoter showed variable expression levels for the different life cycle stages [94]. The *Pfef1α* promoter showed good luciferase expression throughout the life cycle stages, however, luciferase activity was not determined for gametocytes [67]. Even though constitutive parasite lines exist we proposed to develop a line that has a luciferase protein that is not fused to a fluorescent protein. Since a luciferase reporter has lower background levels, it does not require external illumination and has improved signal sensitivity compared to a GFP.

Table 1.4: Comparison of existing luciferase-based assays

Assay	Life cycle stage	Promoter controlling expression	Luciferase source	Reference
Dual-luciferase gametocyte	Gametocyte stage II and IV-V	*Pfs16*	*Pyrophorus plagiophthalamus* Click beetle CBG99 and CBR	[79]
Gametocyte-specific GFP-luciferase	Gametocyte stage I-V	*pfULG8*	*P. plagiophthalamus* Click beetle CBG99	[87]
Gametocyte-specific GFP-luciferase	Gametocyte stage I-V	*Pfs16, pfs48/45* and *mal8p1.16*	Copepods LucIAV luciferase	[71]
Gametocyte-specific luciferase	Gametocyte stage I-V	*Pfs16*	Copepods LucIAV luciferase	[85]
Gametocyte-specific luciferase	Gametocyte stage I-V	*Pfs16*	Copepods LucIAV luciferase	[86]
Gametocyte-specific luciferase	Gametocyte stage I-V	*Pfs16*	*P. plagiophthalamus* Click beetle CBG99	[73]
Asexual-specific luciferase	Asexual stages	*Pfhsp86*	*Photinus pyralis* Firefly luciferase	[65]
Asexual-specific luciferase	Asexual stages	*Pfpcna*	*Photinus pyralis* Firefly luciferase	[66]
mCherry-luciferase	Asexual, Gametocyte, Sporozoite and Liver	*Pfetramp10.3*	*Photinus pyralis* Firefly luciferase	[93]
Constitutive GFP-luciferase	All stages	*Pfef1α*	*P. pyralis* Firefly luciferase	[67]
Constitutive GFP-luciferase	All stages	*Pfhsp70*	Copepods LucIAV luciferase	[94]

In this study, we proposed to improve on the shortcomings of existing drug assays by using a highly sensitive luciferase reporter that is scalable for HTS [79, 87]. The CBG99 luciferase emits green light and is from the click beetle *Pyrophorus plagiophthalamus* [79]. Furthermore, the promoters used in this study to control constitutive luciferase expression were selected based on stringent transcriptomic analysis and its ability to upregulate consistent high levels of gene expression across all life cycle stages of the parasite. To create the transgenic lines we used the bacteriophage serine integrase–based integration system since it has a high integration efficiency to place foreign DNA into a specific location in the parasite's genome [95]. Genetic integration into *P. falciparum* occurs upon transient expression of the mycobacteriophage Bxb1 site-specific integrase to mediate recombination between a plasmid containing the *attP* site and an *attB* site, integrated at a known site into the genome [95]. Although assays exist to screen drug activity on every life cycle stage of the parasite, different biochemical methods are used. A constitutively expressing luciferase reporter line will allow the determination of a drug's TCP activity on all stages of the parasite's life cycle in the human host and mosquito vector. This constitutive luciferase assay will allow for the direct comparison between the different stages of the parasite's life cycle since drug activity is determined on the same assay platform for each cell type with the same readout, thus providing less variability in data.

Hypothesis

A constitutive luciferase-expressing *P. falciparum* line can be developed to evaluate the efficacy of potential antiplasmodial compounds across all life cycle stages of the parasite.

Aim

To develop a constitutive luciferase-expressing *P. falciparum* line that will allow screening of drugs on a single assay platform for all life cycle stages.

Objectives

A. Identify genes constitutively expressed across all life cycle stages of *P. falciparum*, including ring, trophozoites, schizonts, gametocytes, ookinetes, oocysts, and sporozoites.

B. Produce transgenic parasite lines expressing luciferase under the control of a promoter that activates constitutive gene expression using the Bxb1 integration system.

C. Prove luciferase expression under the control of the constitutive promoters occurs in the asexual and gametocyte stages of the transgenic lines.

D. Validate the use of the new constitutive luciferase-expressing lines for its ability to detect antimalarial drug efficacy.

Research output associated with this dissertation

A part of this work was presented in a poster format at the 4th annual South African Medical Research Council - Malaria Research Conference from 30 July to 1 August 2018, Johannesburg, South Africa. Title: Transmission-blocking antimalarial drug discovery. Authors: **Dorè Joubert**, Bianca Brider, Giulia Siciliano, Pietro Alano and Lyn-Marie Birkholtz.

Chapter 2: Materials and Methods

2.1 Ethics statement

All experiments were carried out in the Malaria Parasite Molecular Laboratory (M^2PL) that is a certified P2 facility (registration number 39.2/University of Pretoria-19/160) in which *P. falciparum* parasites were cultivated for this study. All *in vitro* experiments involving human blood donors holds ethics approval from the University of Pretoria Research Ethics Committee, Health Sciences Faculty (506/2018) and the *in vitro* cultivation of human malaria parasites are covered by approved umbrella ethics (NAS ethics approval no 180000094) for the SARChI program under Prof. Birkholtz.

2.2 *In vitro* cultivation of asexual *P. falciparum* parasites

P. falciparum NF54 parasites were cultured for transfection and luciferase assay experiments based on the methods created by Trager and Jensen [96]. Asexual parasites were cultured in human erythrocytes (predominantly O^+ or A^+) at 5 % haematocrit in RPMI-1640 (Sigma-Aldrich, Germany) culture medium supplemented with 0.024 mg/mL gentamycin (Fresensius Kabi Manufacturing, South Africa), 25 mM HEPES (Sigma-Aldrich, Germany), 0.2 % (w/v) glucose (Merck, South Africa), 0.2 mM hypoxanthine (Sigma-Aldrich, Germany), 23.8 mM sodium bicarbonate (Sigma-Aldrich, Germany), and 5 g/L Albumax II (Thermo Fisher Scientific, USA) [96, 97].

Parasite cultures were incubated at 37°C under hypoxic conditions in a 90 % N_2, 5 % O_2 and 5 % CO_2 atmosphere (AFROX, South Africa) at ~60 rpm to allow single parasite invasion events and increase parasitaemia and survival rates [97, 98]. Parasitaemia was routinely determined by Giemsa staining (Merck, South Africa) of a thin blood smear and visualised under a light microscope (Nikon, Japan) at 1000x magnification. Parasitaemia is defined as the percentage of parasite-infected erythrocytes found in more than 500 erythrocytes. Cultures were maintained at ~8 % for ring- or ~4 % for trophozoite-stage parasites by adding fresh uninfected erythrocytes and changing media daily.

Parasite cultures were synchronised to obtain parasites in the same developmental stage for stage-specific experiments. For asexual synchronisation, 5 % (w/v) D-sorbitol (Sigma-Aldrich, Germany) was applied to ring-stage parasites (for ~10 min) to selectively kill late asexual stages by lysis due to the membrane structure of their erythrocytes being permeable to sorbitol [99, 100]. After incubation, the parasites were resuspended in fresh media and erythrocytes and cultured as mentioned above.

2.3 *In vitro* gametocyte induction and maintenance of *P. falciparum* parasites

P. falciparum NF54 cultures (>90 % ring stage) were induced to undergo gametocytogenesis by nutrient starvation and a drop in the haematocrit [50]. Synchronised parasites in the ring stage were reduced to a 0.5 % parasitaemia in 6 % haematocrit (day -3) and transferred to glucose-deprived complete culture media (RPMI-1640, 0.024 mg/mL gentamycin, 25 mM HEPES, 0.2 mM hypoxanthine, 23.8 mM sodium bicarbonate and 5 g/L Albumax II) [50]. The cultures were maintained under hypoxic conditions as above at 37°C in a stationary incubator. Parasites were stressed even more by not changing culture media on day -2. After 72 h (day 0), the haematocrit was dropped from 6 % to 4 % to induce gametocyte production [101]. Gametocytogenesis was monitored daily with Giemsa-stained smears under a light microscope and only media was changed. Once gametocytes were mostly in stage II (day 3), media was changed to glucose-enriched and asexual parasites were removed from day 5 onwards by supplementing the media with 50 mM N-acetyl glucosamine (Sigma-Aldrich, USA) [50, 102]. The gametocyte cultures were maintained until day 10 for late stage IV/V gametocytes as required for downstream assays.

2.4 Identification of constitutively expressed genes in *P. falciparum*

Candidate gene regulatory regions, containing promoter regions, that efficiently activate gene expression across asexual, sexual and mosquito stages of *P. falciparum* parasites were selected by examining microarray and RNA sequencing (RNAseq) expression profiles obtained from the PlasmoDB database [103-106]. These constitutive regulatory regions were used for downstream experiments to create transgenic parasite lines, constitutively expressing a luciferase gene. For the identification of novel constitutive promoters, extensive data analysis was performed in R [107], as explained below, and heatmaps were also created in R.

Three datasets were used to obtain the constitutive gene candidates, consisting of a microarray dataset from van Biljon *et al.* [108] and two RNAseq datasets from López-Barragán *et al.* [103] and Zhangi *et al.* [104]. Firstly, k-means clustering for the RNAseq datasets was performed in R to obtain maintained or constitutive genes in each dataset (clustering was already available for the microarray dataset). After clustering, the overlapping genes between the selected clusters were determined. The genes present in all three datasets or the microarray dataset [108] and one RNAseq dataset were kept for further analysis [103, 104]. An essentiality analysis was performed to ensure that parasites undergoing drug treatment or stress will not cause downregulation of the promoter, which will result in less or no gene expression. Essentiality information of genes was obtained from PlasmoGEM to remove any slow or dispensable genes [109].

Next, translationally repressed genes were removed based on data from Lasonder, *et al.* [30] to ensure that a gene transcript will be translated into a gene product in the sexual stages. Genes were further reduced by selecting for strong expression in all the life cycle stages with a Fragments Per Kilobase of transcript per Million mapped reads (FPKM) threshold of 100 (log_2[100+1]) for RNAseq data. Lastly, genes were selected that showed similar and strong expression in male and female mature gametocytes [30]. The upstream regulatory regions of the genes that showed the strongest expression across all life cycle stages were selected and used for downstream cloning to create the transgenic luciferase-expressing lines.

2.5 Cloning promoter regions into expression plasmids

A multistep cloning strategy (Figure 2.1) was followed to produce the final plasmids, as based on the study by Siciliano *et al.* [87]. The plasmids used for cloning, pEX-myc-CBG99, pASEX-5'*nap*-GFP-3'*nap* and pCR2.1-*attP*-FRT-hDHFR/GFP, were kindly provided by Pietro Alano and Giulia Siciliano (Istituto Superiore di Sanita, Rome, Italy), and their constructs and use are defined in the sections below. The pASEX-5'*nap*-GFP-3'*nap* was modified to the pASEX-5'*nap*-myc-CBG99-3'*nap* plasmid (kindly modified and provided by Elisha Mugo from our lab) to consist of a myc-tagged CBG99 luciferase fusion gene (click beetle luciferase [79]) under control of the 5' upstream and 3' downstream regulatory regions of the nucleosome assembly protein gene (*nap*, PF3D7_0919000). The pCR2.1-*attP*-FRT-hDHFR/GFP plasmid was constructed with our chosen promoter(s) and reporter gene for transfection into the parasite. Modification of these plasmids to contain our chosen promoter regions are described in the sections below.

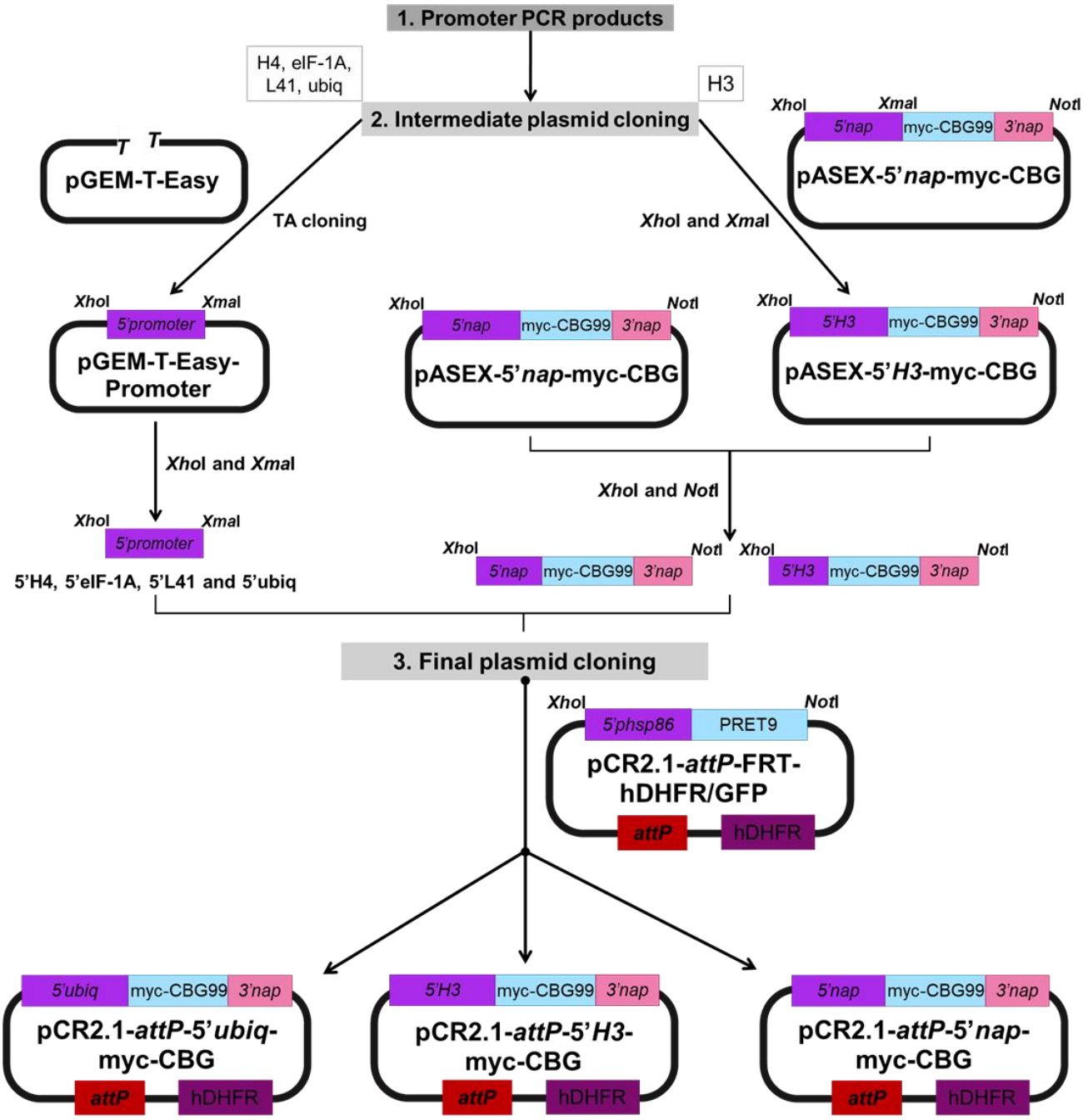

Figure 2.1: Cloning strategy to produce luciferase-expressing plasmids for transfection. The 5' promoter regions for histone H3 (H3), histone H4 (H4), translation initiation factor eIF-1A (eIF-1A), 60S ribosomal protein L41 (L41) and ubiquitin-60S ribosomal protein L40 (ubiq) were PCR amplified and cloned into plasmids for transfection into the *P. falciparum* parasite. Plasmid constructs are explained in more detail in the following sections.

2.5.1 Amplification of promoter regions

Firstly, the upstream regulatory regions containing the promoter sequence, 1400-1600 bp from the translation start site, of the identified constitutive genes were PCR amplified. Forward and reverse primers (Table 2.1) were designed with Benchling [110] and the restriction enzyme sites' *Xho*I, for forward primers and *Xma*I, for reverse primers were added. Restriction sites were added to the

primers along with three extra nucleotides at the end of the sites to increase restriction digestion efficiency to allow cloning into the desired locations of the plasmids. PCR amplification was performed with 1.25 U TaKaRa ExTaq polymerase, 1X ExTaq buffer, 0.2 mM dNTPs (Takara Bio Inc., Japan), 10 pmol of each primer and 30-100 ng of gDNA (*P. falciparum* NF54). Optimised PCR conditions include denaturation at 95°C for 5 min, followed by 30 cycles of denaturation at 95°C for 10 s and combined annealing and extension at 60°C for 4 min, and a final extension of 60°C for 7 min. DNA bands were obtained for the amplified promoter regions on 1 % (w/v) agarose/ Tris-Acetate-EDTA (TAE) gels that were stained with ethidium bromide for ~10 min and visualised with the Gel Doc EZ Imaging system (Bio-rad, USA). The NEB quick-load purple 1kb plus DNA ladder (New England Biolabs, UK) was used to determine DNA fragment sizes on a gel.

Table 2.1: Primer sequences of constitutive gene promoter regions.

nr	Gene name	Gene ID	Forward/ Reverse	Primer sequence (5' - 3' orientation) *
1	Histone H3	PF3D7_0610400	F	ccgctcgagTTCTATTCATAGCTATTATATATGATGTTTC
			R	ccccccgggATGATATAAAATATATTGTGTGTATTTTGTG
2	Histone H4	PF3D7_1105000	F	ccgctcgagTTGCAATTTTGTGTTATATTACTG
			R	ccccccgggAAAGTTTTTTTGAATAATTTTAAATATATATAAC
3	Histone H2A	PF3D7_0617800	F	ccgctcgagAGAATTGACAAAAAAAATGAAAGG
			R	ccccccgggTTTAATTTAAATAAAATTATGTGAAAAATTGC
4	Translation initiation factor eIF-1A, putative	PF3D7_1143400	F	ccgctcgagTTCGTAAATAAAATAATTCAACCTTAC
			R	ccccccgggAAATATAAAATTTGTGAATTCTTTAAAAATG
5	60S ribosomal protein L41	PF3D7_1144300	F	ccgctcgagATACTTAAATATTTACATAATGTGGAGAG
			R	ccccccgggTTTTTAATATTTATTAATTAAACTTTGTTTTTG
6	Ubiquitin-60S ribosomal protein L40	PF3D7_1365900	F	ccgctcgagTTTCTTGTTGATATAATTTAGTACATTC
			R	ccccccgggTTTCTTAAAAATAATGAAATGAAAAAAAAAAATTTAG

*Restriction sites with 3 extra nucleotides were added to primer sequences: *Xho*I (ctcgag) and *Xma*I (cccggg), as underlined

The PCR-amplified promoter regions were excised and recovered from agarose gels using a Zymoclean Gel DNA Recovery Kit (Zymo Research, USA), following manufacturer's instructions. The concentration of each sample was determined with a NanoDrop ND-1000 spectrophotometer (Thermo Fisher Scientific, USA) by measuring nucleic acid absorbance at 260 nm and purity established by evaluating contaminating proteins (A_{280}) and salt, carbohydrate, phenol, or protein (peptide bonds detected) contamination at A_{230}. Eluted DNA purity was determined by the A_{260}/A_{280} and A_{260}/A_{230} ratios, with a ratio of 1.8-2.0 regarded as pure DNA. Purified DNA was stored at -20°C until required for experiments.

2.5.2 Cloning promoter regions into an intermediate plasmid

The intermediate pASEX-5'*nap*-myc-CBG99-3'*nap* plasmid (Figure 2.2) was used since this vector already had a myc-tagged CBG99 luciferase fusion gene inserted under control of the 5' and 3' regulatory regions of the *nap* gene. This allowed for the insertion of the chosen promoter regions upstream of the myc-tag CBG99 luciferase gene by replacing the 5' *nap* promoter sequence, through directional cloning using *Xho*I and *Xma*I restriction sites (as outlined in the Figure 2.1 scheme).

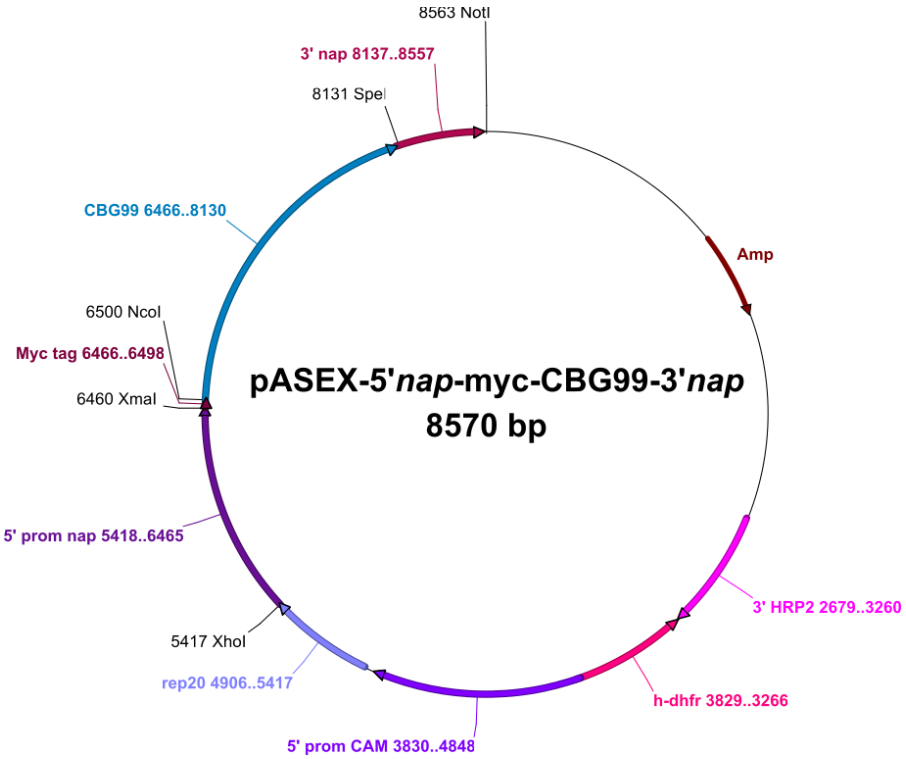

Figure 2.2: Intermediate pASEX-5'*nap*-myc-CBG99-3'*nap* plasmid.
The plasmid contains a myc-tag CBG99 luciferase fusion gene under control of the upstream (5' prom, promoter) and downstream (3') regulatory regions of the nucleosome assembly protein gene (*nap*, PF3D7_0919000). The *Xho*I and *Xma*I restriction enzyme sites were used to clone the selected PCR-amplified promoter regions into the intermediate plasmid. The plasmid contains an ampicillin resistance gene (Amp) for selection in Dh5α *E. coli* cells. The other plasmid components were not used for this study.

The PCR amplified promoter regions and pASEX-5'*nap*-myc-CBG99-3'*nap* plasmid were digested with 1 U/µg *Xho*I (New England Biolabs, UK) and 1 U/µg *Xma*I (New England Biolabs, UK) in 1x CutSmart buffer for 3 h at 37°C followed by heat inactivation at 65°C for 20 min. After digestion, the plasmid backbone was excised from a 1 % agarose gel. Next, the promoter regions and plasmid were column purified using the NucleoSpin Gel and PCR Clean-up kit (Macherey-Nagel GmbH & Co.KG, Germany). The promoter regions were ligated to the digested pASEX plasmid with T4 DNA ligase (New England Biolabs, UK) in a 1:3 vector to insert ratio (as shown in the equation below) and incubated overnight at 4°C.

$$\text{ng of insert} = \frac{\text{ng of vector} \times \text{kb size of insert}}{\text{kb size of vector}} \times \frac{1 \text{ vector}}{3 \text{ insert}}$$

Competent Dh5α *E. coli* cells were prepared from a saturated culture that was grown overnight in Luria-Bertani (LB) broth [pH 7.5, 1 % (w/v) tryptone, 0.5 % (w/v) yeast extract, 1 % (w/v) NaCl], in an incubator at 37°C with shaking at 180 rpm. The overnight bacterial culture was diluted 1:50 in LB broth and grown until the OD_{600} reached ~0.4 for the log-phase growth of cells. Cells were incubated on ice for 10 min and centrifuged at 1865 x*g* for 30 min at 4°C in an Avanti JE Centrifuge (Beckman Coulter, United States). The supernatant was decanted, and the bacterial cell pellet was resuspended in ice-cold 0.1 M $CaCl_2$ and centrifuged as before. The supernatant was again decanted, resuspended in 0.1 M $CaCl_2$ with 13 % (v/v) glycerol and incubated on ice for 1 h, after which cells were aliquoted and stored at -80°C.

The ligation mixture was added to 100 µL of competent cells and incubated on ice for ~30 min. Cells were heat shocked at 42°C for 90 s (water bath) and immediately incubated on ice for 2 min, followed by the addition of 900 µL pre-warmed LB-glucose (LB broth, 20 mM glucose). Cells were incubated in a shaking incubator at 37°C for ~1 h. The transformation reactions were plated onto LB-agar-amp plates [LB broth, 1 % (w/v) agar, 100 µg/mL ampicillin] and incubated overnight at 37°C in a stationary incubator. A positive control, pUC19 plasmid, and blank control, with no plasmid, were also included in the transformation experiments.

Single positive colonies were picked and inoculated in LB-broth with 50 µg/mL ampicillin and grown overnight at 37°C in a shaking incubator at 180 rpm. Colony PCR was performed to confirm positive transformants with the same primers (Table 2.1) as used for amplification. A PCR reaction was set up as before but with 1 µL of bacterial culture (instead of DNA) along with an added initial denaturation step of 95°C for 5 min to lyse bacterial cells and release DNA. PCR reactions were visualised on a 1 % agarose gel and positive clones were determined based on bands specific to the PCR product of the promoter regions. After positive transformants were confirmed, plasmid DNA was purified using the Wizard Plus SV Minipreps DNA Purification System (Promega, USA) as per manufacturer's instructions. In short, an overnight culture was centrifuged to remove culture media and lysed to release DNA. Next, the plasmid DNA was bound to a spin column, washed to remove unwanted content, and eluted from the column with nuclease-free water. Eluted plasmid DNA was assessed for concentration and purity with a spectrophotometer and stored at -20°C. Only the promoter region for the histone H3 gene, PF3D7_0610400, could be successfully cloned into the pASEX plasmid from its PCR product forming pASEX-5'*H3*-myc-CBG99-3'*nap* (Figure 2.1 and Figure 2.3).

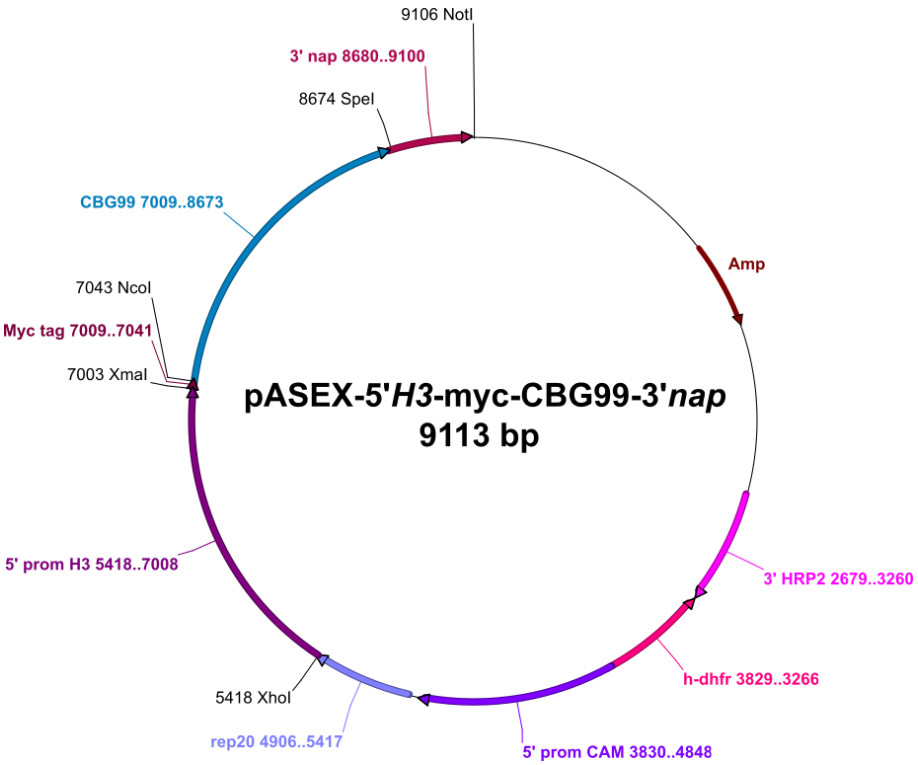

Figure 2.3: New intermediate pASEX-5'*H3*-myc-CBG99-3'*nap* plasmid generated.
The plasmid contains a myc-tag CBG99 luciferase fusion gene under control of the 5' promoter (prom) of histone H3 gene, PF3D7_0610400, and 3' regulatory region of the nucleosome assembly protein gene (*nap*). The plasmid contains an ampicillin resistance gene (Amp) for selection in Dh5α *E. coli* cells. The other plasmid components were not used for this study.

The other promoter regions needed an alternative strategy where they were in the first instance cloned into a pGEM-T Easy vector (Promega, USA) through TA-cloning before subcloning into the final pCR2.1-*attP*-5'*H3*-myc-CBG plasmid (see next section)(Figure 2.1). The linearised pGEM-T Easy vector has a single 3´-terminal thymidine at both ends and the promoter regions have an adenine that was added by the TaKaRa ExTaq during PCR amplification. The ligation was set up with 50 ng of pGEM-T Easy vector, 1x Rapid Ligation Buffer (Promega, USA), 1 Weiss unit of T4 DNA Ligase (Promega, USA) and PCR product in a 1:3 vector to insert ratio as previously shown in the calculation. The ligation reactions were incubated overnight at 4°C, followed by transformation of competent cells as previously described. The transformation reactions were plated onto LB-agar-amp plates spread with IPTG and X-Gal (LB-agar-amp, 100 µL of 100 mM IPTG, 50 µL of 20 mg/mL X-Gal) and incubated overnight at 37°C in a stationary incubator. Recombinant plasmids were identified by blue/white screening since an insert interrupts the coding sequence of β-galactosidase in the pGEM-T Easy vector thereby producing white colonies. Positive white colonies were selected and screened as previously explained. All the promoter regions were successfully cloned into the pGEM-T Easy vector and the promoter regions were then cloned into the final plasmid as below (Figure 2.1 for scheme).

2.5.3 Cloning of promoter regions into the final Bxb1, *attP* plasmid

From the above, the following cassettes were inserted into the pCR2.1-*attP*-FRT-hDHFR/GFP plasmid (Figure 2.4) by replacing the *phsp86* promoter and PRET9 luciferase reporter gene that was initially present in the plasmid with the: 5'*H3*-myc-CBG99-3'*nap* cassette and the 5'*nap*-myc-CBG99-3'*nap* cassette (Figure 2.1 for scheme). Please note, the *nap* promoter was included since it was already present in the intermediate plasmid. The pCR2.1 plasmid contains the required *attP* site needed for integration into the genome at the *attB* site, as explained in the following section.

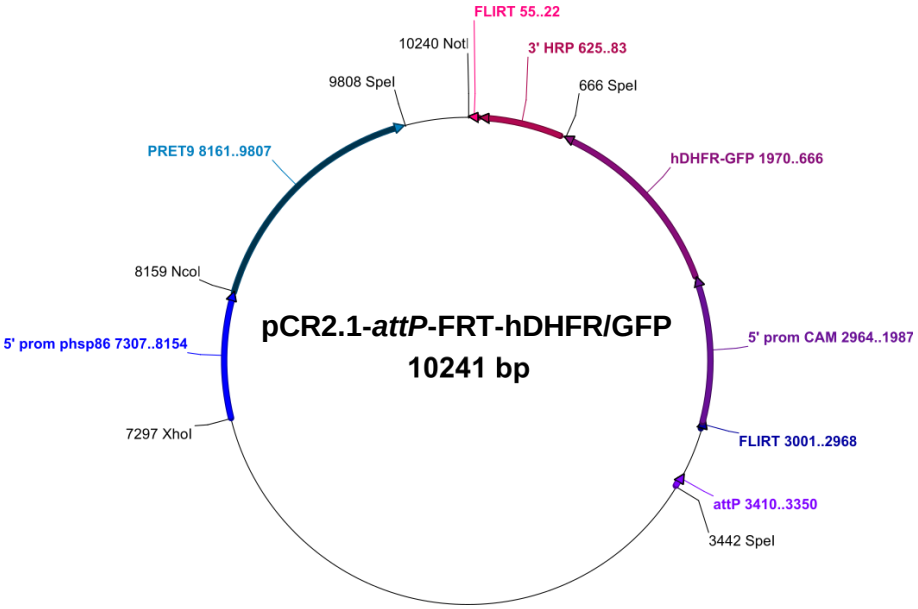

Figure 2.4: Final attP-containing plasmid used for creating transfection plasmids.
The pCR2.1-*attP*-FRT-hDHFR/GFP plasmid contains a PRET9 luciferase gene under control of the 5' heat shock protein 86 (*hsp86*) promoter (prom). The plasmid contains a human dihydrofolate reductase (hDHFR fused to a GFP) resistance gene under control of the 5' *calmodulin* promoter for selection in *P. falciparum* parasites. The *attP* site is used for the Bxb1 *attB*-*attP* integration system.

The promoter myc-tagged CBG99 luciferase cassettes were inserted into the pCR2.1-*attP*-FRT-hDHFR/GFP by digesting the intermediate plasmids (pASEX-5'*nap*-myc-CBG99-3'*nap*, pASEX-5'*H3*-myc-CBG99-3'*nap*) with 1 U/µg each of *Xho*I and *Not*I (New England Biolabs, UK) for 3 h at 37°C. The digested plasmids were run on a 1 % (w/v) agarose gel and the desired bands were excised from the gel. The pCR2.1-*attP*-FRT-hDHFR/GFP plasmid backbone and cassettes (5'*nap*-myc-CBG99-3'*nap*, 5'*H3*-myc-CBG99-3'*nap*) were column purified as before and the DNA concentration and purity were determined. The insert regions were ligated to the pCR2.1-*attP*-FRT-hDHFR/GFP plasmid and transformed into competent cells as previously described. Positive colonies were confirmed by PCR (primers promoter F1 and CBG R3 as shown in Table 2.2), and plasmids were isolated using the NucleoSpin Plasmid Isolation Kit (Macherey-Nagel GmbH & Co.KG, Germany) according to the manufacturer's instructions.

The final plasmids, pCR2.1-*attP*-FRT-hDHFR/GFP-5'*nap*-myc-CBG99-3'*nap* (hereinafter referred to as pCR2.1-*attP*-5'*nap*-myc-CBG, Figure 2.5A) and pCR2.1-*attP*-FRT-hDHFR/GFP-5'*H3*-myc-CBG99-3'*nap* (hereinafter referred to as pCR2.1-*attP*-5'*H3*-myc-CBG, Figure 2.5B) were mapped with restriction enzyme digestion (*Xho*I/*Spe*I) and the 5' promoter region and myc-tag CBG99 luciferase gene was sequenced to confirm the correct sequences were cloned. The sequencing reaction (20 µL) for each primer (Table 2.2) consisted of 10 % (v/v) BigDye (2 µL) and 2x Big Dye buffer (4 µL) from the Big Dye Direct Sequencing kit (Life Technologies Corporation, USA), 5 pmol primer and 100 ng/kb plasmid template (kb refers to region being sequenced). The sequencing PCR comprised of an initial denaturation at 96°C for 1 min, followed by 25 cycles of denaturation at 96°C for 10 s, annealing at 50°C for 5 s and extension at 60°C for 4 min.

Table 2.2: Primer sequences to sequence the promoter and myc-tag CBG99 luciferase gene

Forward/ Reverse	Primer sequence (5' - 3' orientation)
Promoter F1	ACTCACTATAGGGCGAATTG
CBG R1	AACTTCCCATCCATCACACTG
CBG R2	ATATCCAAAATCACCAGAATGC
CBG R3	TTCTCCACAGTGTCCAAGATG

Sequencing reactions were cleaned by ethanol precipitation before being sent for sequencing. The sequencing reaction (20 µL) was mixed with 1/10th 3 M sodium acetate (pH 5.2, 2 µL) and 2.5x ice-cold 100 % absolute ethanol (50 µL) and incubated on ice for ~15 min. The samples were centrifuged at 11000 x*g* for 30 min at 4°C, after which the supernatant was removed and 250 µL of ice-cold 70 % ethanol was added. The samples were centrifuged again at 11000 x*g* for 10 min at 4°C and the supernatant completely removed. The tube was left open on a heating block at 50°C for 5 min to allow all residual ethanol to evaporate. The sequences were evaluated by Sanger sequencing at the UP sequencing facility (South Africa) using an ABI 3500xl genetic analyser and analysed with CLC Main Workbench 8 and online Benchling software.

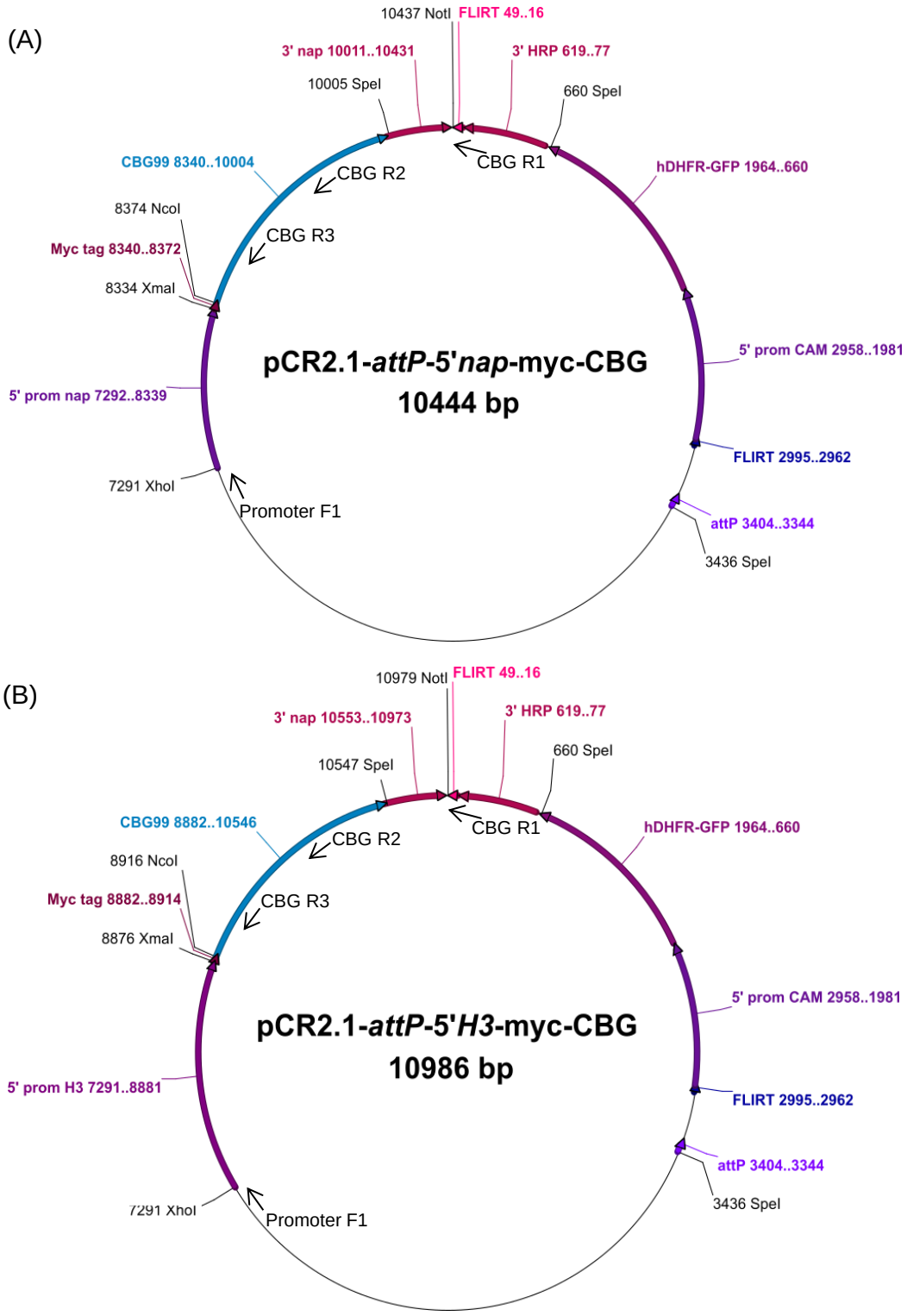

Figure 2.5: Final luciferase- and *attP*-containing plasmids used for transfection.
The (A) pCR2.1-*attP*-5'*nap*-myc-CBG and (B) pCR2.1-*attP*-5'*H3*-myc-CBG plasmids contain a myc-tag CBG99 luciferase fusion gene under control of the 5' (A) nucleosome assembly protein (*nap*) promoter (prom) or (B) *histone H3* promoter, and the 3' regulatory region of the *nap* gene. The plasmid contains a human dihydrofolate reductase (hDHFR fused to a GFP) resistance gene under control of the 5' *calmodulin* promoter for selection in *P. falciparum* parasites. The *attP* site is used for the Bxb1 *attB-attP* integration system. The promoter F1, CBG R1, CBG R2, and CBG R3 primers (Table 2.2) are used for sequencing.

Since only the *H3* and *nap* promoters could be inserted into the pCR2.1 plasmid via the pASEX intermediate plasmid system, the remaining promoter elements (*H4, eIF-1A, ubiq* and *L41*) had to be subcloned into pGEM-T-Easy via TA-cloning first. The promoter elements were subsequently cut from this vector with 1 U/µg each of *Xho*I and *Xma*I (New England Biolabs, UK) for 3 h at 37°C. The pCR2.1-*attP*-5'*H3*-myc-CBG plasmid was used as the backbone to replace the 5' promoter region with the promoter region from pGEM-T-Easy vectors. The digested plasmids were run on a 1 % (w/v) agarose gel and the desired bands were excised and purified. The pCR2.1-*attP*-myc-CBG plasmid backbone and promoter elements (5'*H4*, 5'*eIF-1A*, 5'*ubiq*, 5'*L41*) were ligated and cloned as previously described. However, only the promoter region for the ubiquitin-60S ribosomal protein L40 (PF3D7_1365900) could be successfully cloned, thereby, producing the final plasmid pCR2.1-*attP*-5'*ubiq*-myc-CBG. The pCR2.1-*attP*-5'*ubiq*-myc-CBG plasmid (Figure 2.6) was also mapped and sequenced but was not transfected into the parasite.

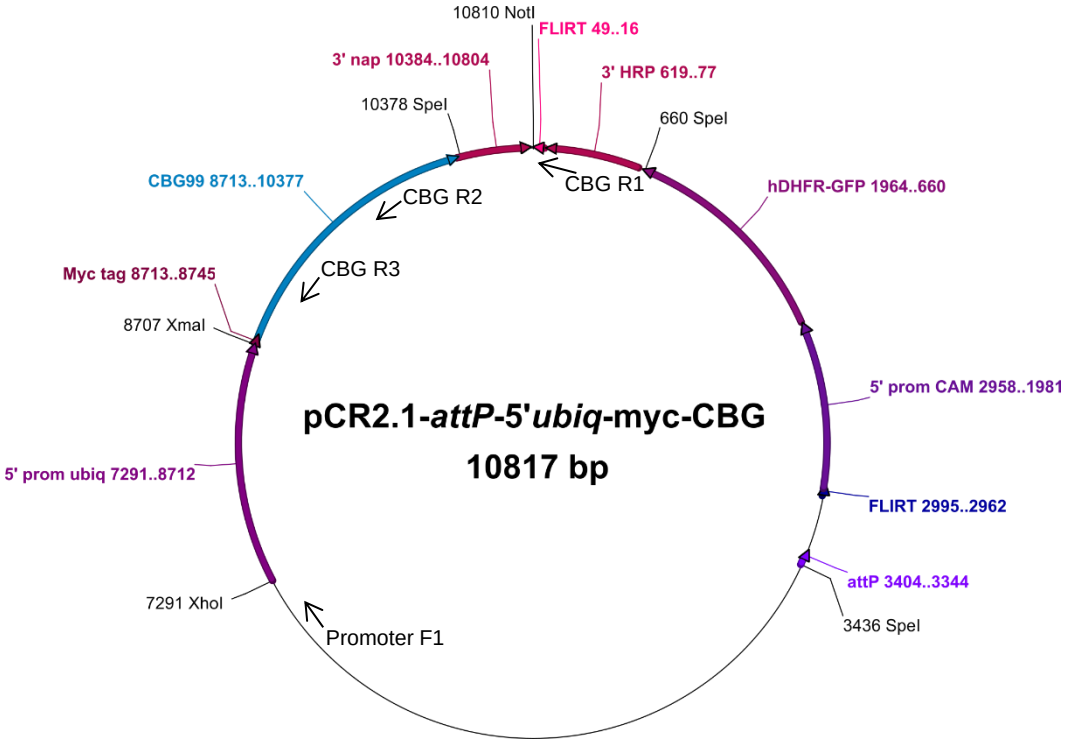

Figure 2.6: Final pCR2.1-*attP*-5'*ubiq*-myc-CBG plasmid.
The pCR2.1-*attP*-5'*ubiq*-myc-CBG plasmid contains a myc-tag CBG99 luciferase fusion gene under control of the 5' ubiquitin-60S ribosomal protein L40 (*ubiq*) promoter (prom), and the 3' regulatory region of the *nap* gene. The plasmid contains a human dihydrofolate reductase (hDHFR fused to a GFP) resistance gene under control of the 5' *calmodulin* promoter for selection in *P. falciparum* parasites. The *attP* site is used for the Bxb1 *attB*-*attP* integration system. The promoter F1, CBG R1, CBG R2, and CBG R3 primers (Table 2.2) are used for sequencing.

2.6 Plasmid integration and parasite transfection

2.6.1 Large scale plasmid isolation

The final plasmids were isolated using the NucleoBond® Xtra Midi purification kit (Macherey-Nagel GmbH & Co.KG, Germany) as per manufacturer's instructions from separate saturated Dh5α *E. coli* cells for pCR2.1-*attP*-5'*nap*-myc-CBG, pCR2.1-*attP*-5'*H3*-myc-CBG and the pINT plasmid (Figure 2.7) that expresses Bxb1 mycobacteriophage integrase. The eluted plasmid DNA was ethanol precipitated as previously described, however, the pellet was airdried at room temperature inside a flow hood. The DNA was reconstituted in Cytomix (120 mM KCl, 0.15 mM $CaCl_2$, 2 mM EGTA, 5 mM $MgCl_2$, 10 mM K_2PO_4, 25 mM HEPES, pH 7.6) at a concentration of 500-600 ng/µL and stored at 4°C until transfection.

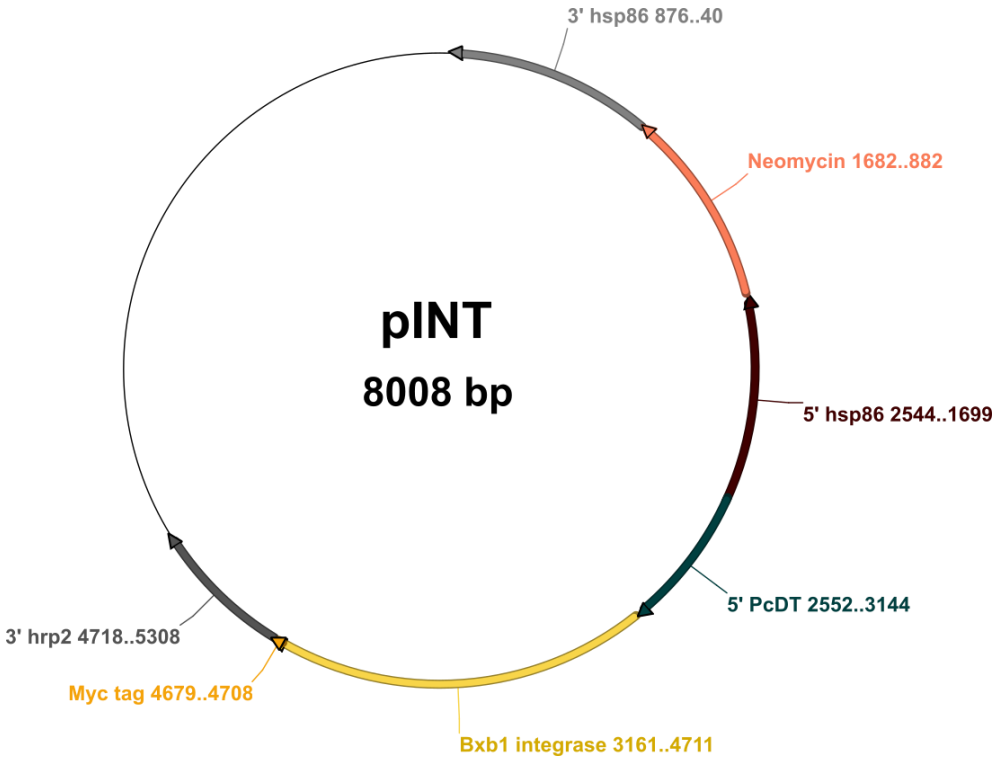

Figure 2.7: pINT plasmid for expression of Bxb1 mycobacteriophage integrase.
The pINT plasmid contains a myc tag Bxb1 mycobacteriophage integrase fusion gene under control of the 5' *P. chabaudi* DHFR/TS (*PcDT*) promoter and the 3' regulatory region of the *hrp2* gene. The plasmid contains a neomycin resistance gene under control of the 5' and 3' *hsp86* promoter for selection in *P. falciparum* parasites.

2.6.2 Parasite transfection

The site-specific Bxb1 *attB-attP* integration system (Figure 2.8) was used to efficiently integrate promoter and reporter gene fragments into the *Plasmodium* genome in the dispensable *cg6* gene of the transgenic NF54-*cg6-attB* parasite line ($NF54^{attB}$, a kind gift from Pietro Alano and Giulia Siciliano, Istituto Superiore di Sanita, Rome, Italy) [71, 95]. The system relies on the site-specific

integration action of the mycobacteriophage Bxb1 integrase, expressed by the pINT plasmid, which catalyses the homology-directed recombination between an *attP*-containing plasmid (pCR2.1) and the target, chromosomal *attB* site in the *cg6* gene [71, 95]. This site-specific recombination event at the *attB* site integrates the expression plasmid to produce two new asymmetric sites, *attL* and *attR,* on both sides of the inserted region that can only recombine with an exogenous excision factor thereby making the integration stable [71, 95].

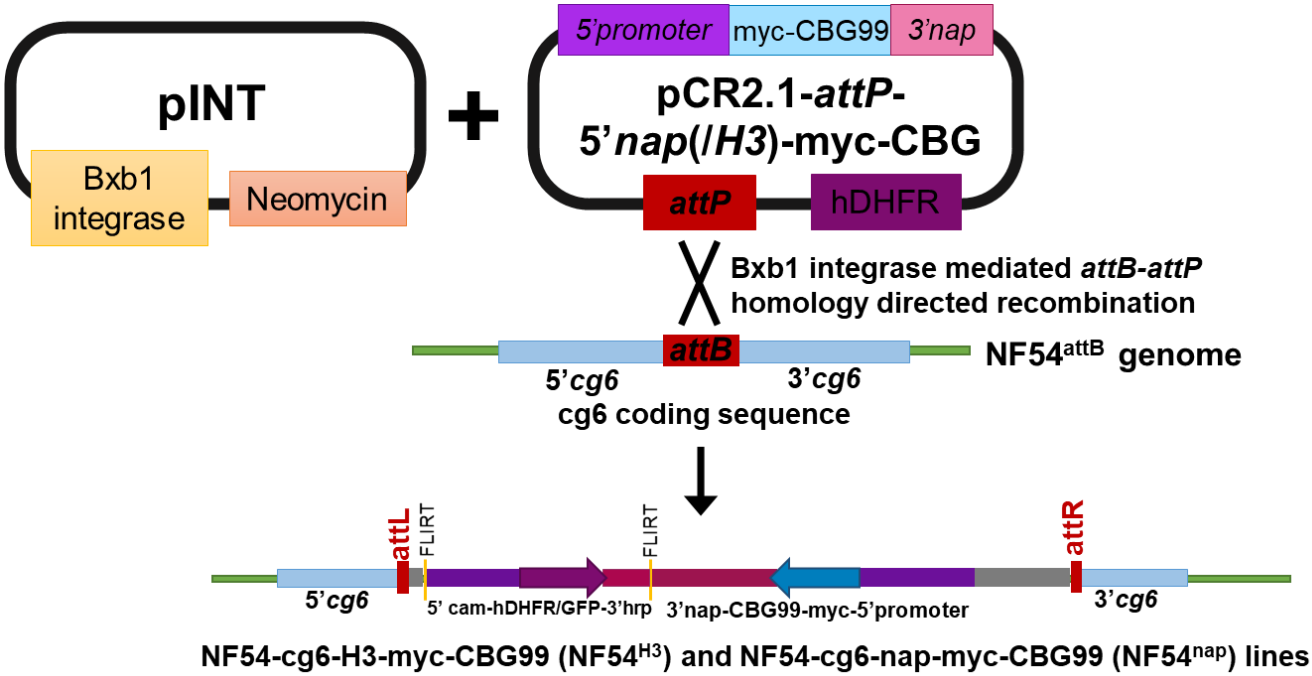

Figure 2.8: Bxb1 integration system to produce the NF54^{H3} and NF54^{nap} reporter lines.
The pCR2.1-*attP*-5'*nap*-myc-CBG or pCR2.1-*attP*-5'*H3*-myc-CBG and the pINT plasmid were transfected into ring-stage NF54^{attB} parasites. The pINT plasmid expresses a mycobacteriophage Bxb1 integrase to catalyse the homology-directed recombination between the *attB* and *attP* sites to produce asymmetric *attL* and *attR* sites around the inserted region. Recombinant parasites were selected for by double drug pressure with G418 (selects for neomycin resistance gene in pINT) and WR99210 (selects for hDHFR resistance gene in pCR2.1-*attP*) to produce two transgenic lines - NF54^{H3} and NF54^{nap}. The transgenic lines consist of a myc-CBG99 luciferase fusion gene under expression control of the 5' *H3/nap* promoter and 3' *nap* regulatory region.

The *P. falciparum* NF54^{attB} line at 5-6 % ring-stage parasites (5 % haematocrit) was centrifuged (3000 x*g* for 2 min) to remove spent media and washed once with cytomix (1:1). The parasite-infected erythrocyte pellet (200 µl) was resuspended in cytomix that contained either 60 µg of pINT (100 µL) and 60 µg of pCR2.1-*attP*-5'*nap-myc*-CBG (100 µL) or 60 µg of pINT (100 µL) and 50 µg pCR2.1-*attP*-5'*H3-myc*-CBG (100 µL) to produce a final volume of 400 µL. The cytomix mixture was added to a pre-chilled electroporation cuvette and electroporated with a BioRad Gene Pulser Xcell™ Electroporation System at a capacitance of 950 µF, a voltage of 310 V, and at maximum resistance to ensure optimal time constants of 10-15 ms.

After electroporation, the infected erythrocytes were combined with 5 mL of culture media (5 % haematocrit) and allowed to recover in the stationary incubator for 2 h at 37°C. The recovered parasites were centrifuged (3000 x*g* for 2 min) and then lysed erythrocytes were aspirated. The transfected erythrocytes were resuspended in pre-warmed culture media (5 mL) with 100 µL erythrocytes (50 % haematocrit) and transferred back to the stationary incubator at 37°C in a 90 % N_2, 5 % O_2 and 5 % CO_2 atmosphere.

2.6.3 Drug selection of transgenic parasites

Twenty-four hours after transfection, double selection for transgenic parasites started by adding 250 µg/mL G418 (neomycin) and 2.5 nM WR99210. After 6 days of double drug treatment, parasites were treated with 2.5 nM WR99210 for 3 days after which parasites could recover in drug-free medium. The G418 drug blocks polypeptide synthesis to ensure only parasites that have the neomycin resistance marker in the pINT integration plasmid survive. The antifolate drug, WR99210, [71] was used to select for the resistance marker human dihydrofolate reductase (DHFR, found in the *attP*-containing plasmid) since the drug disables the *Plasmodium* DHFR enzyme thereby stopping nucleic acid synthesis [111]. Therefore, only the parasites that contained the *attP*-containing plasmid survived since the expression of human DHFR takes over the function of the malaria DHFR [111].

The parasitaemia was calculated daily for the duration of drug selection to monitor parasite death and proliferation. Fresh erythrocytes (50 % haematocrit) were added once a week to replace old lysing erythrocytes and maintain a 5 % haematocrit. Parasites started to appear again after ~17 days. Once parasite cultures were >1 % parasitaemia, PCR screening was performed as explained below (Section 2.6.4) and showed a mixed population of recombinant (integrated) and wild-type parasites. Therefore, parasite cultures were placed under another round of 2.5 nM WR99210 drug selection for 7 days and screened again. Once an increase in parasitaemia (>1 %) was seen, the transgenic parasite cultures (3 mL) were expanded to 10 ml cultures, returned to the shaking incubator, and cultured as normal.

2.6.4 Screening of transgenic parasites

The new transgenic parasite lines, NF54-*cg6*-*H3*-myc-CBG99 ($NF54^{H3}$) and NF54-*cg6*-*nap*-myc-CBG99 ($NF54^{nap}$) were screened by PCR amplification for episomal uptake and genomic integration of the pCR2.1-*attP*-5'*nap*-myc-CBG or pCR2.1-*attP*-5'*H3*-myc-CBG plasmid. As soon as the transfected parasites were >1 % parasitaemia, samples were collected for screening. Genomic parasite DNA was extracted from parasite cultures using the Qiagen DNeasy® Blood & Tissue kit (Qiagen, USA).

Integration of the *attP*-containing plasmid was determined by amplification of template DNA from NF54^{attB} (negative wild-type control) and transgenic parasite lines (NF54^{H3} and NF54^{nap}) using primers (Table 2.3) binding at the *attL* and *attR* sites. Wild-type parasites were identified by positive amplification of the *attB* site (Table 2.3). PCR amplification and analysis with gel electrophoresis was performed as previously described. The 1kb or 100bp Promega DNA ladder (Promega, USA) was used to determine DNA fragment sizes on a gel. The transgenic lines, NF54^{H3} and NF54^{nap} were sequenced to confirm successful integration by the creation of an *attL* and *attR* site from an *attB* site in the NF54^{attB} (also sequenced) genome. The *attL* and *attR* sites were PCR amplified, cleaned and then the PCR products were sequenced with the *attL* forward (F1) and *attR* reverse (R1) primers, respectively.

Table 2.3: Primer sequences for screening and sequencing of transgenic parasite lines

Amplification area	Forward/ Reverse	Primer sequence (5' - 3' orientation)	PCR product (bp)
attB	F1	CATCCTGTGAAGTTACCCAGGATCCA	713
	R1	CATGCAATTCTTGCAACTTGTCTATG	
	R2	TGATAAAACAAACCACAAGCACATA	1100
attR	F2	CGCAGGAAAGAACATGTGAGCA	903
	R1	CATGCAATTCTTGCAACTTGTCTATG	
attL	F1	CATCCTGTGAAGTTACCCAGGATCCA	701
	R3	GATTACTTTGATTAACAAAGGCACGC	

2.6.5 Analysing the growth rate and morphology of the transgenic lines

Parasite morphology of the new transgenic NF54^{H3} and NF54^{nap} lines was assessed by visualising the asexual stage parasites across the 48-h cycle with Giemsa-stained blood smears. After 48 h, the parasitaemia increase of the transgenic asexual stage parasites was compared to that of NF54^{attB} (wild-type control). The new lines' ability to undergo gametocytogenesis was also determined and compared to that of NF54^{attB}. The five gametocyte stages were evaluated for NF54^{nap} over the 12-day development period since NF54^{H3} could not produce gametocytes. Routine culturing and gametocyte induction were performed as previously described.

2.7 Luciferase reporter assay

The luciferase assay was performed in white 96-well plates, to maximise bioluminescent output signal, which was read within 5 min after adding 1 mM D-luciferin substrate (0.1 M citric acid and 0.1 M trisodium citrate 2-hydrate, pH 5.5) to the parasite suspensions, at a 1:1 ratio at room temperature [79]. Bioluminescence (in relative light units, RLU) was detected at an integration constant of 10 s with the GloMax® Explorer Detection System (Promega, USA). The non-lysing

substrate, D-luciferin, was used for detection of luciferase activity since it is more cost-effective than commercial luciferase kits and does not have any lysis buffer, ATP, or enhancers [79]. The bioluminescent signals were normalised to the background control, which was culture media without parasites.

2.7.1 Proof of luciferase expression in transgenic lines

Luciferase expression under control of the constitutive promoters was determined, as described above, in the asexual stages of the NF54^{H3} and NF54^{nap} lines. The CBG99 luciferase enzyme kinetics was analysed for a mixed population of asexual parasites (1 % haematocrit, 6 % parasitaemia) by monitoring the bioluminescent signal over a 1 h timeframe (reading every 10 min). The luciferase activity was further determined in the asexual stages (1 % haematocrit, 1 % parasitaemia) and stage IV/V gametocytes (only NF54^{nap}, 1 % haematocrit and 0.8 % gametocytaemia). To determine the correlation between the luciferase activity and asexual parasitaemia, mixed populations of asexual parasite cultures were prepared at 1 % haematocrit and 1-3 % parasitaemia. The haematocrit was also evaluated as 1 and 2 % using a 2 % parasitaemia. To ensure that the CBG99 luciferase could be detected at the small volumes found in a 384-well plate, the parasite suspensions were plated in white 96-well plates to measure the luciferase activity at a volume of 200 µL and 60 µL, as described before.

2.7.2 Luciferase reporter assay with the new transgenic lines

The optimised luciferase assay conditions were used to validate the new constitutive luciferase-expressing lines for its ability to detect antimalarial drug efficacy. For validation, the IC_{50} of MB, CQ, MMV390048 and DHA was determined against the NF54^{H3} and NF54^{nap} parasite lines. Antiplasmodial activity of the compounds against the asexual stage parasites was determined with both lines but gametocyte activity was only determined with the NF54^{nap} line. Compounds were dissolved in 1x PBS (MMV390048 and CQ) or dimethyl sulfoxide (DMSO, Sigma-Aldrich, USA) (MB and DHA) and diluted fresh for each assay with complete culture medium to achieve a specific final concentration [final DMSO at sublethal concentrations < 0.1 % (v/v)]. The antimalarial drugs underwent 2-fold serial dilutions for a total of 8-9 concentrations in 96-well plates. The final concentration ranges for asexual stage assays were as follows: 100-0.8 nM or 120-0.9 nM MB, 160-1.25 nM or 300-1.17 nM CQ, 160-1.25 nM or 300-1.17 nM MMV390048, and 40-0.31 nM or 100-0.4 nM DHA. The final concentration ranges for stage IV/V gametocyte assays were as follows: 1500-11.7 nM MB, 8 µM - 62.5 nM or 10 µM - 78.1 nM CQ, 2240-17.5 nM MMV00048, and 176-1.4 nM or 200-1.6 nM DHA. The kill control was excess (5 µM) MB and the live cell control contained parasites with culture media. The assays were set up in duplicate or triplicate in a volume

of 200 µL at 1 % haematocrit and 1.5 % parasitaemia (>90 % ring stage) or 0.6-0.8 % gametocytaemia (stage IV/V gametocytes for $NF54^{nap}$). MB activity was also determined at a volume of 60 µL for asexual stage parasites. The plates were incubated for 96 h for asexual stages and 48 h for stage IV/V gametocytes in a gas chamber under hypoxic conditions at 37°C in a stationary incubator. After drug exposure, luciferase activity was determined as described above. Non-linear regression analysis was performed using GraphPad Prism v6.0 (GraphPad Software, Inc., USA) and the determined IC_{50} values were compared to existing data for assay validation. Assay quality was also evaluated in the asexual stages and stage IV/V gametocytes for signal-to-background (S/B) and signal-to-noise (S/N) ratio, Z'-factor and inter-assay reproducibility via % coefficient of variation (%CV) [66, 112].

Chapter 3: Results

3.1 Identification of constitutively expressed genes in *P. falciparum*

To create transgenic parasite lines that constitutively express luciferase as a reporter in all life cycle stages of *P. falciparum*, constitutively expressed genes first needed to be identified. DNA microarray and RNAseq expression profile datasets [103, 104, 108] were probed to identify constitutive genes based on their expression profiles for ring stages, early and late trophozoites and schizonts, stage I to stage V gametocytes, ookinetes, oocysts, and sporozoites of *P. falciparum* parasites.

K-means clustering was performed on all three datasets to obtain clusters containing maintained or constitutively expressed genes. K-means clustering was previously performed on the microarray dataset by van Biljon *et al.* [108], therefore, these ten clusters were used for analysis (Figure 3.1). Three clusters containing constitutively expressed genes were previously identified by this study [108]. These clusters (6-8) show good expression throughout gametocyte development, consequently, these genes were selected for downstream analysis. Cluster 8 shows genes with an increase in gene expression during gametocyte development, while cluster 6 has a more maintained gene expression profile. Cluster 7 also has a maintained expression profile but has four days showing lower gene expression compared to the other days. Although clusters 1 and 2 also have genes that are maintained throughout development, the genes were not selected as they show a weak expression profile. Furthermore, clusters 3-5 and 9-10 show downregulation or weak expression during gametocyte induction or while gametocytes are developing from stage I to stage V, as such these clusters were also not included.

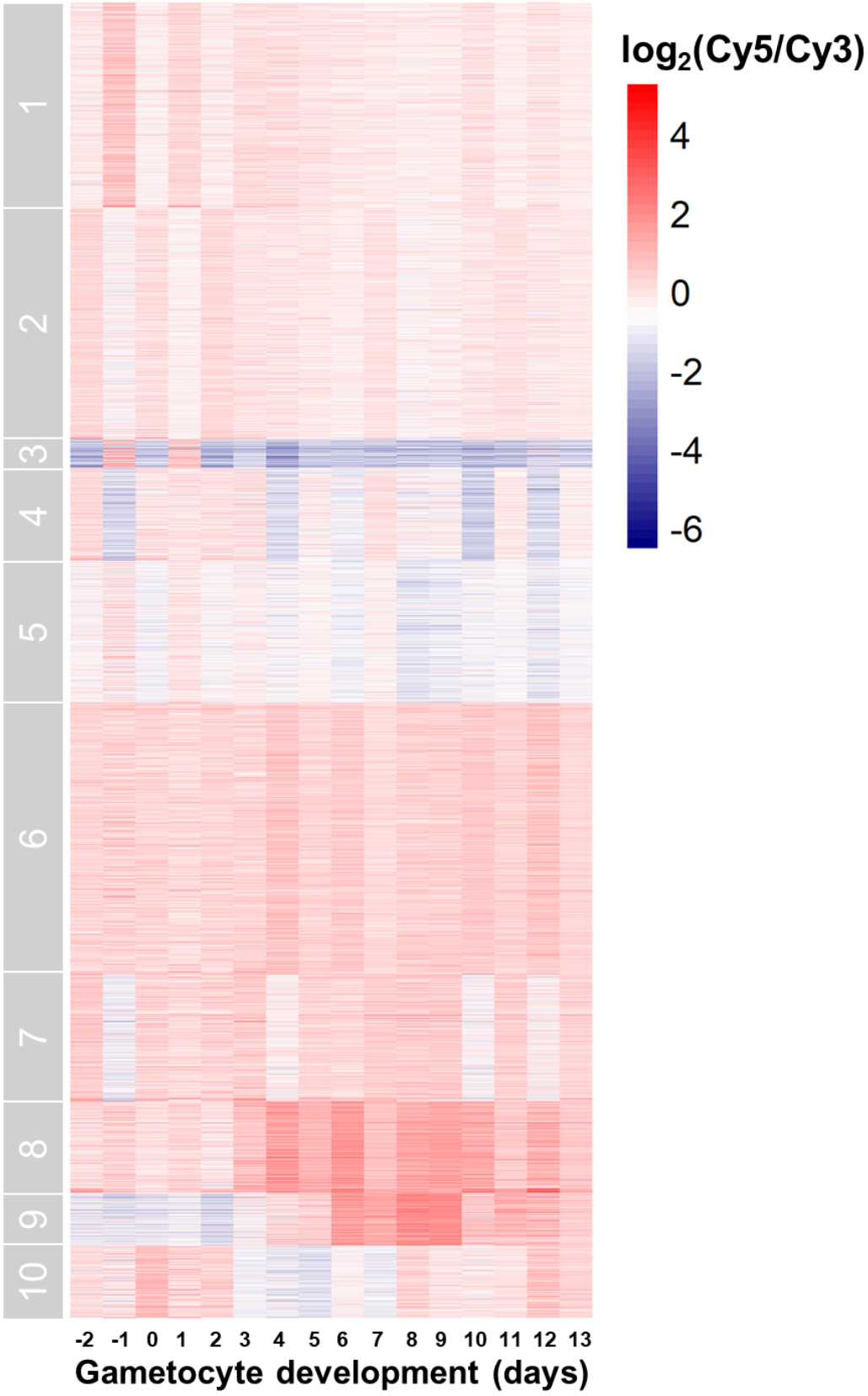

Figure 3.1: K-means clustering of gametocyte development expression profiles.
The gene expression profiles and clustering were obtained from a microarray dataset of van Biljon *et al.* [108]. K-means clustering (10 clusters) with the gene expression profiles during gametocyte development of *P. falciparum* parasites from day -2 to 13, with day 0 being gametocyte induction day. Gene expression is shown as a $\log_2$(Cy5/Cy3) ratio with blue indicative of low, white indicative of moderate and red indicative of high expression. Clusters' 6-8 were used for downstream filtering.

Next, the RNAseq dataset by Lopez *et al.* [103] was also clustered into ten clusters. From these, four clusters were identified to have strong constitutively expressed genes within them, cluster 1, 3, 4 and 5 (Figure 3.2). Although cluster 1 contains genes with weak expression in the asexual stages, there are many genes within the cluster with strong expression profiles throughout the stages. Clusters 4 and 5 show the most promising genes with high and constitutive expression profiles. Although clusters 9 and 10 show genes with constitutive expression, they were not selected for further analysis due to the weak expression profiles of these genes with the majority of expression being ≤ $\log_2(5)$. Furthermore, clusters 6-8 were also removed as they show weak expression overall, especially during the asexual stages.

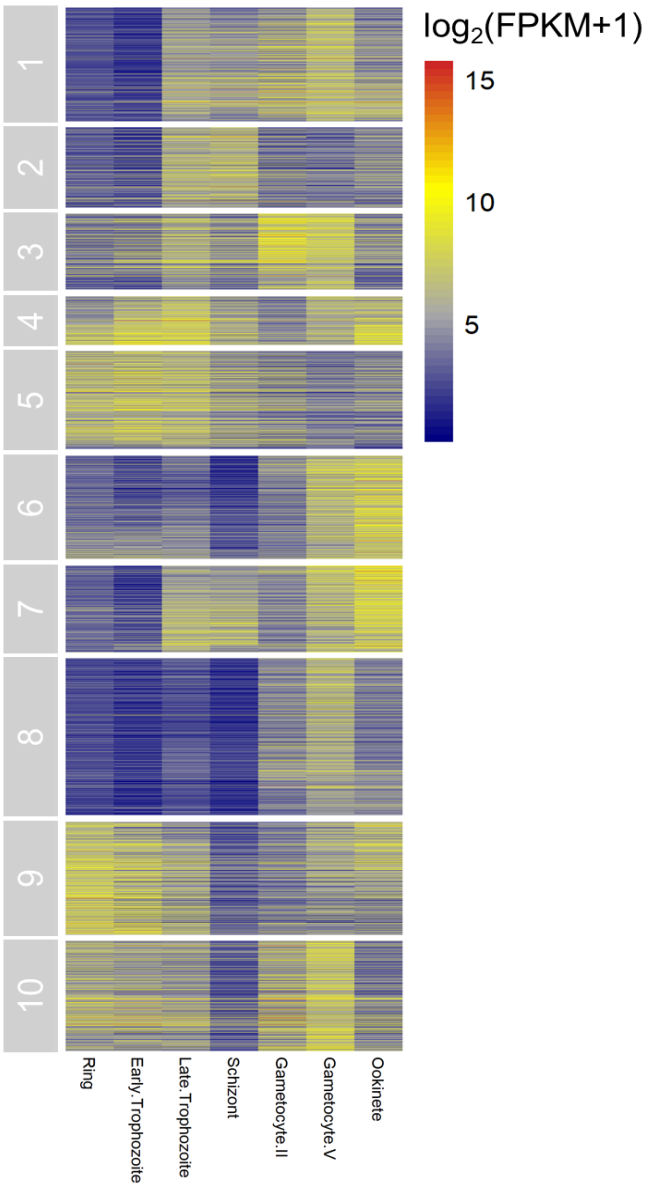

Figure 3.2: K-means clustering of Lopez-Barragan *et al*. RNAseq dataset.
The K-means clustering (10 clusters) of the gene expression profiles for the asexual and sexual stages of *P. falciparum* parasites. Data were taken from previously published RNA sequencing datasets of López-Barragán *et al.* [103]. Gene expression is shown as $\log_2$(FPKM+1) (blue = low, grey to yellow = moderate and orange to red = high expression). Data analysis was performed and heatmaps created on R [107]. Clusters 1, 3-5 were used for downstream filtering.

Lastly, the RNAseq dataset by Zanghi *et al.* [104] was clustered into ten clusters, producing five clusters that potentially have constitutively expressed genes (Figure 3.3). Upon closer examination of the clusters, clusters 1-5 clearly showed the most promising constitutive expression profiles. Although clusters 2, 3 and 5 show weak expression in the sporozoite stages, closer examination shows genes that have strong expression in all three stages. Clusters 1 and 4 show the most promising genes with strong constitutive expression profiles. Clusters 6-10 were removed as they showed weak expression [≤ $\log_2(5)$] in all three stages, especially in the ring stage of the parasite.

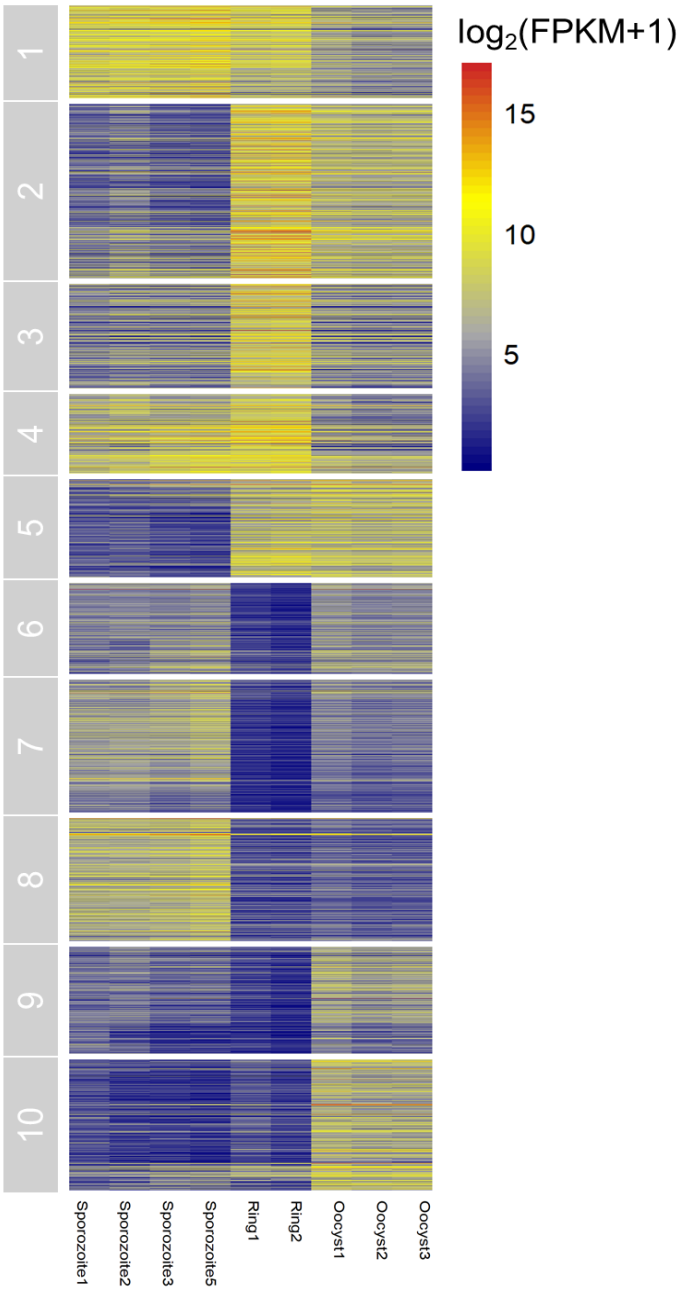

Figure 3.3: K-means clustering of Zanghi *et al*. RNAseq dataset.
K-means clustering (10 clusters) of the gene expression profiles for the sporozoite, ring and oocyst stages of *P. falciparum* parasites. Data were taken from previously published RNA sequencing datasets of Zanghi *et al.* (2-4 replicates are shown) [104]. Gene expression is shown as $\log_2$(FPKM+1) (blue = low, grey to yellow = moderate and orange to red = high expression). Data analysis was performed and heatmaps created on R [107]. Clusters' 1-5 were used for downstream filtering.

The genes within the clusters containing constitutively expressed genes from all the datasets were combined and resulted in the identification of 823 overlapping genes (Figure 3.4). These include genes that were present in the RNAseq data and also in the microarray data. Genes that were shared only in the two RNAseq datasets were excluded, as RNAseq is a more sensitive technique compared to DNA microarray and would pick up low-level RNA being expressed. Since we were attempting to identify constitutively expressed genes which were expressed also at high levels to allow subsequent luciferase detection (implying expression is correlated to strong promoters), we only included genes that were identified in both RNAseq and DNA microarray datasets.

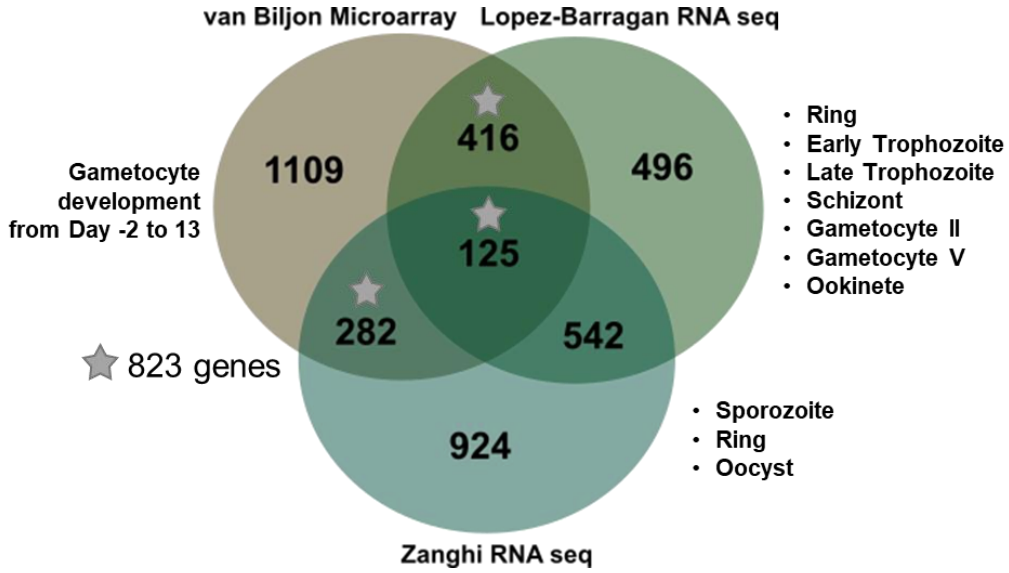

Figure 3.4: Overlapping genes that are maintained or constitutively expressed in three datasets. K-means clustering produced clusters containing maintained or constitutively expressed genes in three datasets. The overlapping genes that were present in the RNAseq data and also in the microarray data identified 823 overlapping genes that were used for downstream filtering.

We subsequently interrogated the essential nature of the 823 constitutively expressed genes, to identify important genes for parasite survival, which could translate to their continuous expression in different life cycle stages similar to household genes. By using the promoters of these essential genes, we will then potentially have increased insurance of continuous expression of luciferase under these promoters. Essentiality data were obtained from PlasmoGEM [109] for *P. berghei* parasites as knockout studies for *P. falciparum* are limited but more data is in the process of being generated by PlasmoGEM. Genes from *P. berghei* that show homology for *P. falciparum* genes were used for analysis. Genes were classified either as causing slow parasite proliferation, or faster progression or genes that were essential and completely abrogated parasites, or lastly was dispensable. In total, 51 'slow' genes and 102 dispensable genes were removed from the dataset, as these gene promoters might result in less or no luciferase expression while under drug pressure.

This resulted in 671 genes which are either known to be essential or for which essentiality data was not known since essentiality data are limited.

Since *P. falciparum* parasites make use of several mechanisms of post-transcriptional regulation [113], we interrogated the 671 gene set for the presence of genes that were for instance translationally repressed [30] as translationally repressed motifs have been identified in upstream and downstream regulatory regions [113]. This removed a further 102 genes to reduce the gene set to 569. In a second-to-last filtering step, the remaining 569 genes from above were filtered to identify genes with the highest expression profiles, on the assumption that this is correlated to strong promoter action. An FPKM threshold of 100 ($\log_2$ FPKM+1 > 6.64) was used for RNAseq data [103, 104], which drastically reduced the number of genes from 569 to 70. From these 70 genes, only 29 genes were shared between the two RNA sequencing datasets as such these were chosen as the top constitutive genes. A threshold was not set for the microarray dataset [108] since it shows a very narrow gene expression profile for gametocyte development.

To inspect the gene expression profiles, a heatmap was created for the RNAseq datasets (Figure 3.5). From the expression profiles for the top 29 genes, genes can be seen with very high expression throughout the life cycle stages. The four genes (PF3D7_0610400, PF3D7_0617800, PF3D7_1105000 and PF3D7_1105100) with the highest gene expression profiles all encode for histone proteins illustrating the need for transcriptional control throughout the parasite's life cycle. These four genes also showed the highest expression in the microarray dataset. Furthermore, some genes show almost equal expression while others have stronger expression in certain stages compared to other stages, albeit being present throughout (i.e. constitutively expressed). This indicates the importance of specific gene products for specific stages of the parasite's life cycle. Overall the asexual stages had the highest gene expression profiles, particularly associated with the transcriptionally active trophozoite and schizont stages, while the mosquito stages had the lowest gene expression profiles.

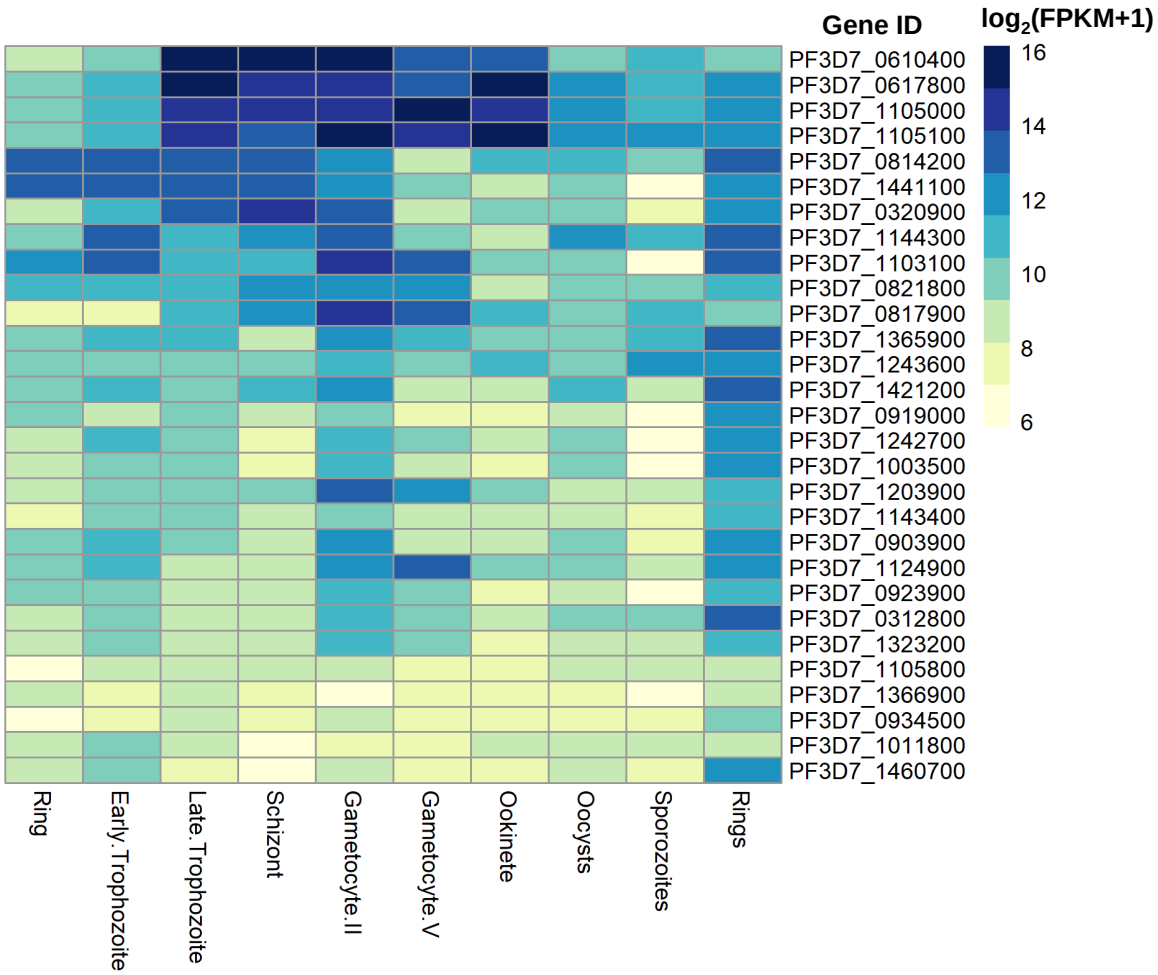

Figure 3.5: Expression profiles of top 29 constitutive genes throughout the parasite's life cycle. The gene expression profiles for the asexual, sexual and mosquito stages of *P. falciparum* parasites for the top constitutive genes. Data was obtained from RNAseq of López-Barragán *et al.* [103] (ring to ookinete stage) and Zanghi *et al.* [104] (oocysts to rings). Gene expression is shown as $\log_2$(FPKM+1) values (cut-off was set at $\log_2$(FPKM+1) > 6.64, therefore, all genes have high expression) with cream indicative of moderate, light blue indicative of high and dark blue indicative of very high expression. Gene ID refers to the PlasmoDB gene number (www.plasmodb.org). Data analysis was performed and heatmaps created in R [107].

Lastly, the differences in gene expression between male and female stage IV/V gametocytes were assessed since genes are not expressed in the same abundance between the two sexes [30]. From this, 14 genes displayed almost equal expression in both sexes of which six genes were selected for cloning as they showed the strongest expression in stage IV/V gametocytes and had known gene products (Table 3.1). These six genes included 3 histone genes (H3, H2A and H4), and 3 genes who's products are involved in protein translation: translation initiation factor 1A (eIF-1A), 60s ribosomal protein L41 and ubiquitin-60s ribosomal protein L40 (ubiq) (Table 3.1). Another gene, the nuclear assembly protein (*nap*, PF3D7_091900) shows a slight bias towards male gametocyte expression (Table 3.1) but was included as it is one of the top constitutive gene

markers. From these seven genes, all except 60s ribosomal protein L41, are essential to parasite survival [114].

Table 3.1: Essentiality phenotypes and transcript abundance of *P. falciparum* gametocytes. Transcript abundance of male and female stage IV/V gametocytes are shown as FPKM values from previously published RNA sequencing data of Lasonder *et al.* [30]. The gene phenotypes are indicative of their essentiality for the parasite [109, 114]. Gene ID refers to the PlasmoDB gene number (www.plasmodb.org) and those in bold refer to the 7 genes selected for further analysis.

Gene ID	Product Description	Male gametocyte	Female gametocyte	Phenotype
PF3D7_0617800	histone H2A	6902,59	9094,48	Essential
PF3D7_0610400	histone H3	3324,25	4657,54	Essential
PF3D7_1105000	histone H4	2479,6	3239,24	Essential
PF3D7_1365900	ubiquitin-60S ribosomal protein L40	1211,86	1330,01	Essential
PF3D7_1144300	60S ribosomal protein L41	954,79	715,32	Unknown
PF3D7_1441100	conserved Plasmodium protein, unknown function	793,66	853,91	Essential
PF3D7_1143400	translation initiation factor eIF-1A, putative	429,61	329,16	Essential
PF3D7_1460700	60S ribosomal protein L27	392,38	484,23	Essential
PF3D7_0919000	nucleosome assembly protein (nap)	384,57	72,55	Essential
PF3D7_0320900	histone H2A.Z	352,26	291,05	Essential
PF3D7_1242700	40S ribosomal protein S17, putative	294,91	336,86	Essential
PF3D7_1003500	40S ribosomal protein S20e, putative	270,75	255,14	Essential
PF3D7_1323200	V-type proton ATPase subunit G, putative	173,82	253,31	Essential
PF3D7_0903900	60S ribosomal protein L32	169,24	244,32	Essential
PF3D7_0923900	polyadenylate-binding protein 2, putative	157,63	175,93	Essential

The RNAseq profiles of previously identified ‘constitutive genes’ were compared to the newly identified constitutive genes. This included *Pfetramp10.3* (PF3D7_1016900) [93], *Pfhsp70* (PF3D7_0818900) [94] and *Pfeef1α* (PF3D7_1357000) [67], which were not part of our gene set as it was filtered out by the constitutive gene cluster in the microarray dataset. These genes were compared to the seven newly identified constitutive genes that were used in cloning of their promoter regions (Figure 3.6). *Pfetramp10.3* and *Pfeef1α* have variable expression profiles between the different life cycle stages. Furthermore, as seen on the graph *Pfetramp10.3* and *Pfeef1α* had gene expression levels below the FPKM threshold of 100 that was set for strong gene expression. Although *Pfhsp70* had high expression, the expression profile was not confirmed as constitutive based on the microarray dataset. All the newly identified genes show constitutive expression in all life cycle stages with the three histone genes having the highest overall expression profile. Although *nap* and *eIF-IA* genes show lower overall expression, in both instances, these genes have the most consistent expression profile over all the life cycle stages, similar to *ubiq*.

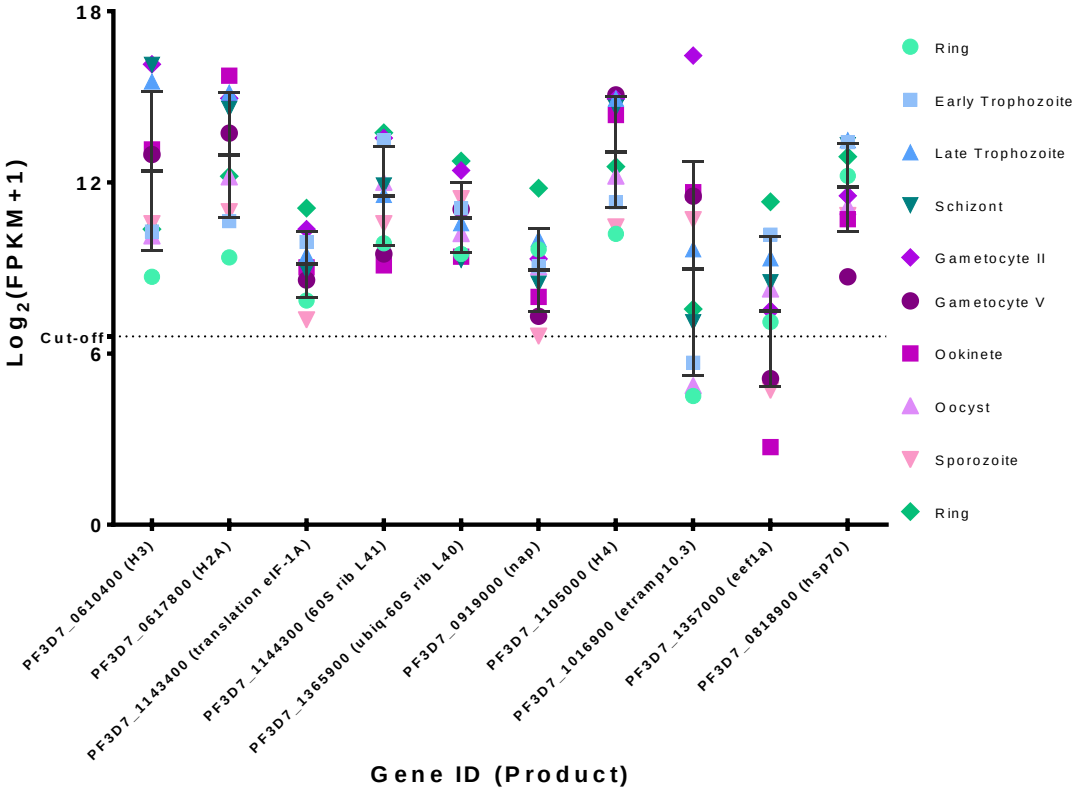

Figure 3.6: Expression profiles for constitutive genes in the *P. falciparum* life cycle.
The RNA expression profiles are shown for the final seven genes that were used to clone a luciferase gene under control of their promoter regions. The three constitutive gene expression controls: *Pfetramp10.3*, *Pfhsp70* and *Pfeef1α,* are shown for comparison. Data for the ring to ookinete stages are from an RNA sequencing dataset of López-Barragán *et al.* [103] and oocyst to ring stages are from Zanghi *et al.* [104]. Gene expression is shown as $\log_2$(FPKM+1) and the cut-off value is an FPKM threshold of 100 ($\log_2$ FPKM+1 > 6.64). The average gene expression with standard deviations is shown for each gene across all the life cycle stages.

3.2 Amplification of promoter regions

The upstream regulatory regions of the identified constitutive gene markers were amplified for cloning upstream of the luciferase gene. The upstream regulatory region is known to contain a promoter region, 5' untranslated region (UTR) and transcription start sites. A previous study has shown that transcription start sites are found within a 1000 nt upstream of the gene's start codon in *Plasmodia* [115]. Although information on the promoter's architecture has been studied [115], the exact sequences are still unknown since the AT-rich genome of the parasite makes identification of AT-rich promoter elements challenging. Therefore, to ensure the promoter regions are present in the regulatory regions amplified, we designed primers that amplify between 1400-1600 nt upstream of the start codon of a gene (Figure 3.7).

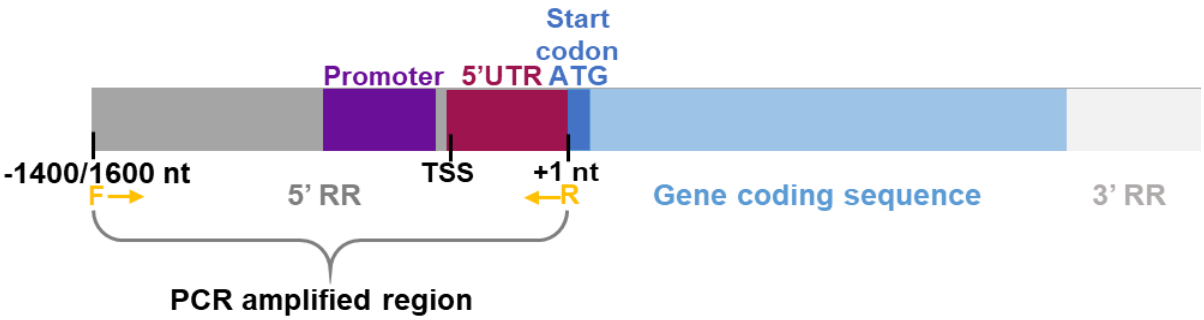

Figure 3.7: Gene map indicative of promoter region PCR amplified for cloning.
The forward (F) and reverse (R) primers were designed to PCR amplify 1400-1600 nucleotides (nt) upstream of the constitutive gene's start codon (ATG) (RR, regulatory region; TSS, transcription start site; UTR, untranslated region).

The promoter regions were amplified from genomic DNA isolated from trophozoite stage NF54 *P. falciparum* parasites. PCR optimisation included changes in annealing temperature and changing extension time and temperature. Annealing at 50°C did result in the required product but also produced numerous misprimed products (Figure 3.8A). This was improved when the annealing temperature was increased to 60°C, with associated specificity of priming, for three of the promoter regions amplified (Figure 3.8A). As such, the remaining two promoter regions were also amplified with an annealing temperature of 60°C (Figure 3.8B). The *nap* promoter region did not require amplification as it was already present in the intermediate plasmid.

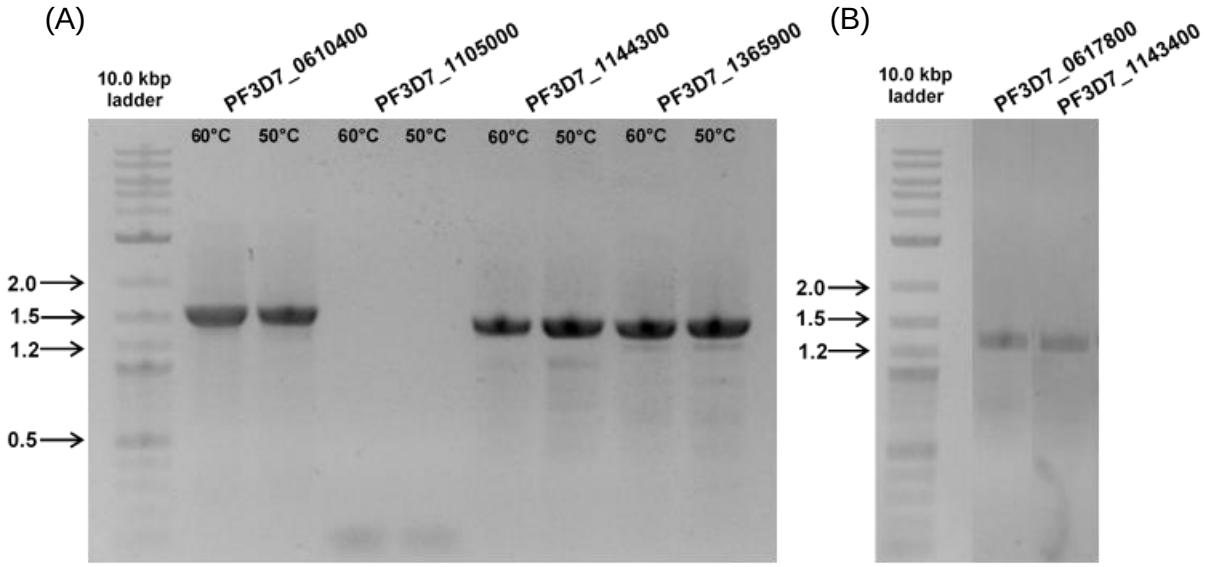

Figure 3.8: PCR amplification of promoter regions for the top constitutive gene markers.
Promoter regions were PCR amplified with genomic DNA from NF54 parasites using primers shown in Table 2.1. PCR conditions had an annealing temperature of (A and B) 60°C or (A) 50°C. The expected promoter region band sizes were obtained for five of the six constitutive markers: 1597 bp (PF3D7_0610400), 1463 bp (PF3D7_0617800), 1480 bp (PF3D7_1143400), 1454 bp (PF3D7_1144300) and 1428 bp (PF3D7_1365900). The PF3D7_1105000 promoter region could not be amplified. NEB quick-load purple 1 kb plus DNA ladder and DNA fragments were separated on a gel and visualised with ethidium bromide staining. (For complete gel picture of Figure 3.8B see supplementary information Figure S1).

The promoter region for PF3D7_1105000 could not be amplified even after numerous optimisation attempts. This promoter region has an AT-content of 89 %, which could explain its refractory amplification, also the primer pair might have produced primer dimers as seen in the two bands at <100bp (Figure 3.8A), therefore, this gene was excluded. DNA bands of the correct size for each remaining promoter were subsequently gel extracted and purified. Purified DNA yielded concentrations between 138-192 ng/µL DNA with A_{260}/A_{280} and A_{260}/A_{230} purity ratios ranging between 1.8-2.1.

3.3 Cloning *H3* and *nap* promoter regions into plasmids

A two-step cloning strategy was followed to obtain the promoters and luciferase gene in the correct arrangement in the final pCR2.1-*attP*-FRT-hDHFR/GFP plasmid needed to enable Bxb1 integrase mediated generation of the transgenic lines (Figure 2.1). As stated before, an intermediate plasmid, pASEX-5'*nap*-myc-CBG99-3'*nap*, was already available in the lab. This plasmid already had the correct click beetle luciferase (CBG99) under control of the *nap* promoter and was used as such to evaluate the *nap* promoter. However, in addition, the amplified *H3* promoter region was exchanged for the *nap* promoter region in this plasmid as the first step in the cloning strategy (Figure 2.1), The pASEX-5'*nap*-myc-CBG99-3'*nap* plasmid (8570 bp) was digested with *Xho*I and *Xma*I (Figure 3.9) to remove the 5' *nap* promoter (1048 bp), followed by gel extraction and purification of the plasmid backbone (7522 bp).

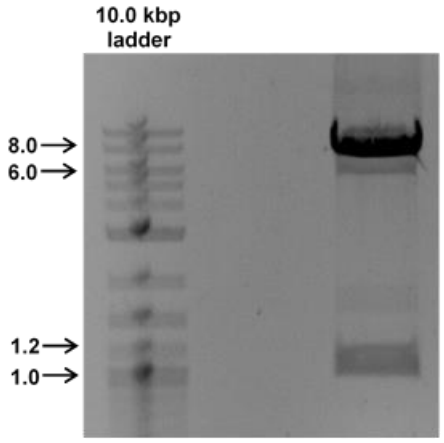

Figure 3.9: Restriction enzyme digestion of pASEX-5'*nap*-myc-CBG99-3'*nap* plasmid.
Restriction enzyme digestion with *Xho*I and *Xma*I of the pASEX-5'*nap*-myc-CBG99-3'*nap* plasmid with expected sizes for digested 7522 bp plasmid backbone and 1048 bp 5' *nap* promoter region. NEB quick-load purple 1 kb plus DNA ladder and DNA fragments were separated on a gel and visualised with ethidium bromide staining.

The promoter region of the *H3* promoter (digested and purified PCR product) was subsequently ligated to the digested pASEX plasmid, and positive clones obtained after colony PCR screening (Supplementary information Figure S2). Subsequently, the pASEX-5'*nap*-myc-CBG99-3'*nap* and

pASEX-5'*H3*-myc-CBG99-3'*nap* were isolated from bacterial cells the identity confirmed with *Xho*I and *Not*I restriction mapping (Figure 3.10). This resulted in cutting of the promoter-CBG99-3'*nap* cassette in each instance, confirming the identity of the plasmids, but also allowing subsequent purification of these cassettes for cloning into the final *attP* transfection plasmid (pCR2.1-*attP*-FRT-hDHFR/GFP). The nap cassette (5'*nap*-myc-CBG99-3'*nap)* was successfully obtained at ~3.1 kb and 5'*H3*-myc-CBG99-3'*nap* cassette at ~3.7 kb (Figure 3.10).

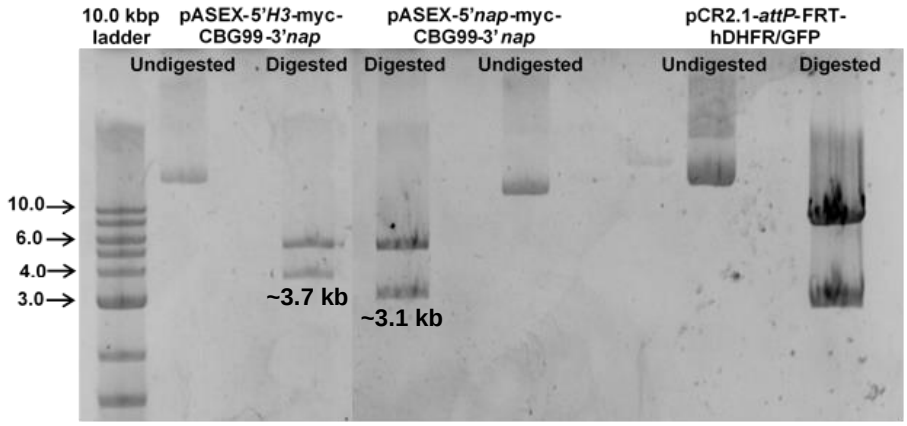

Figure 3.10: Restriction enzyme digestion of pASEX-5'*H3/nap*-myc-CBG99-3'*nap* and pCR2.1-*attP*-FRT-hDHFR/GFP plasmids.
*Xho*I and *Not*I restriction enzyme digestion of the pASEX-5'*H3*-myc-CBG99-3'*nap* (9113 bp), pASEX-5'*nap*-myc-CBG99-3'*nap* (8570 bp), and pCR2.1-*attP*-FRT-hDHFR/GFP (10241 bp) plasmids showed the expected band sizes. Undigested and digested plasmids can be seen on the gel. NEB quick-load purple 1 kb plus DNA ladder and DNA fragments were separated on a gel and visualised with ethidium bromide staining. (For complete gel picture see supplementary information Figure S3).

These cassettes were gel-extracted, purified and ligated to the digested pCR2.1-*attP*-FRT-hDHFR/GFP plasmid backbone (7290 bp, Figure 3.10), which was also cut with the same restriction sites to allow directional, sticky-end cloning. The plasmids were successfully transformed into competent cells as confirmed by colony PCR screening (Supplementary information Figure S4). This resulted in the final plasmids for the *H3* and *nap* promoters: pCR2.1-*attP*-5'*nap*-myc-CBG and pCR2.1-*attP*-5'*H3*-myc-CBG, which were mapped by restriction enzyme digestion as a first evaluation of correct assembly of the plasmids (Figure 3.11). The pCR2.1-*attP*-5'*H3*-myc-CBG plasmid with the *H3* promoter was completely digested with *Xho*I and *Spe*I and gave the expected band sizes on the gel. However, the pCR2.1-*attP*-5'*nap*-myc-CBG plasmid was completely digested with *Spe*I but, based on the restriction enzyme sites on the plasmid (see Figure 2.5A for plasmid map), the *Xho*I enzyme did not digest completely at all the sites resulting in a 6569 bp DNA band instead of just the expected 3855 bp and 2714 bp bands.

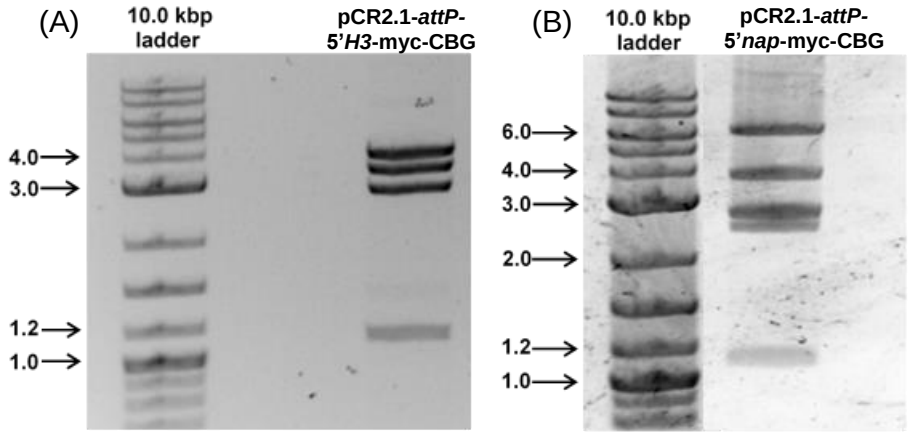

Figure 3.11: Restriction enzyme mapping of final pCR2.1-*attP*-FRT-hDHFR/GFP plasmid clones. Restriction enzyme mapping with *Xho*I and *Spe*I of (A) pCR2.1-*attP*-5'*H3*-myc-CBG showed expected DNA band sizes for complete digestion (3855, 3256, 2776, 1099 bp). (B) However, pCR2.1-*attP*-5'*nap*-myc-CBG showed complete and partial digestion on the gel (6569, 3855, 2776, 2714, 1099 bp). NEB quick-load purple 1 kb plus DNA ladder and DNA fragments were separated on a gel and visualised with ethidium bromide staining. (For complete gel picture of Figure 3.11B see supplementary information Figure S5).

As ultimate confirmation of the correct construction of the above plasmids, the promoter regions and the myc-CBG99 regions were sequenced to ensure the correct sequence was cloned (Figure 3.12). The cloning sites, myc-tag and CBG99 regions, as well as the promoter regions visible, were sequenced correctly. These regions were also in-frame to ensure that CBG99 luciferase will be successfully expressed once integrated into the genome. Successful cloning and construction of the pCR2.1-*attP*-5'*H3*-myc-CBG and pCR2.1-*attP*-5'*nap*-myc-CBG plasmids were therefore achieved for transfection.

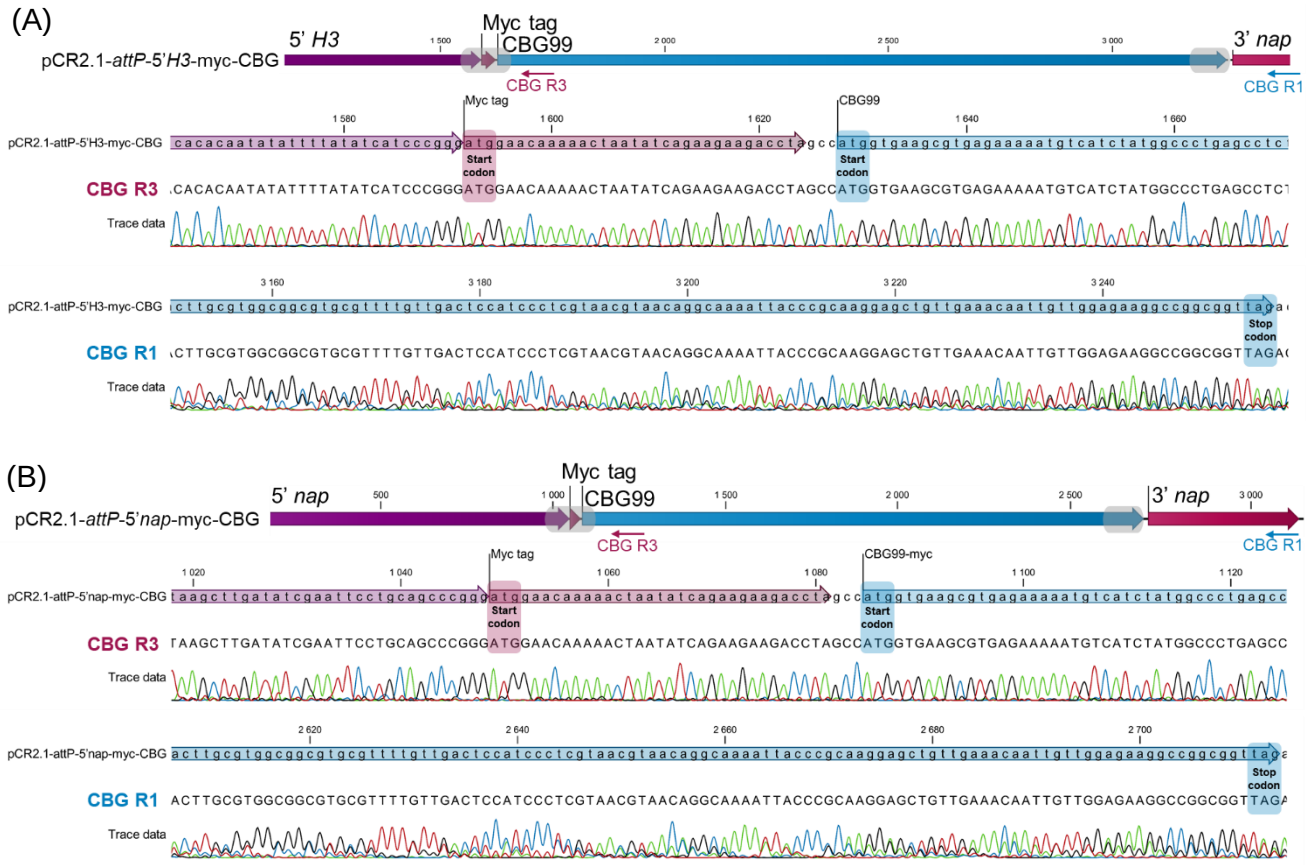

Figure 3.12: Sequencing of final pCR2.1-*attP*-FRT-hDHFR/GFP plasmid clones for the *H3* and *nap* promoters.
Sequencing results are shown for regions in the (A) pCR2.1-*attP*-5'*H3*-myc-CBG and (B) pCR2.1-*attP*-5'*nap*-myc-CBG plasmids consisting of the start and end of the myc-CBG99 luciferase fusion gene. The two different sequencing results are from reverse primers (CBG R1 and CBG R3) as seen in Table 2.2 aligned to the expected reference sequence. The start and stop codons are indicated on the sequences.

3.4 Cloning *H4, eIF-1A, ubiq* and *L41* promoter regions into plasmids

The promoter regions (*H4, eIF-1A, ubiq* and *L41*) that could not be successfully cloned into the intermediate plasmid from their PCR products, were first cloned into pGEM-T Easy vectors via TA-cloning and subsequently subcloned from there. All four promoters were correctly cloned into pGEM-T Easy as seen with colony screening PCR (Figure 3.13). Two bacterial clones were positively screened for each gene, except for PF3D7_0617800.

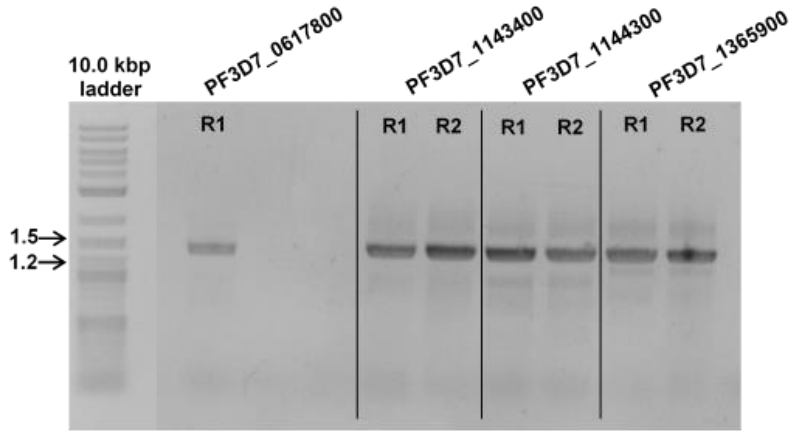

Figure 3.13: PCR screening of pGEM-T Easy vector clones.
Screening of promoter regions cloned into pGEM-T Easy vectors by colony PCR using primers shown in Table 2.1. The expected promoter region band sizes were obtained 1463 bp (PF3D7_0617800), 1480 bp (PF3D7_1143400), 1454 bp (PF3D7_1144300) and 1428 bp (PF3D7_1365900). (R indicates bacterial clone replicates). NEB quick-load purple 1 kb plus DNA ladder and DNA fragments were separated on a gel and visualised with ethidium bromide staining. (For complete gel picture see supplementary information Figure S6).

The promoter regions were digested from pGEM-T Easy with *Xho*I and *Xma*I (Figure 3.14) for restriction enzyme mapping (Figure 3.14) and to subsequently replace the *H3* promoter in the pCR2.1-*attP*-5'*H3*-myc-CBG plasmid. After multiple colony PCR screenings and restriction enzyme mapping of potential clones, only the ubiquitin-60S ribosomal protein (PF3D7_1365900, *ubiq*) promoter could be successfully cloned into the final plasmid.

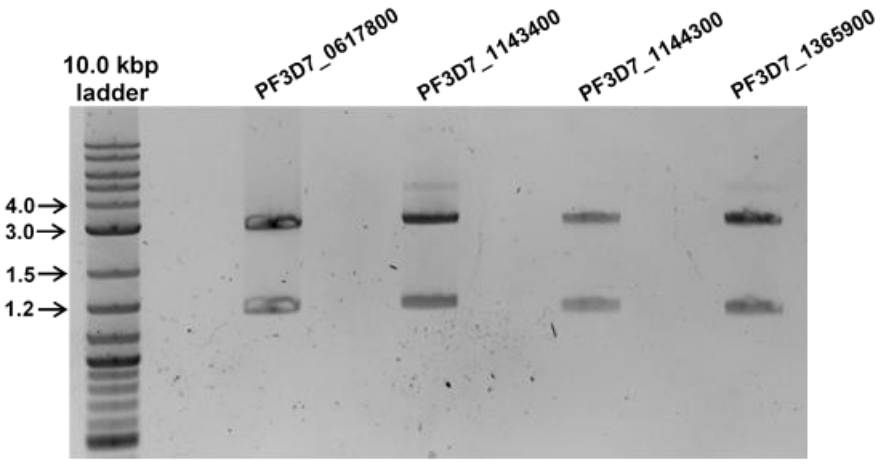

Figure 3.14: Restriction enzyme digestion of pGEM-T Easy vector clones.
Restriction enzyme digestion with *Xho*I and *Xma*I of pGEM-T Easy vector clones showed complete digestion with the expected band sizes: 3015 bp for plasmid backbone and 1463 bp (PF3D7_0617800), 1480 bp (PF3D7_1143400), 1454 bp (PF3D7_1144300) and 1428 bp (PF3D7_1365900) for promoter regions. NEB quick-load purple 1kb plus DNA ladder and DNA fragments were separated on a gel and visualised with ethidium bromide staining.

The pCR2.1-*attP*-5'*ubiq*-myc-CBG plasmid was mapped by restriction enzyme digestion to ensure that the plasmid was correctly assembled (Figure 3.15). The pCR2.1-*attP*-*ubiq*-myc-CBG clone was incompletely digested with *Xho*I and *Xma*I, resulting in faint DNA bands for the small amount of digested plasmid and dark bands for a large amount of undigested plasmid. Partial sequencing of the promoter region (Supplementary information Figure S7) confirmed the successful construction of this plasmid for use in future transfection experiments.

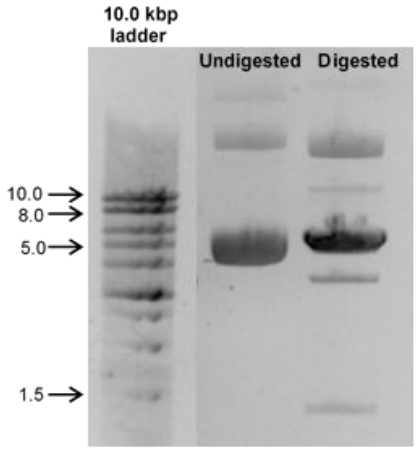

Figure 3.15: Restriction enzyme digestion of pCR2.1-*attP*-5'ubiq-myc-CBG plasmid.
Restriction enzyme mapping with *Xho*I and *Xma*I of pCR2.1-*attP*-5'*ubiq*-myc-CBG showed incomplete digestion as seen by digested (9401 and 1428 bp) and undigested bands in the same lane on the gel. First lane shows undigested plasmid (10.83 kb) in different forms. NEB quick-load purple 1kb plus DNA ladder and DNA fragments were separated on a gel and visualised with ethidium bromide staining.

3.5 Plasmid integration and parasite transfection

The site-specific Bxb1 *attB*-*attP* integration system (Figure 2.8) was used to produce NF54 transgenic reporter lines expressing luciferase under control of constitutive promoters. The pINT plasmid expressed the mycobacteriophage Bxb1 integrase to catalyse the homology-directed recombination between an *attP* site from the promoter-containing pCR2.1 plasmids and a target *attB* site integrated into the *P. falciparum* genome of the NF54^{attB} parasite line [71, 95]. Sequencing of the *attB* site (Figure 3.16) showed no mutations, therefore, transfection with this parasite line could occur.

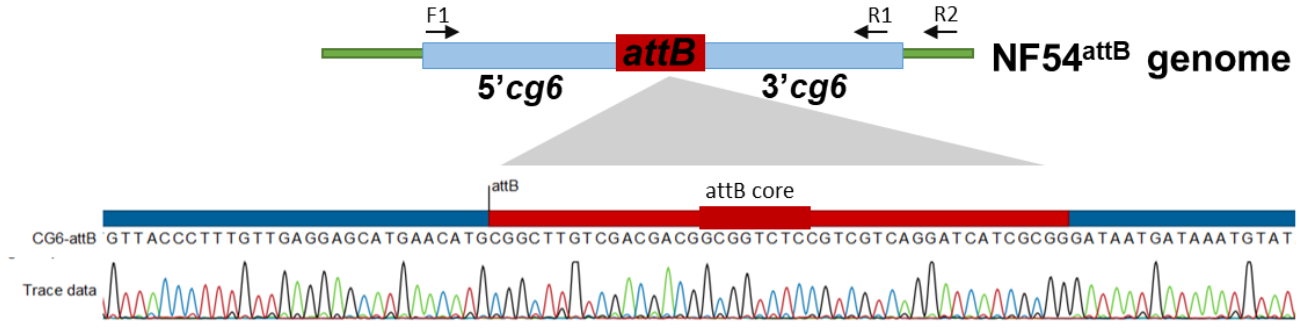

Figure 3.16: Sequencing result of the *attB* site in the NF54^{attB} line before transfection.
The sequence within the *attB* site of the *cg6* gene in NF54^{attB} parasites was sequenced before transfection to ensure integration would be possible. The *attB* site was PCR amplified with forward (F1) and reverse (R1) primers as seen in Table 2.3 and then the PCR product was sequenced with F1.

A double transfection strategy was applied by co-transfecting ring-stage NF54^{attB} parasites with the pINT plasmid and either the pCR2.1-*attP*-5'*nap*-myc-CBG or pCR2.1-*attP*-5'*H3*-myc-CBG plasmid. Large scale plasmid isolation was done from bacterial cells to obtain enough DNA (50-60 µg) for transfection. Positive transfectants were double drug selected with G418 (for pINT plasmid) and WR99210 (for pCR2.1 plasmid) for 6 days followed by 3 days of only WR99210 selection. After drug pressure, parasites could recover in drug-free media and possible recombinant parasites started to appear ~17 days post-transfection. The recovered parasites were PCR screened by amplifying the *attL* (5' integration) and *attR* (3' integration) regions from gDNA of these parasites, which showed integration of the pCR2.1-*attP*-FRT-hDHFR/GFP plasmid for both constructs (Figure 3.17A). The *attB* site was also amplified by PCR and showed that a small portion of wild-type NF54^{attB} parasites was still present in the recovered culture, therefore, the parasites were placed under another round of WR99210 selection for 7 days. After the second round of drug selection, only recombinant parasites (NF54^{H3} and NF54^{nap}) were present (Figure 3.17B).

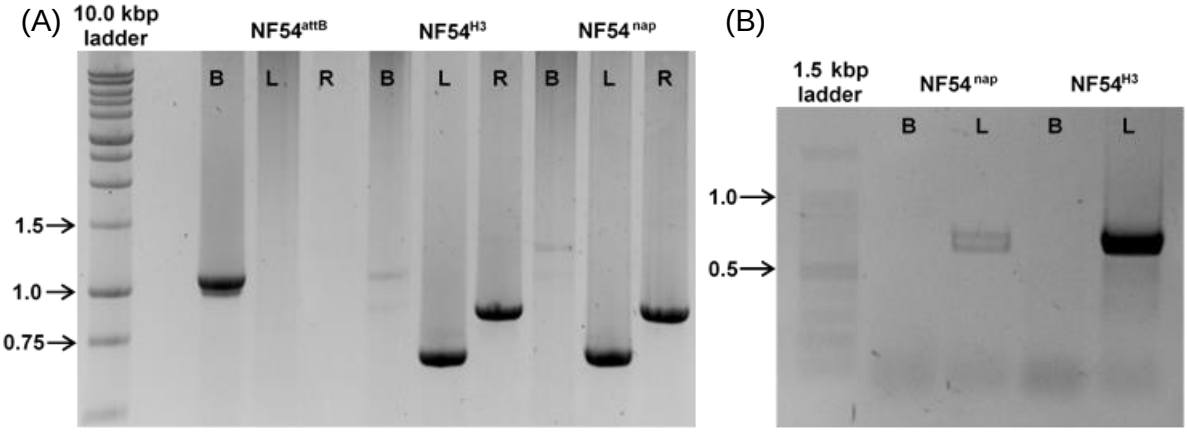

Figure 3.17: Screening of recovered parasites to confirm pCR2.1-*attP* plasmid integration.
(A) After the first round of drug selection, the wild-type NF54^{attB} (control) and two transgenic lines NF54^{H3} and NF54^{nap} were PCR screened for the *attB* (B) sites which would denote wild-type, unintegrated parasites, whilst the presence of both *attL* (L) and *attR* (R) regions will indicate successful integration using primers shown in Table 2.3 and Figure 3.18. The expected DNA band sizes were

obtained on the gels (*attB*: 1100 bp, *attL*: 701 bp and *attR*: 903 bp). (B) After the second round of drug selection, the two transgenic lines NF54^{H3} and NF54^{nap} were PCR screened for the *attB* and *attL* regions. No bands were obtained for the *attB* region as no wild-type parasites were present but the 701 bp *attL* region showed the expected band sizes for the transgenic lines. Promega DNA ladder [(A) 1kb and (B) 100bp] and DNA fragments were separated on a gel and visualised with ethidium bromide staining.

Integration was further confirmed by sequencing of the asymmetric *attL* and *attR* sites in the *cg6* gene of the NF54^{H3} and NF54^{nap} transgenic lines (Figure 3.18). The sequencing results are similar to the expected *attL* and *attR* sequences with the core sequence in both sites remaining the same as the *attB* site. Thus, two transgenic parasite lines NF54^{H3} and NF54^{nap} were successfully created, consequently, the lines were assessed for growth rate, morphology and luciferase expression.

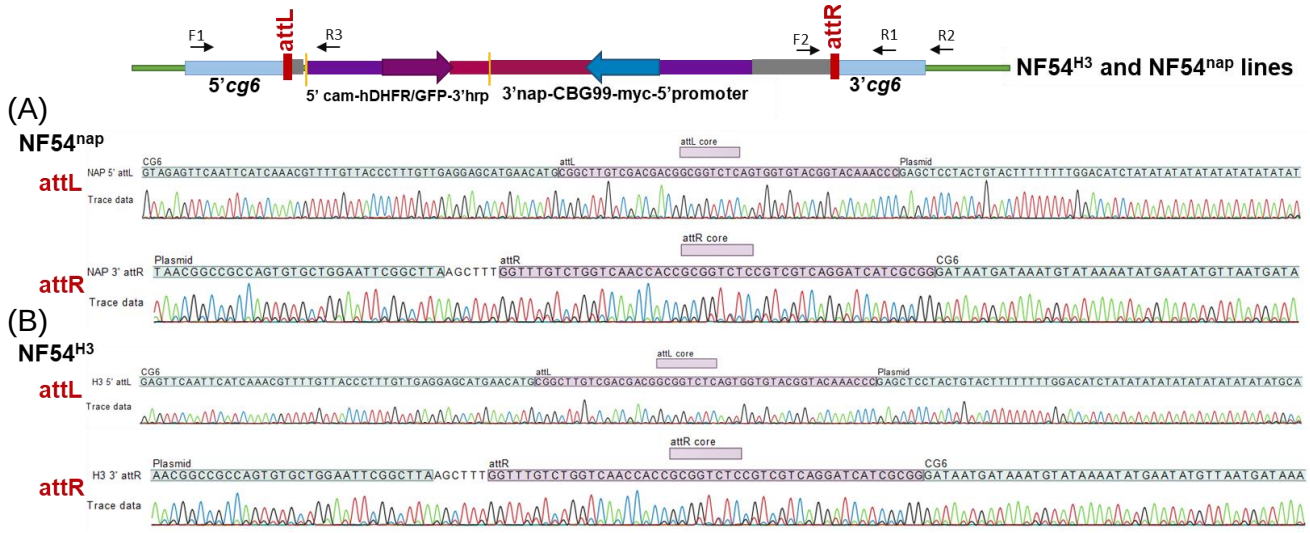

Figure 3.18: Sequencing the integration sites for the NF54^{H3} and NF54^{nap} reporter lines.
The *attB* × *attP* homology-directed recombination produced asymmetric *attL* and *attR* sites, with the core remaining the same, in the (A) NF54^{nap} and (B) NF54^{H3} lines. Primers used for screening and sequencing of transgenic lines are shown on the figure and seen in Table 2.3. The *attL* and *attR* sites were PCR amplified (F1 and R3 for *attL*, and F2 and R1 for *attR*), and then the PCR products were sequenced with the *attL* forward (F1) and *attR* reverse (R1) primers, respectively.

3.6 Analysis of transgenic parasite lines

3.6.1 Growth rate and morphology

The NF54^{H3} and NF54^{nap} transgenic lines were compared to the NF54^{attB} untransfected line as a wild-type control with regards to growth rate and morphology of the parasite in the asexual and sexual stages. The transgenic parasites were visualised (Figure 3.19) by Giemsa-stained light microscopy to evaluate morphology for the intra-erythrocytic asexual stages.

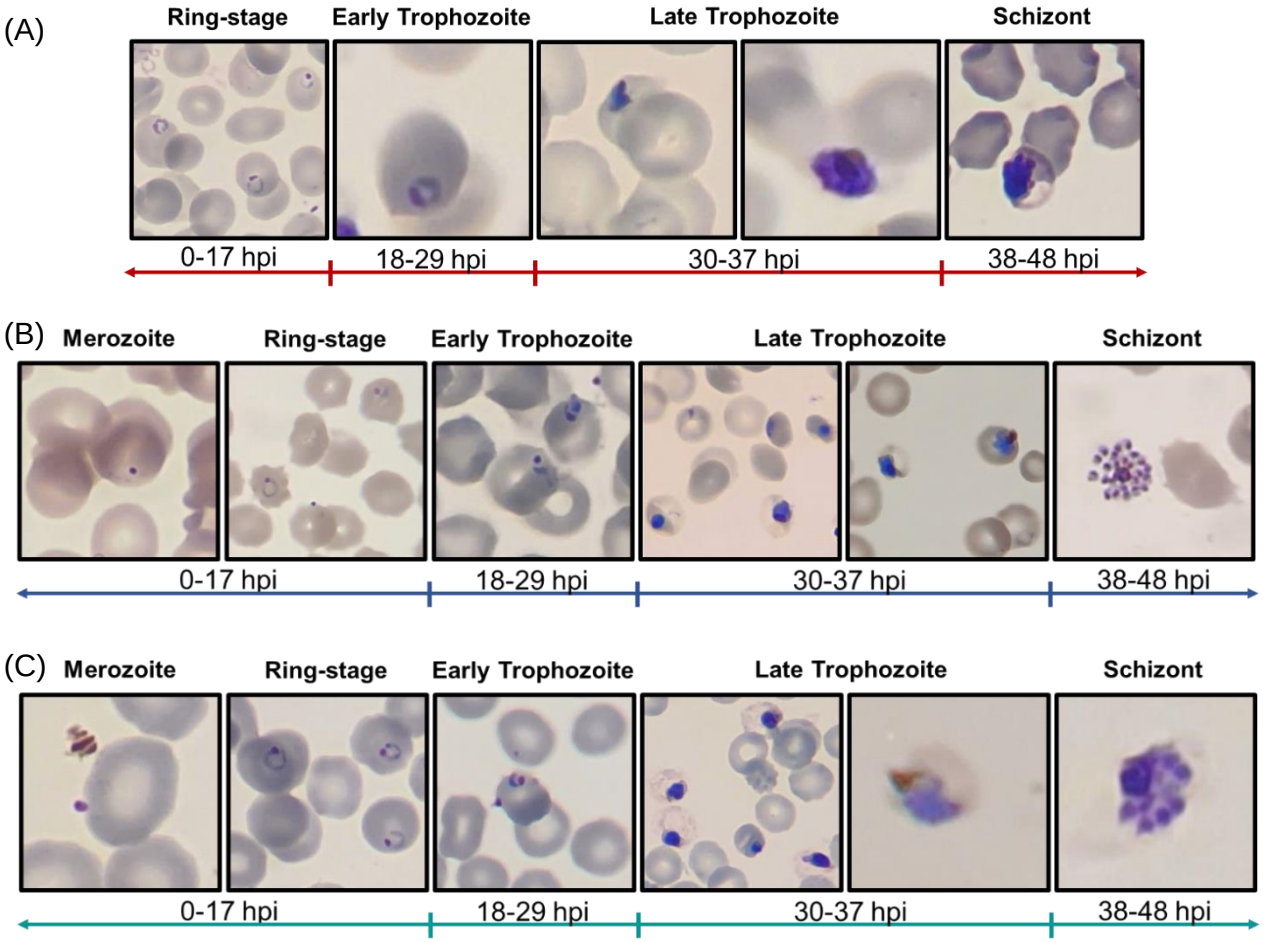

Figure 3.19: Morphological evaluation of transgenic parasites in the asexual stages. Intra-erythrocytic development of (A) NF54^{attB} (wild-type control), (B) NF54^{H3} and (C) NF54^{nap} asexual-stage parasites for the 48-h cycle were visualised by Giemsa-staining under a light microscope at 1000x magnification. After merozoite invasion at 0 hours post invasion (hpi), parasites are seen inside host erythrocytes. Parasites develop into the ring stage between 0-17 hpi as noted by the flat, circular shape. Parasites mature from early (18-29 hpi) to late (30-37 hpi) trophozoites as seen by an increase in the surface area of the cytoplasm due to the breakdown of haemoglobin to form haemozoin crystals that are added to the pigment vacuole. The final schizont stage (38-48 hpi) can be distinguished by a large, dense pigment vacuole and multiple nuclei being present that from merozoites. In early schizont development, (A and C) the merozoites can be seen inside a thin erythrocyte membrane and at the end, (B) the membrane burst open to release merozoites (48 hpi) [116].

The morphology of the NF54^{H3} and NF54^{nap} parasites was similar to the untransfected, wild-type NF54^{attB} parasites for the intra-erythrocytic development and stayed within the 48 h timeframe. Parasitaemia increase was also monitored over a 72 h period by using synchronised ring-stage parasites (Figure 3.20). To avoid human error, only trophozoite stages were counted at 24 and 72 h as they are easily observed under the microscope, whereas ring stages can be missed when counting. Results showed similar fold change increases after one asexual replication cycle between the untransfected and transfected transgenic parasites.

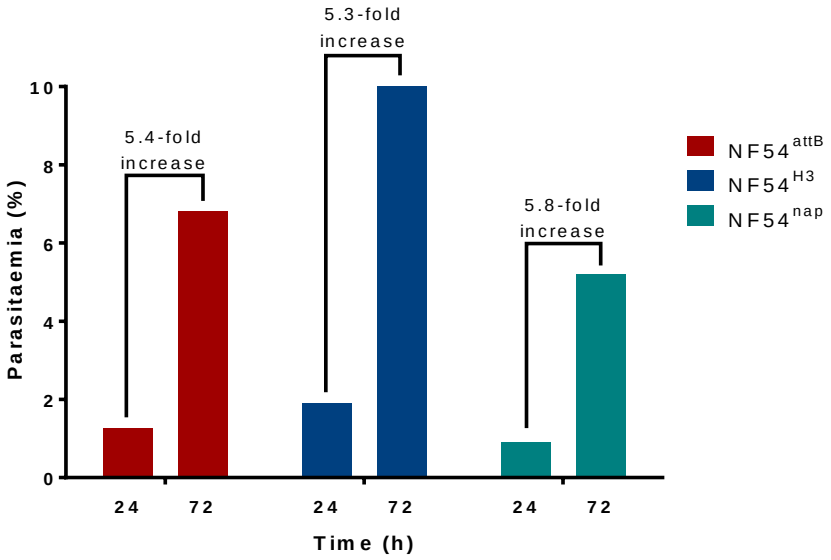

Figure 3.20: Growth rate of NF54^{attB}, NF54^{H3} and NF54^{nap} asexual stage parasites.
Increase in parasitaemia of NF54^{attB} (untransfected control), NF54^{H3} and NF54^{nap} intra-erythrocytic asexual-stage parasites. Synchronised parasites were monitored from ring-stage (0 h) and parasitaemia was determined at 24 and 72 h (trophozoite stages).

Next, parasites were induced to undergo gametocytogenesis, however, after three independent biological repeats, the NF54^{H3} line did not produce gametocytes. Therefore, only the NF54^{nap} parasite line was analysed in the sexual stages for morphology (Figure 3.21).

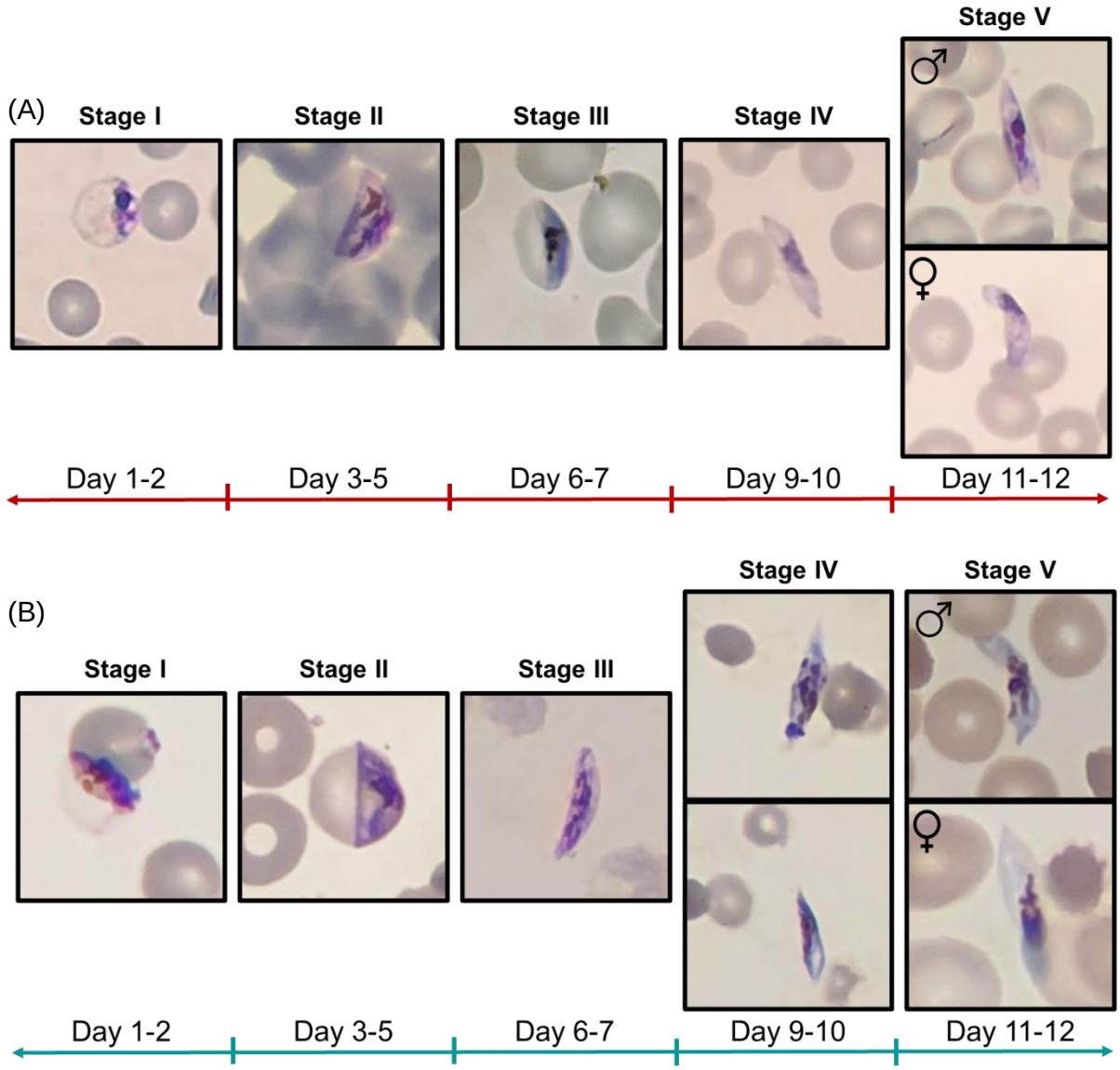

Figure 3.21: Morphological evaluation of NF54^{attB} and NF54^{nap} parasites in the sexual stages. Gametocytogenesis of (A) NF54^{attB} (untransfected wild-type control) and (B) NF54^{nap} parasites were visualised by Giemsa-staining under a light microscope at 1000x magnification. Committed asexual parasites undergo gametocytogenesis from day 1 to day 12 post-induction to develop into five distinct morphological stages. Stage I gametocytes look like trophozoites by having a large cytoplasm surface area. From stage II onwards gametocytes can be easily set apart with elongation of the infected erythrocyte. Stage II gametocytes have a D-shaped cytoplasm and elongate further to form stage III. Stage IV becomes round on both sides with sharp ends and shows a clear distinction between male and female gametocytes, with females having a smaller nucleus and more concentrated pigment pattern. The gametocyte further matures into the transmissible stage V as notable by the round ends and a slight curve.

The development of gametocyte stages for NF54^{nap} as visually inspected corresponded to the untransfected NF54^{attB} parent line in morphology (Figure 3.21) and timeframe of development. NF54^{nap} was further analysed for the amount of gametocytes being produced and the conversion factor (Table 3.2), which is the number of asexual stage parasites that commit to gametocytogenesis.

Table 3.2: Analysis of gametocyte production in sexual stages.
Comparison of gametocytaemia and conversion factor between untransfected (control) and transfected transgenic *P. falciparum* parasite lines. Data are representative of (n) biological replicates, ± SD.

Parasite line	Gametocytaemia [a]	Conversion factor [b]
$NF54^{attB}$ (Control)	1.1 % (n=1)	15 % (n=1)
$NF54^{nap}$	0.6 ± 0.1 % (n=3)	2.3 % (n=1)
$NF54^{H3}$	Not detected (n=3)	-

[a] Day 10 after gametocyte induction

[b] Conversion factor = $\frac{\text{number of stage II gametocytes on day 5}}{\text{number of rings on day 2}}$

The amount $NF54^{nap}$ parasites that committed to sexual development were very low compared to the $NF54^{attB}$ parasites. Based on the analysis, $NF54^{nap}$ parasites are suitable for downstream application in both asexual and sexual stages but $NF54^{H3}$ can only be used in asexual stages.

3.6.2 Prove luciferase expression

Luciferase expression under control of constitutive promoters was confirmed in the newly generated transgenic lines - $NF54^{H3}$ and $NF54^{nap}$. Firstly, the emission kinetics of the CBG99 luciferase was analysed with a mixed population of ring and trophozoite stage parasites to ensure that a stable bioluminescent signal (in RLU) can be obtained within a broad time-frame (Figure 3.22).

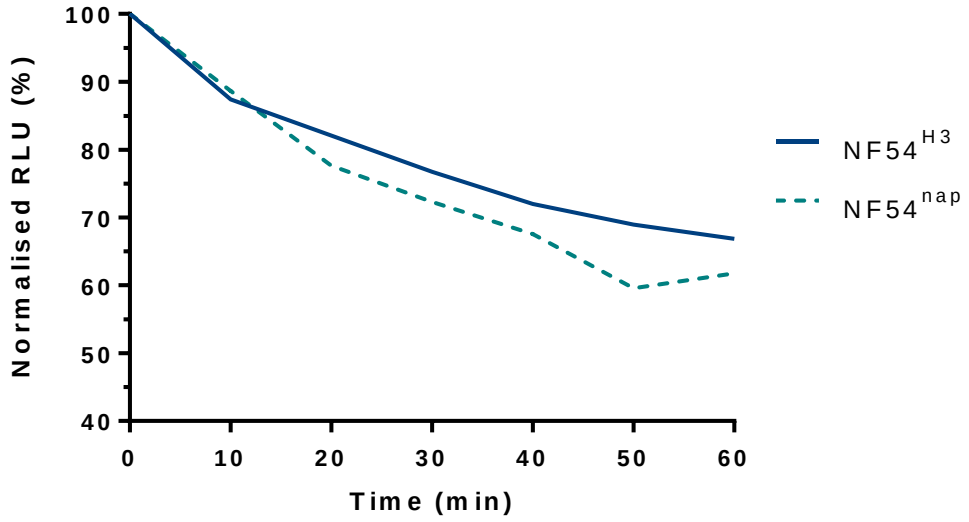

Figure 3.22: Emission kinetics of the CBG99 luciferase over a one-hour time-frame.
The normalised bioluminescent signal in relative light units (RLU) based on CBG99 activity was assessed at 10 min intervals over 1 h for the $NF54^{H3}$ and $NF54^{nap}$ transgenic lines at 6 % parasitaemia (mixed population of rings and trophozoites) and 1 % haematocrit. Data are from one biological replicate, performed in technical triplicates. The highest RLU is set at 100 %. Figure was created using GraphPad Prism 6.0 software.

As seen on the graph, the bioluminescent signal remained relatively stable after one hour, with a signal loss of ~33 % for NF54^{H3} and ~38 % for NF54^{nap}. Notably, within the first 10 min, a time in which a 96-well plate is typically measured, there is a loss of only ~12 % of the initial RLU.

The level of expression of luciferase between the *H3* and *nap* promoters was evaluated next, for expression in asexual stages (Figure 3.23). From this, it is clear that in asexual stages, and as a reflection of the strength of the promoter, the luciferase signal under the *H3* promoter was almost two orders of magnitude stronger compared to when expressed under the *nap* promoter.

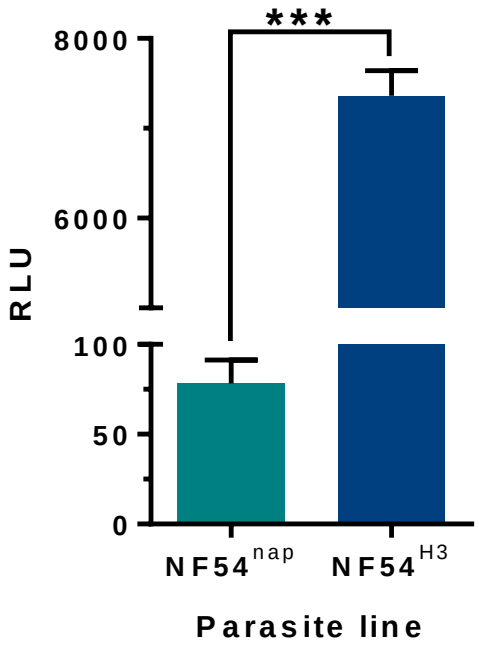

Figure 3.23: Luciferase activity for mixed asexual stage parasites.
The bioluminescent signal based on CBG99 luciferase activity for NF54^{H3} and NF54^{nap} was measured at 1 % parasitaemia for mixed asexual stages consisting of rings, trophozoites and schizonts (1 % haematocrit). Data are from 2-3 biological replicates, performed in technical triplicates, mean ± SEM. (RLU, relative luminescence unit). An unpaired t-test was performed to determine statistical significance between the different parasite lines (*** = P<0.001). Figure was created using GraphPad Prism 6.0 software.

Subsequently, the stage-specific expression of luciferase was evaluated for the parasite stages during asexual development (ring and trophozoite stages) for both NF54^{H3} and NF54^{nap} as well as for stage IV/V gametocytes for the NF54^{nap} line (Figure 3.24).

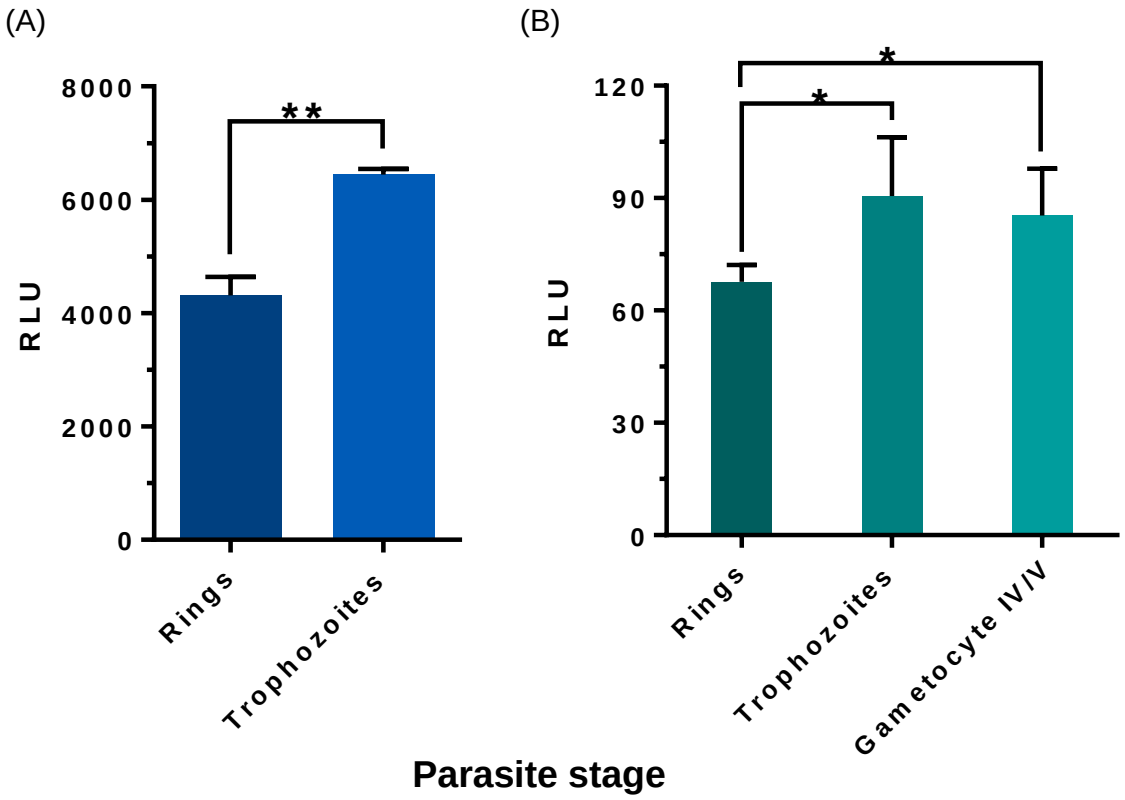

Figure 3.24: Luciferase activity at different life cycle stages of the parasite.
The bioluminescent signal based on CBG99 luciferase activity for (A) NF54^{H3} and (B) NF54^{nap} was measured at 1 % parasitaemia for asexual stages and 0.8 % gametocytaemia for stage IV/V gametocytes (1 % haematocrit in 200 µL). Ring stages = 70-75 % rings and trophozoite stages = 70-95 % trophozoites. Data are from 2-3 biological replicates, performed in technical triplicates, mean ± SEM. Unpaired t-tests were performed to determine statistical significance between the different parasite stages, where not indicated the stages are not significantly different (* = P<0.05; ** = P<0.01). (RLU, relative luminescence unit). Figures were created using GraphPad Prism 6.0 software.

In the NF54^{H3} line, luciferase was detectable in both rings and trophozoite stages, albeit trophozoites at a significantly higher level compared to rings (n=3, P<0.01, unpaired student t-test). This same profile was observed for NF54^{nap} line, with significantly higher luciferase expression observed in trophozoites (n=2-3, P<0.05, unpaired student t-test). However, luciferase expression was also present in the NF54^{nap} line in stage IV/V gametocytes, similar to that observed in trophozoites. The latter provides confidence in the use of the NF54^{nap} line to evaluate luciferase expression in asexual and gametocyte stages of *P. falciparum*.

3.6.3 Evaluation of the lines for plate-reader signal detection of luciferase

To use the NF54^{H3} and NF54^{nap} lines in a plate-reader format to detect luciferase activity, several parameters were evaluated to influence luciferase readout, including parasitaemia, haematocrit and inoculum volume. Firstly, the correlation between luciferase activity and asexual parasitaemia was evaluated for both lines. Mixed ring- and trophozoite-stage parasite samples were diluted into

1, 2 and 3 % parasitaemia and the bioluminescent signal was measured (Figure 3.25). Both the NF54^{H3} and NF54^{nap} parasite lines showed a linear relationship (R^2=0.98) between parasitaemia and bioluminescent signal, with increased parasitaemia resulting in a similar fold-increase in RLU.

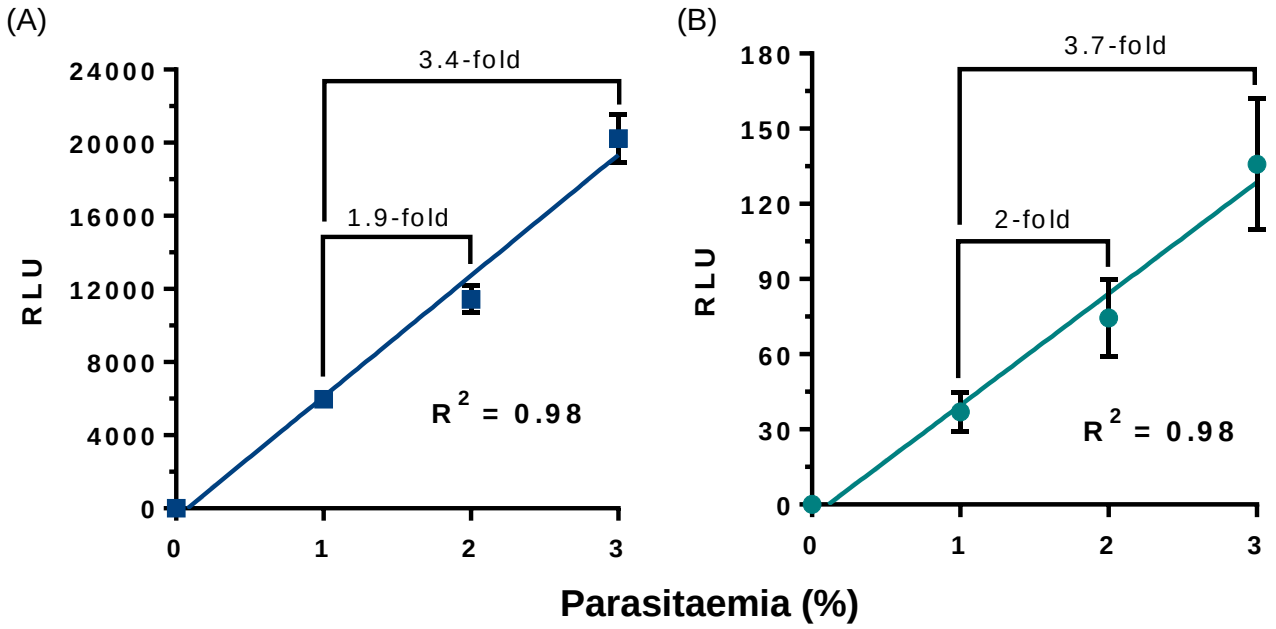

Figure 3.25: Correlation of luciferase activity with parasitaemia.
The bioluminescent signal based on CBG99 luciferase activity for (A) NF54^{H3} and (B) NF54^{nap} was measured at 1, 2 and 3 % parasitaemia and 1 % haematocrit in 200 µL. Data are from three biological replicates, performed in technical triplicates, mean ± SEM. The linear correlation (R^2) and fold change increases are shown on each graph. (RLU, relative luminescence unit). Figures were created using GraphPad Prism 6.0 software.

Next, the haematocrit was evaluated at 1 and 2 % using a mixed population of parasites, at a constant 2 % parasitaemia (Figure 3.26). Increased haematocrit would have the advantage of higher numbers of parasites present (even at constant parasitaemia) but could interfere with assay readout. Although the 2 % haematocrit gave a higher bioluminescent signal, this increase was not significant (n=2, P>0.05, unpaired student t-test) for the NF54^{nap} line, possibly due to the smaller margin of luciferase expression above background. Therefore, a 1 % haematocrit was used for subsequent experiments.

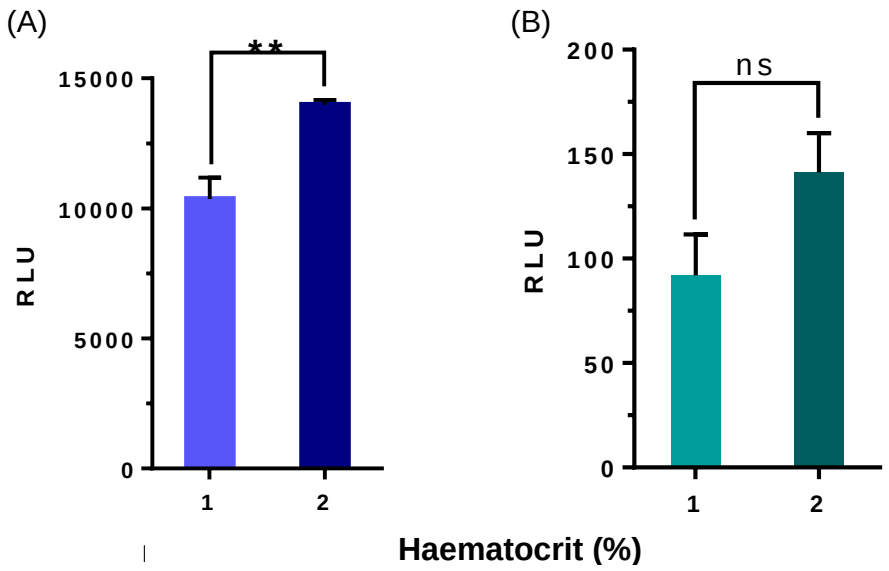

Figure 3.26: Bioluminescent signal using different haematocrits.
The bioluminescent signal based on CBG99 luciferase activity for (A) NF54^{H3} and (B) NF54^{nap} was measured at 1/2 % haematocrit and 2 % parasitaemia in 200 µL. Data are from 2 biological replicates, performed in technical triplicates, mean ± SEM. An unpaired t-test was performed to determine statistical significance between the different haematocrits (ns, not significant; ** = P<0.01). (RLU, relative luminescence unit). Figures were created using GraphPad Prism 6.0 software.

Lastly, different volumes were also evaluated for assay setup to detect signal at 200 µL for a standard 96-well plate and also at 60 µL for a 384-well plate for higher throughput assays (Figure 3.27).

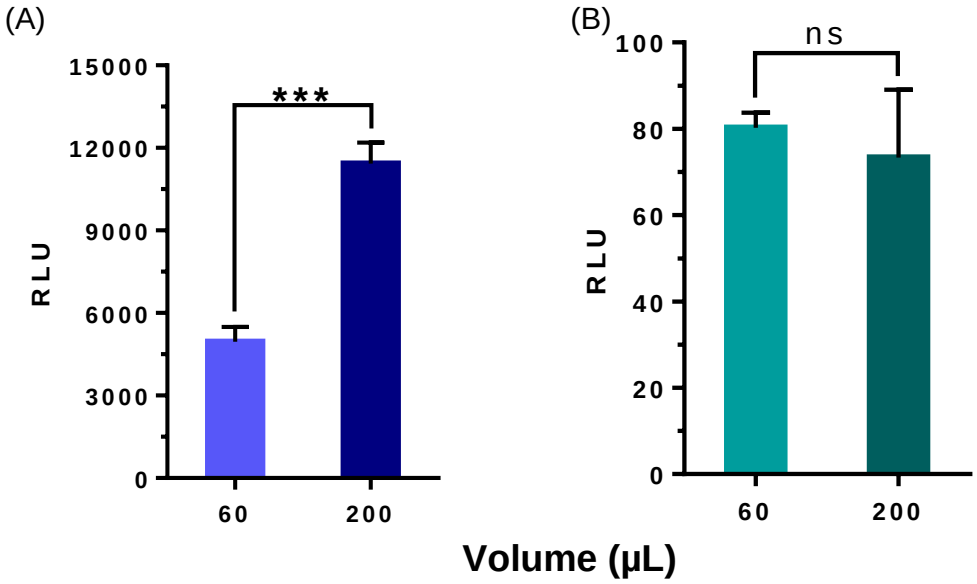

Figure 3.27: Bioluminescent signal at different volumes for assay setup.
The bioluminescent signal based on CBG99 luciferase activity for (A) NF54^{H3} and (B) NF54^{nap} was measured at 2 % parasitaemia and 1 % haematocrit in 60 µL and 200 µL. Data are from three biological replicates, performed in technical triplicates, mean ± SEM. An unpaired t-test was performed to determine statistical significance between the different volumes (ns, not significant; *** = P<0.001). (RLU, relative luminescence unit). Figures were created using GraphPad Prism 6.0 software.

Both volumes for the NF54^{H3} line provided detectable signal, with the expected increased signal obtained with increased inoculum volume. However, for the NF54^{nap} line, there was no significant difference between inocula (n=3, P>0.05, unpaired student t-test).

3.7 Validate the use of the lines to determine drug efficacy through the luciferase assay

Finally, the two new luciferase-expressing lines NF54^{H3} and NF54^{nap} were used to determine their efficacy in detecting antimalarial drug activity. Assay performance and quality were evaluated in the asexual stages and stage IV/V gametocytes for detection range, Z'-factor and inter-assay reproducibility via %CV (Table 3.3) [66].

Table 3.3: Performance indicators of the luciferase assay for NF54^{H3} and NF54^{nap}.
The luciferase assay was performed after 96 h drug exposure for asexual stages and 48 h drug exposure for stage IV/V gametocytes (0.6-0.8 % gametocytaemia). The assay performance parameters were determined for data from 2-4 biological replicates performed in technical triplicates.

Assay performance parameters	Asexual stages (avg ± SD)		Stage IV/V gametocyte (avg ± SD)
	NF54^{H3}	NF54^{nap}	NF54^{nap}
Signal of live cell control (RLU)	100230 ± 31970	3354.6 ± 827.7	214.8 ± 23.7
Background signal (RLU)	74.1 ± 10.7	74.02 ± 6.25	71.93 ± 11.15
S/B	1367.3 ± 161.4	45.2 ± 12.2	3.00 ± 0.26
S/N	10551.2 ± 4056.7	366.3 ± 219.2	14.4 ± 4.9
Z'-factor	0.10 - 0.46	0.02 - 0.59	0.19 - 0.57
%CV for no-drug control	32 %	24 %	11 %

The NF54^{H3} line showed a wide dynamic range based on S/B and S/N values and high bioluminescent signal indicative of strong luciferase expression. The NF54^{nap} line showed a smaller dynamic range for asexual stages but still good enough to distinguish signal from noise. The luciferase assay with the NF54^{nap} line allowed quantification of 0.6-0.8 % late stage IV/V gametocytes showing that the luciferase expression is strong enough for signal detection and with further optimisation of gametocyte production and assay setup the signal could improve. However, both lines show poor reproducibility with low Z'-factors between different assays due to the large variation in bioluminescent signal for the control samples. The %CV between independent experiments was relatively high, with NF54^{H3} showing the highest variation making data slightly inconsistent within an assay plate thereby contributing to the poor Z'-factors. These variations in signal during the plate reading might be because no stabilisers or enhancers are present during the assay as is the case with standard luciferase kits.

The two lines were further evaluated for their ability to accurately determine the IC_{50} of four compounds with known activity against asexual stage parasites, including MB, CQ, MMV390048 and DHA (Figure 3.28).

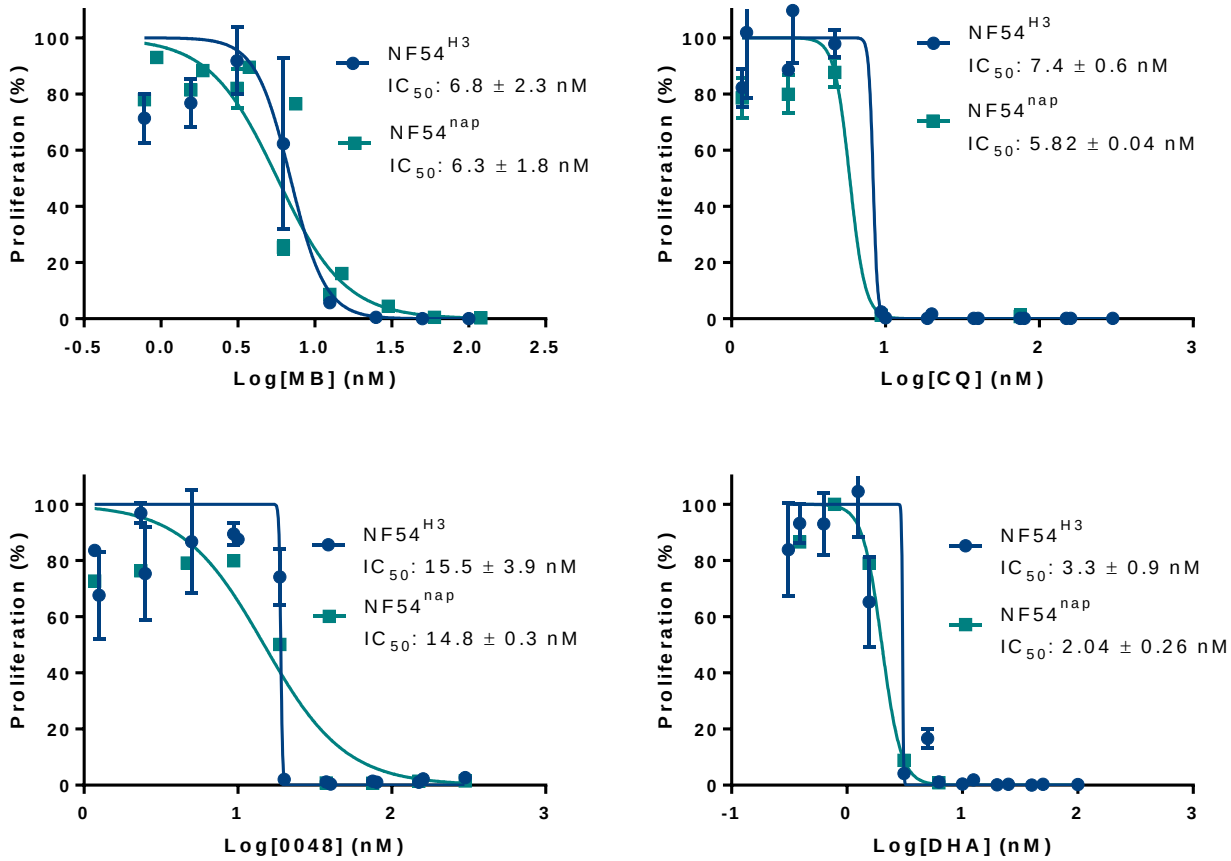

Figure 3.28: IC_{50} values for intra-erythrocytic asexual stage $NF54^{H3}$ and $NF54^{nap}$ parasites. The luciferase assay was performed after 96 h of drug exposure with methylene blue (MB), chloroquine (CQ), MMV390048 (0048) and dihydroartemisinin (DHA). Data are from 2-4 biological replicates, performed in technical duplicates/triplicates, ± SEM. Figures were created using GraphPad Prism 6.0 software.

Both lines reported low nM activities for all four compounds, similar to previously published values [45, 60, 71, 72] indicating these lines are suitable for asexual stage drug assays. Also, $NF54^{nap}$ gave less variation in the IC_{50} values and smaller standard deviations compared to $NF54^{H3}$. However, the hill slope of all the drugs on the $NF54^{H3}$ line is extraordinarily steep, indicating that these parasites are very sensitive to changes in drug concentration. The lines were further evaluated to accurately determine IC_{50} values of MB at 200 µL for a standard 96-well plate and 60 µL for a 384-well plate (Figure 3.29).

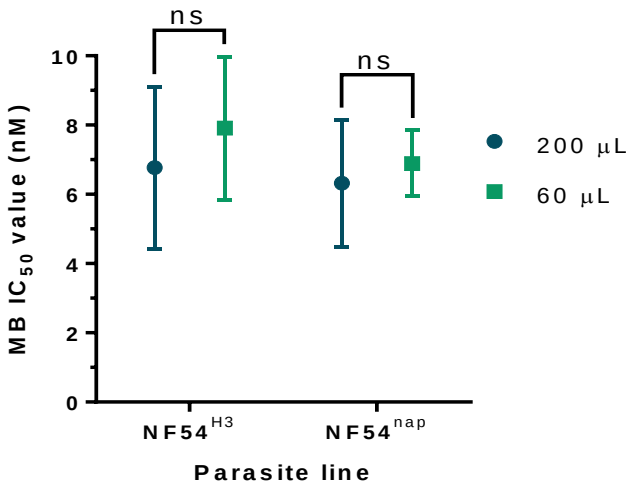

Figure 3.29: Methylene blue IC_{50} values at different volumes for intra-erythrocytic asexual stages.
The luciferase assay was performed with $NF54^{H3}$ and $NF54^{nap}$ after 96 h of drug exposure with methylene blue (MB) in 200 µL and 60 µL volumes. Data are from 4 biological replicates, performed in technical duplicates/triplicates, ± SEM. An unpaired t-test was performed and showed no significant difference (ns) between the 200 µL and 60 µL volumes for MB. Figure was created using GraphPad Prism 6.0 software.

The IC_{50} values for MB showed no significant difference (n=4, P>0.05, unpaired student t-test) between the 200 µL and 60 µL volumes and produced accurate IC_{50} values indicating that the bioluminescent signal is detectable at small volumes required for higher-throughput formats than 96-well plates.

The $NF54^{nap}$ line was further evaluated to accurately determine the IC_{50} of the four compounds against the late stage IV/V gametocytes (Figure 3.30). CQ and DHA failed to produce sigmoidal curves. CQ is known not to be active against late stage gametocytes [45, 50, 69, 71], while DHA produce the expected nM IC_{50} although the curve shape is flat. By contrast, MB and MMV390048 did produce sigmoidal curves. However, the error bars are large and the assay has poor reproducibility, thereby compromising the accuracy of the IC_{50} values.

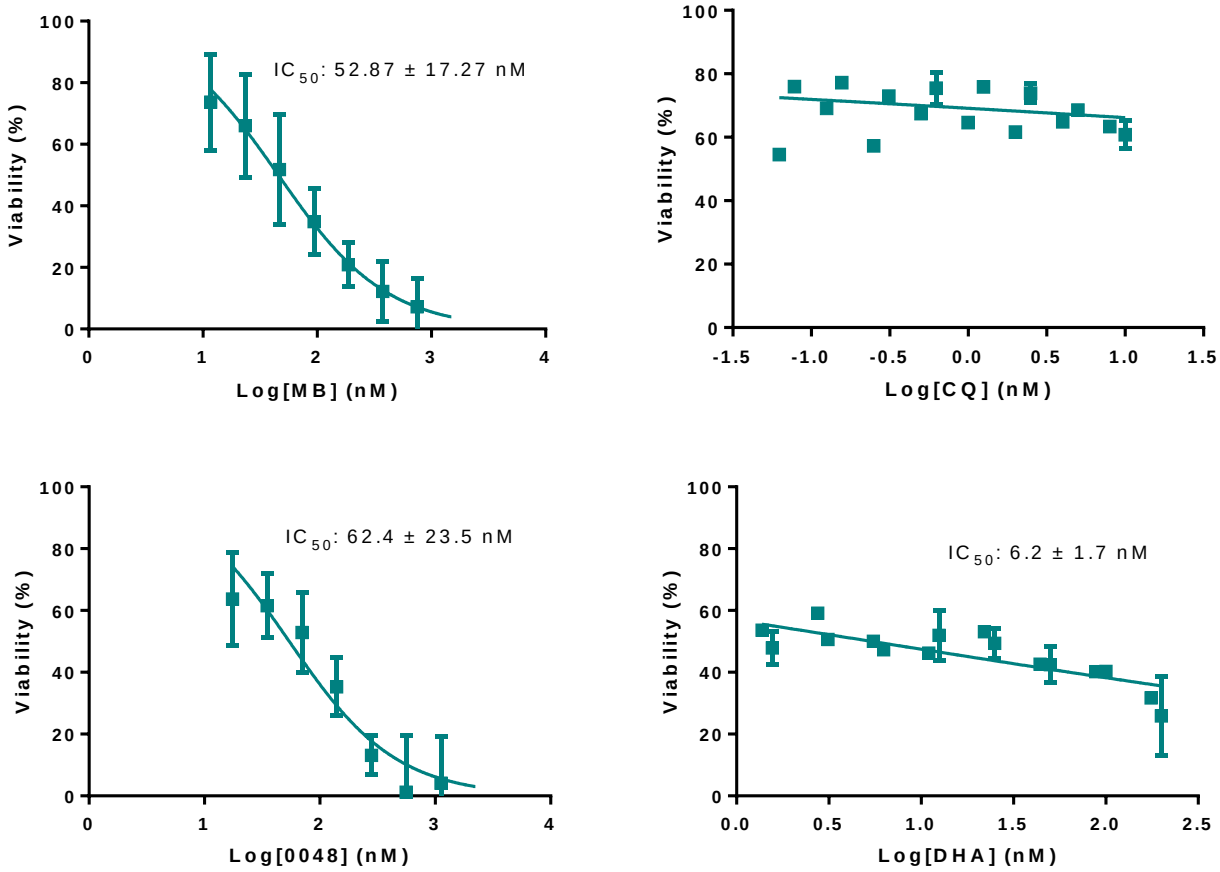

Figure 3.30: IC_{50} values for late stage IV/V gametocytes of $NF54^{nap}$ parasites.
The luciferase assay was performed after 48 h of drug exposure with methylene blue (MB), chloroquine (CQ), MMV390048 (0048) and dihydroartemisinin (DHA). Data are from three biological replicates, performed in technical triplicates, ± SEM. Figures were created using GraphPad Prism 6.0 software.

The IC_{50} against the late stage IV/V gametocytes were further compared to previously published luciferase assay data (Table 3.4).

Table 3.4: IC_{50} values for $NF54^{nap}$ in late stage IV/V gametocytes.
The luciferase assay was performed after 48 h of drug exposure with methylene blue, chloroquine, MMV390048 and dihydroartemisinin. Data are from three biological replicates, performed in technical triplicates, ± SEM. Comparison IC_{50} data are from previously published luciferase assays [50, 72, 117].

Compounds	IC_{50} (mean ± SEM)	Previously published IC_{50} (mean)
Methylene blue	52.87 ± 17.27 nM	143 nM [50]
Chloroquine	Not determined	>20 µM [117]
MMV390048	62.4 ± 23.5 nM	140 nM [72]
Dihydroartemisinin	6.2 ± 1.7 nM	11 nM [50]

CQ showed the poorest potency similar to published data. DHA, MB and MMV390048 showed low nM activity against the sexual stages and a stronger activity than previously published data [60, 71, 72]. As such $NF54^{nap}$ could determine IC_{50} values of known antimalarial compounds in asexual and gametocyte stages of the parasite but with poor accuracy.

Chapter 4: Discussion

Antimalarial drug resistance elevates the need for novel compounds that not only resist resistance formation but also block transmission of the parasite between humans and mosquitoes. Drug discovery is a long process, therefore, it would be helpful to compare drug assay results of similar screening libraries from different laboratories. Furthermore, classifying the TCP of novel compounds is important to find compounds that target the disease-causing asexual stage, the transmissible stage V gametocytes or downstream stages of the parasite. However, TCP identification and standardisation of drug assays are complicated by the fact that each stage of the parasite requires a different assay platform due to biochemical differences in the cell types, thereby creating variability in IC_{50} data. In this study we aimed to develop a constitutive luciferase-expressing *P. falciparum* line to evaluate the efficacy of potential antiplasmodial compounds on a single assay platform across all life cycle stages of the parasite, thereby providing less variability in data. To achieve our aim, we had to find constitutive promoters based on gene expression data that can drive the constitutive luciferase expression. These promoter regions were then cloned into expression plasmids for transfection into the *P. falciparum* $NF54^{attB}$ parasite line to generate our transgenic lines. The newly developed transgenic $NF54^{H3}$ and $NF54^{nap}$ parasite lines were evaluated for their ability to detect antiplasmodial activity in the parasite. Our results show that $NF54^{nap}$ allows direct comparison between the asexual stages and stage IV/V gametocytes by determining drug activity on a single luciferase reporter assay platform.

As part of our study, genes were identified that are constitutively expressed across all life cycle stages of the *P. falciparum* parasite, including asexual, sexual and mosquito stages. Previous studies focused on the promoters for *Pfetramp10.3* [93], *Pfhsp70* [94], and *Pfeef1α* [67] to produce constitutive reporter expression. However, our stringent data analysis revealed novel gene markers to consider for constitutive reporter expression studies. Although we used the promoter regions of these constitutive genes there is no assurance that luciferase expression will behave the same since the transcription factor binding sites within promoter regions are not accurate predictors of gene expression [118]. Furthermore, the regulation of gene expression in *Plasmodium* is still not clearly understood and no well-defined promoters have been identified [119]. In contrast to eukaryotes, transcription factor binding to gene promoters is not the only control of transcription implying that other mechanisms are also important for gene expression [118, 119]. Existing knowledge shows epigenetic and post-transcriptional regulation is important throughout the parasite's life cycle [118], coinciding with our top constitutive gene markers that express proteins involved in chromatin structure regulation (histone H3, histone H2A, histone H4, and nap) and translation (translation initiation factor eIF-1A, 60S ribosomal protein L41, and ubiquitin-60S

ribosomal protein L40). From these top gene markers, the promoter regions for *histone H3* (PF3D7_0610400) and *nap* (PF3D7_0919000) were used to drive luciferase reporter expression. Previous research has attempted to knockout the *histone H3* [109] and *nap* [120] gene without any success indicating the essentiality of these genes for parasite survival.

The NF54^{nap} parasite line expresses the luciferase reporter gene under control of the 5' and 3' UTR of the *nap* gene. An earlier study detected GFP reporter expression in the asexual, sexual and mosquito stages of the parasite using the same UTRs [119], agreeing with our data that showed luciferase expression in the asexual stages and stage IV/V gametocytes. Furthermore, it was shown that the 5' UTR of *nap* drives gene expression regardless of the 3' UTR [119], therefore, the 5' UTR of *histone H3* was combined with the 3' UTR of *nap* to drive luciferase expression. The strength of gene expression for *histone H3* and *nap* agrees with the amount of luciferase being expressed under control of their respective promoter regions in the parasite. The *histone H3* gene shows stronger gene expression compared to *nap*, similar to what is seen with bioluminescence signal intensity in the asexual stages. As the luciferase is constitutively expressed throughout the stages, parasite samples have to be pure to give accurate results for stage-specific studies. Since the parasite controls the expression of these constitutive genes as needed and for different stages, luciferase expression will be controlled in the same way. This might explain why there are variations in the bioluminescence signal for the same parasite stage between different days of measurements. Nonetheless, the data is reliable since these variations are removed by the controls in each experiment.

The transgenic NF54^{H3} and NF54^{nap} parasite lines were created by using the Bxb1 integrase-mediated *attB* × *attP* recombination system [95]. Homology-directed recombination occurred between the *attP* site in the pCR2.1-*attP* plasmid and the *attB* site in the dispensable *cg6* gene to integrate the expression plasmid into the genome of NF54^{attB} [95]. The parasite's genome is a good fit for this Bxb1 system since its AT-rich genome shows no detectable homology to the GC-rich *attB* and *attP* sites [95]. Another advantage of this system is that the recombination event produces asymmetric *attL* and *attR* sites that are not prone to excision by Bxb1 integrase [95]. Previous studies have shown that the disrupted *cg6* gene does not compromise parasite development in the asexual and gametocyte stages [87, 95]. The FLIRT sites that were introduced into the genome was not used in this study but allows for FLP-mediated DNA integration, rearrangement or excision at the FLIRT sites [121] to, for instance, remove the hDHFR resistance marker to prevent potential interference with drug experiments.

NF54^{H3} and NF54^{nap} show comparable growth for asexual stages to the NF54^{attB} wild-type parental line, however, differences are seen for the sexual stages as NF54^{H3} does not produce gametocytes

and NF54^{nap} produces a low number of gametocytes. These results coincide with previous research that showed clones derived from the same isolate differed in their gametocyte production ability [122]. Furthermore, studies have shown that parasites gradually lose their ability to produce gametocytes due to continuous *in vitro* culturing of asexual stage parasites [123]. Since transgenic parasites were continuously cultured during drug selection and screening for over a month, it could have resulted in their reduced ability to produce gametocytes. Therefore, NF54^{H3} parasites can only be used for asexual stage experiments. However, NF54^{nap} parasites are suitable for asexual and sexual stage experiments since gametocytes are detectable and quantifiable by bioluminescence signal.

Since commercially available bioluminescence kits contain lysing components, ATP and other additives to enhance and stabilise the bioluminescence signal, an artefactual signal is produced by treated parasites [79]. To overcome this, a non-lysing D-luciferin substrate was used that requires endogenous ATP to reliably reflect the viability of parasites, at a reduced cost and incubation time [79]. The D-luciferin formulation has previously been optimised to enter cells in other eukaryotic and prokaryotic systems without lysing of cells [79, 124]. Therefore, the bioluminescence signal is lower when the D-luciferin substrate is used, explaining the narrow dynamic range and low signal intensity of the luciferase assays for NF54^{nap}. However, NF54^{H3} has a wide dynamic range due to its strong luciferase expression under the *histone H3* promoter. The reliability to show parasite viability using only D-luciferin substrate can be seen in the linear relationship between the bioluminescence signal intensity and parasitaemia. Another advantage of using a non-lysing substrate is the potential to visualise live parasites at a single-cell level by bioluminescence imaging, which is rare in the malaria parasite [79]. Furthermore, live bioluminescence imaging could allow monitoring of constitutively luciferase-expressing parasites while they interact with host tissues and cells to determine how different cell types affect parasite viability in *in vitro* and *ex vivo* environments [79].

The two transgenic *P. falciparum* parasite lines express a myc-tagged luciferase fusion under the constitutive *histone H3* or *nap* promoter. A luciferase reporter was used instead of a GFP since bioluminescence is easier to measure and less expensive [67]. The CBG99 luciferase reporter was used, as it previously showed to produce the strongest bioluminescence signal compared to other luciferases under control of the same promoter [79]. Although we did not utilise the myc-tag in this study it allows future work to make use of the tag by antibody detection for visualisation under a microscope, western blots, and flow cytometry. The luciferase reporter assay was detectable at a small volume (60 µL) for higher throughput assays and validated with MB for asexual stages, thereby, reducing the number of parasites per well, decreasing assay cost and increasing throughput of the assay [86]. The robustness of the luciferase assay for NF54^{H3} and NF54^{nap} was

low, which is in contrast to previous data [79] that showed good reproducibility. The CBG99 luciferase is known to have a half-life of more than five hours at 37°C [79], which is in contrast to our results that show 33-38 % reduction in the bioluminescence signal after one hour and with drug assay a reduction of ~55 % was seen after only 15 min of plate reading. After incubating the parasites with drugs at 37°C, the assay plates are handled at room temperature for bioluminescence measurements, which could explain the acceleration of the luciferase's half-life. Furthermore, no enhancers or stabilisers are present in the luciferase assay to stabilise the bioluminescence signal, however, to optimise and improve assay reproducibility these additives might have to be considered for future experiments.

Since luciferase activity for NF54^{H3} and NF54^{nap} correlates with parasite numbers, the luciferase activity can be measured between treated and control samples. As such the IC_{50} values of known antimalarial compounds MB, CQ, MMV390048, and DHA were determined to confirm the accuracy of the luciferase assay when using NF54^{H3} and NF54^{nap}. Antiplasmodial activity against the asexual stage parasites was found to be below 20 nM for all four compounds, agreeing with previous data that show these compounds have TCP-1 activity [45, 60, 71, 72]. Since NF54^{H3} is unable to produce gametocytes, this line can only be used to determine antiplasmodial activity against asexual stage parasites. Furthermore, low nM antiplasmodial TCP-5 activity against stage IV/V gametocytes with NF54^{nap} was confirmed for DHA, MB and MMV390048, and the low potency of CQ was also shown [45, 60, 71, 72]. NF54^{nap} showed stronger antiplasmodial activity for all four compounds compared to previous data, indicating that the line might be more sensitive to drug exposure. As such, more compounds with known activity will have to be screened to determine if the line produces false-positive antiplasmodial hits. Nevertheless, NF54^{nap} can determine antiplasmodial activity against the asexual stages and stage IV/V gametocytes on a single assay platform. Thereby, contributing to the discovery of novel antiplasmodial compounds and identifying compounds with TCP-1 activity, TCP-5 activity or both.

Chapter 5: Conclusion

This research aimed to develop a *P. falciparum* line constitutively expressing luciferase across all life cycle stages of the parasite to evaluate antiplasmodial efficacy of compounds on a single assay platform. Constitutive promoters were identified, after stringent analysis of gene expression profiles, to control constitutive luciferase expression in the parasite. The knowledge of luciferase expression under the *histone H3* and *nap* promoters can be useful for future generation of transgenic lines with reporter expression in different stages of the parasite's life cycle. An effective cloning strategy was followed to transfect the expression plasmids into the *P. falciparum* NF54^{attB} parasites. Two transgenic parasite lines were successfully created, namely NF54^{H3} and NF54^{nap}. This research illustrates the effectiveness of the Bxb1 integrase-mediated *attB* × *attP* recombination system to generate transgenic lines, but also raises the concern of gametocyte non-producing parasite lines, like NF54^{H3}. Although luciferase assay quality and reproducibility were variable between drug experiments, IC_{50} data was comparable to previous studies. Optimisation of the luciferase assay is required, by adding additives to the D-luciferin substrate, to stabilise bioluminescence signal during measurements. Nevertheless, NF54^{H3} was able to effectively detect antiplasmodial activity in the asexual stages of the parasite.

NF54^{nap} could detect antiplasmodial activity against the asexual stages and stage IV/V gametocytes, however, the mosquito and liver stages still need confirmation to know whether the line can be used for all life cycle stages. Future work is needed to determine whether the NF54^{nap} line can be used in standard membrane feeding assays (SMFA) to determine drug activity against mosquito stages. Furthermore, the *in vitro* luciferase assay could be used to investigate the dynamics of drug treatment by determining the rate-of-kill of antiplasmodial drugs. The development of the *P. falciparum* NF54^{nap} reporter line allows rapid screening of compounds on a standardised assay platform at different stages of parasite development to discover novel antiplasmodial compounds that are either selective towards a specific stage or active against multiple stages of the parasite. Therefore, NF54^{nap} can be used to identify molecule combinations that fit the TPP-1 criteria, which focuses on case management to treat infected patients, by identifying compounds that can clear asexual blood-stage parasites (TCP-1) and that target gametocytes to block transmission (TCP-5). Thus, compounds can be discovered that will play an important role in malaria elimination by addressing parasite transmission from humans to mosquitoes, while also reducing the risk of resistance development.

References

1 WHO. (2019) World malaria report 2019. Geneva: World Health Organization. Licence: CC BY-NC-SA 3.0 IGO.

2 WHO. (2017) World malaria report 2017. Geneva: World Health Organization. Licence: CC BY-NC-SA 3.0 IGO.

3 White, N. J., Pukrittayakamee, S., Hien, T. T., Faiz, M. A., Mokuolu, O. A. and Dondorp, A. M. (2014) Malaria. Lancet. **383**, 723-735

4 WHO. (2016) Global Technical Strategy for Malaria 2016–2030. Geneva, World Health Organization.

5 Brooke, B., Koekemoer, L., Kruger, P., Urbach, J., Misiani, E. and Coetzee, M. (2013) Malaria vector control in South Africa. South African Medical Journal. **103**, 784-788

6 Phillips, M. A., Burrows, J. N., Manyando, C., van Huijsduijnen, R. H., Van Voorhis, W. C. and Wells, T. N. C. (2017) Malaria. Nature Reviews Disease Primers. **3**, 17050

7 Milner, D. A., Jr. (2018) Malaria Pathogenesis. Cold Spring Harbor Perspectives in Medicine. **8**

8 WHO. (2018) World malaria report 2018. Geneva: World Health Organization. Licence: CC BY-NC-SA 3.0 IGO.

9 Elimination_8. (2015) E8 strategic plan (2015-2020). Elimination 8 Secretariat. Windhoek.

10 Raman, J., Morris, N., Frean, J., Brooke, B., Blumberg, L., Kruger, P., Mabusa, A., Raswiswi, E., Shandukani, B. and Misani, E. (2016) Reviewing South Africa's malaria elimination strategy (2012–2018): progress, challenges and priorities. Malaria Journal. **15**, 438

11 Elimination_8. (2019) SADC Malaria Elimination Eight Inititative: E8 Annual Report 2019. Elimination 8 Secretariat. Windhoek. https://malariaelimination8.org/wp-content/uploads/2020/04/Elimination_8_Annual_Report_2019.pdf.

12 Rabinovich, R. N., Drakeley, C., Djimde, A. A., Hall, B. F., Hay, S. I., Hemingway, J., Kaslow, D. C., Noor, A., Okumu, F., Steketee, R., Tanner, M., Wells, T. N. C., Whittaker, M. A., Winzeler, E. A., Wirth, D. F., Whitfield, K. and Alonso, P. L. (2017) malERA: An updated research agenda for malaria elimination and eradication. PLOS Medicine. **14**, e1002456

13 MalERA Group. (2011) A Research Agenda for Malaria Eradication: Drugs. PLOS Medicine. **8**

14 WHO. (2016) World Malaria Report 2016. ed.)^eds.), World Health Organization, Geneva, Switzerland

15 Lobo, N. F., Achee, N. L., Greico, J. and Collins, F. H. (2018) Modern Vector Control. Cold Spring Harbor Perspectives in Medicine. **8**

16 Ranson, H. (2017) Current and Future Prospects for Preventing Malaria Transmission via the Use of Insecticides. Cold Spring Harbor Perspectives in Medicine. **7**

17 Reddy, M. R., Overgaard, H. J., Abaga, S., Reddy, V. P., Caccone, A., Kiszewski, A. E. and Slotman, M. A. (2011) Outdoor host seeking behaviour of Anopheles gambiae mosquitoes following initiation of malaria vector control on Bioko Island, Equatorial Guinea. Malaria Journal. **10**, 184

18 Rts, S. C. T. P. (2015) Efficacy and safety of RTS,S/AS01 malaria vaccine with or without a booster dose in infants and children in Africa: final results of a phase 3, individually randomised, controlled trial. The Lancet. **386**, 31-45

19 Healer, J., Cowman, A. F., Kaslow, D. C. and Birkett, A. J. (2017) Vaccines to Accelerate Malaria Elimination and Eventual Eradication. Cold Spring Harbor Perspectives in Medicine. **7**

20 Burrows, J. N., Duparc, S., Gutteridge, W. E., Hooft van Huijsduijnen, R., Kaszubska, W., Macintyre, F., Mazzuri, S., Möhrle, J. J. and Wells, T. N. C. (2017) New developments in anti-malarial target candidate and product profiles. Malaria Journal. **16**, 26

21 WHO. (2015) Guidelines for the treatment of malaria, Third edition. Geneva, World Health Organization.

22 CDC. (2017) Malaria Information and Prophylaxis, by Country. Centers for Disease Control and Prevention. **2017**

23 Soulard, V., Bosson-Vanga, H., Lorthiois, A., Roucher, C., Franetich, J. F., Zanghi, G., Bordessoulles, M., Tefit, M., Thellier, M., Morosan, S., Le Naour, G., Capron, F., Suemizu, H., Snounou, G., Moreno-Sabater, A. and Mazier, D. (2015) *Plasmodium falciparum* full life cycle and *Plasmodium ovale* liver stages in humanized mice. Nature Communications. **6**, 7690

24 Bannister, L. and Mitchell, G. (2003) The ins, outs and roundabouts of malaria. Trends in Parasitology. **19**, 209-213

25 Josling, G. A. and Llinas, M. (2015) Sexual development in *Plasmodium* parasites: knowing when it's time to commit. Nature Reviews Microbiology. **13**

26 Ruecker, A., Mathias, D. K., Straschil, U., Churcher, T. S., Dinglasan, R. R., Leroy, D., Sinden, R. E. and Delves, M. J. (2014) A Male and Female Gametocyte Functional Viability Assay To Identify Biologically Relevant Malaria Transmission-Blocking Drugs. Antimicrobial Agents and Chemotherapy. **58**, 7292-7302

27 Kuehn, A. and Pradel, G. (2010) The Coming-Out of Malaria Gametocytes. Journal of Biomedicine and Biotechnology. **2010**

28 Guttery, D. S., Holder, A. A. and Tewari, R. (2012) Sexual Development in *Plasmodium*: Lessons from Functional Analyses. PLOS Pathogens. **8**

29 Silvestrini, F., Alano, P. and Williams, J. L. (2000) Commitment to the production of male and female gametocytes in the human malaria parasite *Plasmodium falciparum*. Parasitology. **121**

30 Lasonder, E., Rijpma, S. R., van Schaijk, B. C., Hoeijmakers, W. A., Kensche, P. R., Gresnigt, M. S., Italiaander, A., Vos, M. W., Woestenenk, R. and Bousema, T. (2016) Integrated transcriptomic and proteomic analyses of *P. falciparum* gametocytes: molecular insight into sex-specific processes and translational repression. Nucleic Acids Research. **44**, 6087-6101

31 Baker, D. A. (2010) Malaria gametocytogenesis. Molecular and Biochemical Parasitology. **172**

32 Kafsack, B. F. C., Rovira-Graells, N., Clark, T. G., Bancells, C., Crowley, V. M. and Campino, S. G. (2014) A transcriptional switch underlies commitment to sexual development in malaria parasites. Nature. **507**

33 Sinha, A., Hughes, K. R., Modrzynska, K. K., Otto, T. D., Pfander, C., Dickens, N. J., Religa, A. A., Bushell, E., Graham, A. L., Cameron, R., Kafsack, B. F. C., Williams, A. E., Llinas, M., Berriman, M., Billker, O. and Waters, A. P. (2014) A cascade of DNA-binding proteins for sexual commitment and development in *Plasmodium*. Nature. **507**, 253-257

34 Robert, V., Read, A. F., Essong, J., Tchuinkam, T., Mulder, B., Verhave, J. P. and Carnevale, P. (1996) Effect of gametocyte sex ratio on infectivity of *Plasmodium falciparum* to *Anopheles gambiae*. Transactions of The Royal Society of Tropical Medicine and Hygiene. **90**, 621-624

35 Ngwa, C. J., Scheuermayer, M., Mair, G. R., Kern, S., Brügl, T., Wirth, C. C., Aminake, M. N., Wiesner, J., Fischer, R. and Vilcinskas, A. (2013) Changes in the transcriptome of the malaria parasite *Plasmodium falciparum* during the initial phase of transmission from the human to the mosquito. BMC genomics. **14**, 256

36 Alano, P. (2007) *Plasmodium falciparum* gametocytes: still many secrets of a hidden life. Molecular microbiology. **66**, 291-302

37 Billker, O., Shaw, M. K., Margos, G. and Sinden, R. E. (1997) The roles of temperature, pH and mosquito factors as triggers of male and female gametogenesis of *Plasmodium berghei* in vitro. Parasitology. **115**

38 Bozdech, Z., Llinás, M., Pulliam, B. L., Wong, E. D., Zhu, J. and DeRisi, J. L. (2003) The transcriptome of the intraerythrocytic developmental cycle of *Plasmodium falciparum*. PLOS biology. **1**

39 Verlinden, B. K., Louw, A. and Birkholtz, L.-M. (2016) Resisting resistance: is there a solution for malaria? Expert opinion on drug discovery. **11**, 395-406

40 Fairhurst, R. M., Nayyar, G. M. L., Breman, J. G., Hallett, R., Vennerstrom, J. L., Duong, S., Ringwald, P., Wellems, T. E., Plowe, C. V. and Dondorp, A. M. (2012) Artemisinin-Resistant Malaria: Research Challenges, Opportunities, and Public Health Implications. The American Journal of Tropical Medicine and Hygiene. **87**, 231-241

41 Menard, D. and Dondorp, A. (2017) Antimalarial Drug Resistance: A Threat to Malaria Elimination. Cold Spring Harbor Perspectives in Medicine. **7**

42 White, N. J. (2004) Antimalarial drug resistance. The Journal of Clinical Investigation. **113**, 1084-1092

43 Birkholtz, L.-M., Coetzer, T. L., Mancama, D., Leroy, D. and Alano, P. (2016) Discovering new transmission-blocking antimalarial compounds: challenges and opportunities. Trends in Parasitology. **32**, 669-681

44 Chen, I., Clarke, S. E., Gosling, R., Hamainza, B., Killeen, G., Magill, A., O'Meara, W., Price, R. N. and Riley, E. M. (2016) "Asymptomatic" Malaria: A Chronic and Debilitating Infection That Should Be Treated. PLOS Medicine. **13**

45 Lucantoni, L. and Avery, V. (2012) Whole-cell in vitro screening for gametocytocidal compounds. Future Medicinal Chemistry. **4**

46 Bousema, T., Okell, L., Felger, I. and Drakeley, C. (2014) Asymptomatic malaria infections: detectability, transmissibility and public health relevance. Nature Reviews Microbiology. **12**

47 Burrows, J. N., Leroy, D., Lotharius, J. and Waterson, D. (2011) Challenges in antimalarial drug discovery. Future Medicinal Chemistry. **3**

48 Delves, M. J. (2012) *Plasmodium* cell biology should inform strategies used in the development of antimalarial transmission-blocking drugs. Future Medicinal Chemistry. **4**, 2251-2263

49 Plouffe, David M., Wree, M., Du, Alan Y., Meister, S., Li, F., Patra, K., Lubar, A., Okitsu, Shinji L., Flannery, Erika L., Kato, N., Tanaseichuk, O., Comer, E., Zhou, B., Kuhen, K., Zhou, Y., Leroy, D., Schreiber, Stuart L., Scherer, Christina A., Vinetz, J. and Winzeler, Elizabeth A. (2016) High-Throughput Assay and Discovery of Small Molecules that Interrupt Malaria Transmission. Cell Host & Microbe. **19**, 114-126

50 Reader, J., Botha, M., Theron, A., Lauterbach, S. B., Rossouw, C., Engelbrecht, D., Wepener, M., Smit, A., Leroy, D., Mancama, D., Coetzer, T. L. and Birkholtz, L.-M. (2015) Nowhere to hide: interrogating different metabolic parameters of *Plasmodium falciparum* gametocytes in a transmission blocking drug discovery pipeline towards malaria elimination. Malaria Journal. **14**, 213

51 Bousema, J. T., Schneider, P., Gouagna, L. C., Drakeley, C. J., Tostmann, A., Houben, R., Githure, J. I., Ord, R., Sutherland, C. J., Omar, S. A. and Sauerwein, R. W. (2006) Moderate effect of artemisinin-based combination therapy on transmission of *Plasmodium falciparum*. The Journal of Infectious Diseases. **193**, 1151-1159

52 White, N. J. (2013) Primaquine to prevent transmission of falciparum malaria. The Lancet Infectious Diseases. **13**, 175-181

53 Lalève, A., Vallières, C., Golinelli-Cohen, M.-P., Bouton, C., Song, Z., Pawlik, G., Tindall, S. M., Avery, S. V., Clain, J. and Meunier, B. (2016) The antimalarial drug primaquine targets Fe–S cluster proteins and yeast respiratory growth. Redox Biology. **7**, 21-29

54 Vale, N., Moreira, R. and Gomes, P. (2009) Primaquine revisited six decades after its discovery. European journal of medicinal chemistry. **44**, 937-953

55 Thriemer, K., Ley, B., Bobogare, A., Dysoley, L., Alam, M. S., Pasaribu, A. P., Sattabongkot, J., Jambert, E., Domingo, G. J., Commons, R., Auburn, S., Marfurt, J., Devine, A., Aktaruzzaman, M. M., Sohel, N., Namgay, R., Drukpa, T., Sharma, S. N., Sarawati, E., Samad, I., Theodora, M., Nambanya, S., Ounekham, S., Mudin, R. N. B., Da Thakur, G., Makita, L. S., Deray, R., Lee, S.-E., Boaz, L., Danansuriya, M. N., Mudiyanselage, S. D., Chinanonwait, N., Kitchakarn, S., Nausien, J., Naket, E., Duc, T. N., Do Manh, H., Hong, Y. S., Cheng, Q., Richards, J. S., Kusriastuti, R., Satyagraha, A., Noviyanti, R., Ding, X. C., Khan, W. A., Swe Phru, C., Guoding, Z., Qi, G., Kaneko, A., Miotto, O., Nguitragool, W., Roobsoong, W.,

Battle, K., Howes, R. E., Roca-Feltrer, A., Duparc, S., Bhowmick, I. P., Kenangalem, E., Bibit, J.-A., Barry, A., Sintasath, D., Abeyasinghe, R., Sibley, C. H., McCarthy, J., von Seidlein, L., Baird, J. K. and Price, R. N. (2017) Challenges for achieving safe and effective radical cure of *Plasmodium vivax*: a round table discussion of the APMEN Vivax Working Group. Malaria Journal. **16**, 141

56 Delves, M. J., Miguel-Blanco, C., Matthews, H., Molina, I., Ruecker, A., Yahiya, S., Straschil, U., Abraham, M., León, M. L., Fischer, O. J., Rueda-Zubiaurre, A., Brandt, J. R., Cortés, Á., Barnard, A., Fuchter, M. J., Calderón, F., Winzeler, E. A., Sinden, R. E., Herreros, E., Gamo, F. J. and Baum, J. (2018) A high throughput screen for next-generation leads targeting malaria parasite transmission. Nature Communications. **9**, 3805

57 Burrows, J. N., Hooft van Huijsduijnen, R., Möhrle, J. J., Oeuvray, C. and Wells, T. N. C. (2013) Designing the next generation of medicines for malaria control and eradication. Malaria Journal. **12**

58 Wells, T. N. C., Hooft van Huijsduijnen, R. and Voorhis, W. C. (2015) Malaria medicines: a glass half full? Nature Reviews Drug Discovery. **14**

59 Gatton, M. L., Martin, L. B. and Cheng, Q. (2004) Evolution of resistance to sulfadoxine-pyrimethamine in *Plasmodium falciparum*. Antimicrobial Agents and Chemotherapy. **48**, 2116-2123

60 Duffy, S. and Avery, V. M. (2013) Identification of inhibitors of *Plasmodium falciparum* gametocyte development. Malaria Journal. **12**, 408

61 Rueda-Zubiaurre, A., Yahiya, S., Fischer, O. J., Hu, X., Saunders, C. N., Sharma, S., Straschil, U., Shen, J., Tate, E. W., Delves, M. J., Baum, J., Barnard, A. and Fuchter, M. J. (2020) Structure-Activity Relationship Studies of a Novel Class of Transmission Blocking Antimalarials Targeting Male Gametes. J Med Chem. **63**, 2240-2262

62 Reader, J., van der Watt, M. E., Taylor, D., Le Manach, C., Mittal, N., Ottilie, S., Theron, A., Moyo, P., Erlank, E., Nardini, L., Venter, N., Lauterbach, S., Bezuidenhout, B., Horatscheck, A., van Heerden, A., Boyle, G. A., Calvo, D., Mancama, D., Coetzer, T. L., Winzeler, E. A., Duffy, J., Koekemoer, L. L., Basarab, G., Chibale, K. and Birkholtz, L.-M. (2020) Multistage and transmission-blocking targeted antimalarials discovered from the open-source MMV Pandemic Response Box. bioRxiv, 2020.2006.2005.133405

63 Lucantoni, L., Loganathan, S. and Avery, V. M. (2017) The need to compare: assessing the level of agreement of three high-throughput assays against *Plasmodium falciparum* mature gametocytes. Scientific Reports. **7**, 45992

64 Van Voorhis, W. C., Adams, J. H., Adelfio, R., Ahyong, V., Akabas, M. H., Alano, P., Alday, A., Aleman Resto, Y., Alsibaee, A., Alzualde, A., Andrews, K. T., Avery, S. V., Avery, V. M., Ayong, L., Baker, M., Baker, S., Ben Mamoun, C., Bhatia, S., Bickle, Q., Bounaadja, L., Bowling, T., Bosch, J., Boucher, L. E., Boyom, F. F., Brea, J., Brennan, M., Burton, A., Caffrey, C. R., Camarda, G., Carrasquilla, M., Carter, D., Belen Cassera, M., Chih-Chien Cheng, K., Chindaudomsate, W., Chubb, A., Colon, B. L., Colon-Lopez, D. D., Corbett, Y., Crowther, G. J., Cowan, N., D'Alessandro, S., Le Dang, N., Delves, M., DeRisi, J. L., Du, A. Y., Duffy, S., Abd El-Salam El-Sayed, S., Ferdig, M. T., Fernandez Robledo, J. A., Fidock, D. A., Florent, I., Fokou, P. V., Galstian, A., Gamo, F. J., Gokool, S., Gold, B., Golub, T., Goldgof, G. M., Guha, R., Guiguemde, W. A., Gural, N., Guy, R. K., Hansen, M. A., Hanson, K. K., Hemphill, A., Hooft

van Huijsduijnen, R., Horii, T., Horrocks, P., Hughes, T. B., Huston, C., Igarashi, I., Ingram-Sieber, K., Itoe, M. A., Jadhav, A., Naranuntarat Jensen, A., Jensen, L. T., Jiang, R. H., Kaiser, A., Keiser, J., Ketas, T., Kicka, S., Kim, S., Kirk, K., Kumar, V. P., Kyle, D. E., Lafuente, M. J., Landfear, S., Lee, N., Lee, S., Lehane, A. M., Li, F., Little, D., Liu, L., Llinas, M., Loza, M. I., Lubar, A., Lucantoni, L., Lucet, I., Maes, L., Mancama, D., Mansour, N. R., March, S., McGowan, S., Medina Vera, I., Meister, S., Mercer, L., Mestres, J., Mfopa, A. N., Misra, R. N., Moon, S., Moore, J. P., Morais Rodrigues da Costa, F., Muller, J., Muriana, A., Nakazawa Hewitt, S., Nare, B., Nathan, C., Narraidoo, N., Nawaratna, S., Ojo, K. K., Ortiz, D., Panic, G., Papadatos, G., Parapini, S., Patra, K., Pham, N., Prats, S., Plouffe, D. M., Poulsen, S. A., Pradhan, A., Quevedo, C., Quinn, R. J., Rice, C. A., Abdo Rizk, M., Ruecker, A., St Onge, R., Salgado Ferreira, R., Samra, J., Robinett, N. G., Schlecht, U., Schmitt, M., Silva Villela, F., Silvestrini, F., Sinden, R., Smith, D. A., Soldati, T., Spitzmuller, A., Stamm, S. M., Sullivan, D. J., Sullivan, W., Suresh, S., Suzuki, B. M., Suzuki, Y., Swamidass, S. J., Taramelli, D., Tchokouaha, L. R., Theron, A., Thomas, D., Tonissen, K. F., Townson, S., Tripathi, A. K., Trofimov, V., Udenze, K. O., Ullah, I., Vallieres, C., Vigil, E., Vinetz, J. M., Voong Vinh, P., Vu, H., Watanabe, N. A., Weatherby, K., White, P. M., Wilks, A. F., Winzeler, E. A., Wojcik, E., Wree, M., Wu, W., Yokoyama, N., Zollo, P. H., Abla, N., Blasco, B., Burrows, J., Laleu, B., Leroy, D., Spangenberg, T., Wells, T. and Willis, P. A. (2016) Open Source Drug Discovery with the Malaria Box Compound Collection for Neglected Diseases and Beyond. PLoS Pathog. **12**, e1005763

65 Cui, L., Miao, J., Wang, J., Li, Q. and Cui, L. (2008) Plasmodium falciparum: development of a transgenic line for screening antimalarials using firefly luciferase as the reporter. Experimental parasitology. **120**, 80-87

66 Hasenkamp, S., Sidaway, A., Devine, O., Roye, R. and Horrocks, P. (2013) Evaluation of bioluminescence-based assays of anti-malarial drug activity. Malar J. **12**, 58

67 Vaughan, A. M., Mikolajczak, S. A., Camargo, N., Lakshmanan, V., Kennedy, M., Lindner, S. E., Miller, J. L., Hume, J. C. C. and Kappe, S. H. I. (2012) A transgenic *Plasmodium falciparum* NF54 strain that expresses GFP–luciferase throughout the parasite life cycle. Molecular and Biochemical Parasitology. **186**, 143-147

68 Delves, M., Plouffe, D., Scheurer, C., Meister, S., Wittlin, S. and Winzeler, E. A. (2012) The activities of current antimalarial drugs on the life cycle stages of Plasmodium: a comparative study with human and rodent parasites. PLoS Med. **9**

69 Bolscher, J. M., Koolen, K. M. J., van Gemert, G. J., van de Vegte-Bolmer, M. G., Bousema, T., Leroy, D., Sauerwein, R. W. and Dechering, K. J. (2015) A combination of new screening assays for prioritization of transmission-blocking antimalarials reveals distinct dynamics of marketed and experimental drugs. Journal of Antimicrobial Chemotherapy. **70**, 1357-1366

70 Lelievre, J., Almela, M. J., Lozano, S., Miguel, C., Franco, V., Leroy, D. and Herreros, E. (2012) Activity of clinically relevant antimalarial drugs on Plasmodium falciparum mature gametocytes in an ATP bioluminescence “transmission blocking” assay. PLoS One. **7**

71 Adjalley, S. H., Johnston, G. L., Li, T., Eastman, R. T., Ekland, E. H., Eappen, A. G., Richman, A., Sim, B. K. L., Lee, M. C. and Hoffman, S. L. (2011) Quantitative assessment of *Plasmodium falciparum* sexual development reveals potent transmission-blocking activity by methylene blue. Proceedings of the National Academy of Sciences. **108**, E1214-E1223

72 Paquet, T., Le Manach, C., Cabrera, D. G., Younis, Y., Henrich, P. P., Abraham, T. S., Lee, M. C. S., Basak, R., Ghidelli-Disse, S., Lafuente-Monasterio, M. J., Bantscheff, M., Ruecker, A., Blagborough, A. M., Zakutansky, S. E., Zeeman, A.-M., White, K. L., Shackleford, D. M., Mannila, J., Morizzi, J., Scheurer, C., Angulo-Barturen, I., Martínez, M. S., Ferrer, S., Sanz, L. M., Gamo, F. J., Reader, J., Botha, M., Dechering, K. J., Sauerwein, R. W., Tungtaeng, A., Vanachayangkul, P., Lim, C. S., Burrows, J., Witty, M. J., Marsh, K. C., Bodenreider, C., Rochford, R., Solapure, S. M., Jiménez-Díaz, M. B., Wittlin, S., Charman, S. A., Donini, C., Campo, B., Birkholtz, L.-M., Hanson, K. K., Drewes, G., Kocken, C. H. M., Delves, M. J., Leroy, D., Fidock, D. A., Waterson, D., Street, L. J. and Chibale, K. (2017) Antimalarial efficacy of MMV390048, an inhibitor of *Plasmodium* phosphatidylinositol 4-kinase. Science Translational Medicine. **9**

73 D'Alessandro, S., Camarda, G., Corbett, Y., Siciliano, G., Parapini, S., Cevenini, L., Michelini, E., Roda, A., Leroy, D. and Taramelli, D. (2016) A chemical susceptibility profile of the *Plasmodium falciparum* transmission stages by complementary cell-based gametocyte assays. Journal of Antimicrobial Chemotherapy. **71**, 1148-1158

74 Delves, M. J., Angrisano, F. and Blagborough, A. M. (2018) Antimalarial Transmission-Blocking Interventions: Past, Present, and Future. Trends in parasitology. **34**, 735-746

75 Hovlid, M. L. and Winzeler, E. A. (2016) Phenotypic screens in antimalarial drug discovery. Trends in Parasitology. **32**

76 Leroy, D., Campo, B., Ding, X. C., Burrows, J. N. and Cherbuin, S. (2014) Defining the biology component of the drug discovery strategy for malaria eradication. Trends in Parasitology. **30**, 478-490

77 Lucantoni, L., Silvestrini, F., Signore, M., Siciliano, G., Eldering, M. and Dechering, K. J. (2015) A simple and predictive phenotypic High Content Imaging assay for *Plasmodium falciparum* mature gametocytes to identify malaria transmission blocking compounds. Scientific Reports. **5**

78 Azevedo, R., Markovic, M., Machado, M., Mendes, A. M., Prudencio, M. and Franke-Fayard, B. (2017) Bioluminescence method for in vitro screening of *Plasmodium* transmission-blocking compounds. Antimicrobial Agents and Chemotherapy. **61**

79 Cevenini, L., Camarda, G., Michelini, E., Siciliano, G., Calabretta, M. M., Bona, R., Kumar, T. S., Cara, A., Branchini, B. R., Fidock, D. A., Roda, A. and Alano, P. (2014) Multicolor bioluminescence boosts malaria research: quantitative dual-color assay and single-cell imaging in *Plasmodium falciparum* parasites. Analytical chemistry. **86**, 8814-8821

80 Duffy, S. and Avery, V. M. (2012) Development and optimization of a novel 384-well anti-malarial imaging assay validated for high-throughput screening. Am J Trop Med Hyg. **86**

81 de Cózar, C., Caballero, I., Colmenarejo, G., Sanz, L. M., Álvarez-Ruiz, E., Gamo, F.-J. and Cid, C. (2016) Development of a Novel High-Density [3H]Hypoxanthine Scintillation Proximity Assay To Assess *Plasmodium falciparum* Growth. Antimicrobial Agents and Chemotherapy. **60**, 5949-5956

82 Delves, M. J., Ruecker, A., Straschil, U., Lelievre, J., Marques, S. and Lopez-Barragan, M. J. (2013) Male and female *Plasmodium falciparum* mature gametocytes show different responses to antimalarial drugs. Antimicrobial Agents and Chemotherapy. **57**

83 Miguel-Blanco, C., Lelièvre, J., Delves, M. J., Bardera, A. I., Presa, J. L., López-Barragán, M. J., Ruecker, A., Marques, S., Sinden, R. E. and Herreros, E. (2015) Imaging-Based High-Throughput Screening Assay To Identify New Molecules with Transmission-Blocking Potential against *Plasmodium falciparum* Female Gamete Formation. Antimicrobial Agents and Chemotherapy. **59**, 3298-3305

84 Almela, M. J., Lozano, S., Lelièvre, J., Colmenarejo, G., Coterón, J. M., Rodrigues, J., Gonzalez, C. and Herreros, E. (2015) A New Set of Chemical Starting Points with *Plasmodium falciparum* Transmission-Blocking Potential for Antimalarial Drug Discovery. PLOS ONE. **10**

85 Lucantoni, L., Duffy, S., Adjalley, S. H., Fidock, D. A. and Avery, V. (2013) Identification of MMV malaria box inhibitors of *Plasmodium falciparum* early-stage gametocytes using a luciferase-based high- throughput assay. Antimicrobial Agents and Chemotherapy. **57**

86 Lucantoni, L., Fidock, D. A. and Avery, V. M. (2016) Luciferase-based, high-throughput assay for screening and profiling transmission-blocking compounds against *Plasmodium falciparum* gametocytes. Antimicrobial Agents and Chemotherapy. **60**

87 Siciliano, G., Kumar, T. R. S., Bona, R., Camarda, G., Calabretta, M. M., Cevenini, L., Davioud-Charvet, E., Becker, K., Cara, A., Fidock, D. A. and Alano, P. (2017) A high susceptibility to redox imbalance of the transmissible stages of *Plasmodium falciparum* revealed with a luciferase-based mature gametocyte assay. Molecular Microbiology. **104**, 306-318

88 Rampersad, S. N. (2012) Multiple Applications of Alamar Blue as an Indicator of Metabolic Function and Cellular Health in Cell Viability Bioassays. Sensors (Basel, Switzerland). **12**, 12347-12360

89 Riss, T. L., Moravec, R. A., Niles, A. L., Duellman, S., Benink, H. A., Worzella, T. J. and Minor, L. (2004) Cell Viability Assays. In Assay Guidance Manual (Sittampalam, G. S., et al., eds.), Bethesda (MD)

90 Jensen, E. C. (2012) Types of Imaging, Part 2: An Overview of Fluorescence Microscopy. The Anatomical Record. **295**, 1621-1627

91 Bray, M. A. and Carpenter, A. (2004) Advanced Assay Development Guidelines for Image-Based High Content Screening and Analysis. In Assay Guidance Manual (Sittampalam, G. S., et al., eds.), Bethesda (MD)

92 Ehrhardt, D. (2003) GFP technology for live cell imaging. Current Opinion in Plant Biology. **6**, 622-628

93 Marin-Mogollon, C., Salman, A. M., Koolen, K. M. J., Bolscher, J. M., van Pul, F. J. A., Miyazaki, S., Imai, T., Othman, A. S., Ramesar, J., van Gemert, G. J., Kroeze, H., Chevalley-Maurel, S., Franke-Fayard, B., Sauerwein, R. W., Hill, A. V. S., Dechering, K. J., Janse, C. J. and Khan, S. M. (2019) A *P. falciparum* NF54 Reporter Line Expressing mCherry-Luciferase in Gametocytes, Sporozoites, and Liver-Stages. Frontiers in Cellular and Infection Microbiology. **9**, 96

94 Vos, M. W., Stone, W. J., Koolen, K. M., Gemert, G. J., Schaijk, B. and Leroy, D. (2015) A semi-automated luminescence based standard membrane feeding assay identifies novel small molecules that inhibit transmission of malaria parasites by mosquitoes. Scientific Reports. **5**

95 Nkrumah, L. J., Muhle, R. A., Moura, P. A., Ghosh, P., Hatfull, G. F., Jacobs Jr, W. R. and Fidock, D. A. (2006) Efficient site-specific integration in *Plasmodium falciparum* chromosomes mediated by mycobacteriophage Bxb1 integrase. Nature Methods. **3**, 615

96 Trager, W. and Jensen, J. B. (1976) Human malaria parasites in continuous culture. Science. **193**, 673-675

97 Verlinden, B. K., Niemand, J., Snyman, J., Sharma, S. K., Beattie, R. J., Woster, P. M. and Birkholtz, L.-M. (2011) Discovery of novel alkylated (bis) urea and (bis) thiourea polyamine analogues with potent antimalarial activities. Journal of Medicinal Chemistry. **54**, 6624-6633

98 Schuster, F. L. (2002) Cultivation of *Plasmodium* spp. Clinical Microbiology Reviews. **15**, 355-364

99 Lambros, C. and Vanderberg, J. P. (1979) Synchronization of *Plasmodium falciparum* erythrocytic stages in culture. The Journal of parasitology. **65**, 418-420

100 Roncalés, M., Vidal, J., Torres, P. A. and Herreros, E. (2015) In Vitro Culture of *Plasmodium falciparum*: Obtention of Synchronous Asexual Erythrocytic Stages. Open Journal of Epidemiology. **5**, 71

101 Verlinden, B. K., de Beer, M., Pachaiyappan, B., Besaans, E., Andayi, W. A., Reader, J., Niemand, J., van Biljon, R., Guy, K. and Egan, T. (2015) Interrogating alkyl and arylalkylpolyamino (bis) urea and (bis) thiourea isosteres as potent antimalarial chemotypes against multiple lifecycle forms of *Plasmodium falciparum* parasites. Bioorganic & medicinal chemistry. **23**, 5131-5143

102 Miao, J., Wang, Z., Liu, M., Parker, D., Li, X., Chen, X. and Cui, L. (2013) *Plasmodium falciparum*: Generation of pure gametocyte culture by heparin treatment. Experimental parasitology. **135**, 10.1016/j.exppara.2013.1009.1010

103 López-Barragán, M. J., Lemieux, J., Quiñones, M., Williamson, K. C., Molina-Cruz, A., Cui, K., Barillas-Mury, C., Zhao, K. and Su, X.-z. (2011) Directional gene expression and antisense transcripts in sexual and asexual stages of *Plasmodium falciparum*. BMC Genomics. **12**, 587-587

104 Zanghi, G., Vembar, S. S., Baumgarten, S., Ding, S., Guizetti, J., Bryant, J. M., Mattei, D., Jensen, A. T. R., Renia, L., Goh, Y. S., Sauerwein, R., Hermsen, C. C., Franetich, J. F., Bordessoulles, M., Silvie, O., Soulard, V., Scatton, O., Chen, P., Mecheri, S., Mazier, D. and Scherf, A. (2018) A Specific PfEMP1 Is Expressed in *P. falciparum* Sporozoites and Plays a Role in Hepatocyte Infection. Cell Reports. **22**, 2951-2963

105 van Biljon, R. (Unpublished) Microarray relative expression values during *P. falciparum* gametocyte development. University of Pretoria.

106 Aurrecoechea, C., Brestelli, J., Brunk, B. P., Dommer, J., Fischer, S., Gajria, B., Gao, X., Gingle, A., Grant, G., Harb, O. S., Heiges, M., Innamorato, F., Iodice, J., Kissinger, J. C., Kraemer, E., Li, W., Miller, J. A., Nayak, V., Pennington, C., Pinney, D. F., Roos, D. S., Ross, C., Stoeckert, C. J., Jr., Treatman, C. and Wang, H. (2009) PlasmoDB: a functional genomic database for malaria parasites. Nucleic acids research. **37**, D539-D543

107 RStudio. (2016) RStudio: Integrated Development for R. RStudio, Inc. Boston, MA. URL http://www.rstudio.com/.

108 van Biljon, R., van Wyk, R., Painter, H. J., Orchard, L., Reader, J., Niemand, J., Llinás, M. and Birkholtz, L.-M. (2019) Hierarchical transcriptional control regulates Plasmodium falciparum sexual differentiation. BMC Genomics. **20**, 920

109 Schwach F, B. E., Gomes AR, Anar B, Girling G, Herd C, Rayner JC and Billker O. PlasmoGEM, a database supporting a community resource for large-scale experimental genetics in malaria parasites. DOI: http://doi.org/10.1093/nar/gku1143. *Nucleic Acids Research*. **43** 1176-1182

110 Benchling. (2018-2019) Benchling (Biology Software). URL: https://benchling.com/.

111 Rug, M. and Maier, A. G. (2013) Transfection of *Plasmodium falciparum*. Methods in Molecular Biology. **923**, 75-98

112 Zhang, J. H., Chung, T. D. and Oldenburg, K. R. (1999) A simple statistical parameter for use in evaluation and validation of high throughput screening assays. Journal of Biomolecular Screening. **4**

113 Miao, J., Fan, Q., Parker, D., Li, X., Li, J. and Cui, L. (2013) Puf mediates translation repression of transmission-blocking vaccine candidates in malaria parasites. PLOS Pathogens. **9**, e1003268

114 Zhang, M., Wang, C., Otto, T. D., Oberstaller, J., Liao, X., Adapa, S. R., Udenze, K., Bronner, I. F., Casandra, D., Mayho, M., Brown, J., Li, S., Swanson, J., Rayner, J. C., Jiang, R. H. Y. and Adams, J. H. (2018) Uncovering the essential genes of the human malaria parasite Plasmodium falciparum by saturation mutagenesis. Science. **360**, eaap7847

115 Adjalley, Sophie H., Chabbert, Christophe D., Klaus, B., Pelechano, V. and Steinmetz, Lars M. (2016) Landscape and Dynamics of Transcription Initiation in the Malaria Parasite Plasmodium falciparum. Cell Reports. **14**, 2463-2475

116 Bannister, L. H., Hopkins, J. M., Fowler, R. E., Krishna, S. and Mitchell, G. H. (2000) A Brief Illustrated Guide to the Ultrastructure of *Plasmodium falciparum* Asexual Blood Stages. Parasitology Today. **16**, 427-433

117 Macedo, T. S., Colina-Vegas, L., Da PaixÃO, M., Navarro, M., Barreto, B. C., Oliveira, P. C. M., Macambira, S. G., Machado, M., PrudÊNcio, M., D'Alessandro, S., Basilico, N., Moreira, D. R. M., Batista, A. A. and Soares, M. B. P. (2016) Chloroquine-containing organoruthenium complexes are fast-acting multistage antimalarial agents. Parasitology. **143**, 1543-1556

118 Read, D. F., Cook, K., Lu, Y. Y., Le Roch, K. G. and Noble, W. S. (2019) Predicting gene expression in the human malaria parasite *Plasmodium falciparum* using histone modification, nucleosome positioning, and 3D localization features. PLOS Computational Biology. **15**, e1007329

119 Pace, T., Olivieri, A., Sanchez, M., Albanesi, V., Picci, L., Siden Kiamos, I., Janse, C. J., Waters, A. P., Pizzi, E. and Ponzi, M. (2006) Set regulation in asexual and sexual *Plasmodium* parasites reveals a novel mechanism of stage-specific expression. Molecular Microbiology. **60**, 870-882

120 Gill, J., Kumar, A., Yogavel, M., Belrhali, H., Jain, S. K., Rug, M., Brown, M., Maier, A. G. and Sharma, A. (2010) Structure, localization and histone binding properties of nuclear-associated nucleosome assembly protein from *Plasmodium falciparum*. Malaria Journal. **9**, 90

121 Huang, L. C., Wood, E. A. and Cox, M. M. (1997) Convenient and reversible site-specific targeting of exogenous DNA into a bacterial chromosome by use of the FLP recombinase: the FLIRT system. J Bacteriol. **179**, 6076-6083

122 Graves, P., Carter, R. and McNeill, K. (1984) Gametocyte Production in Cloned Lines of *Plasmodium falciparum*. The American Journal of Tropical Medicine and Hygiene. **33**, 1045-1050

123 Alano, P. and Carter, R. (1990) Sexual Differentiation in Malaria Parasites. Annual Review of Microbiology. **44**, 429-449

124 Michelini, E., Cevenini, L., Mezzanotte, L., Ablamsky, D., Southworth, T., Branchini, B. R. and Roda, A. (2008) Combining intracellular and secreted bioluminescent reporter proteins for multicolor cell-based assays. Photochemical & Photobiological Sciences. **7**, 212-217

Supplementary Information

Figure S1 shows the entire gel for Figure 3.8B in the main text.

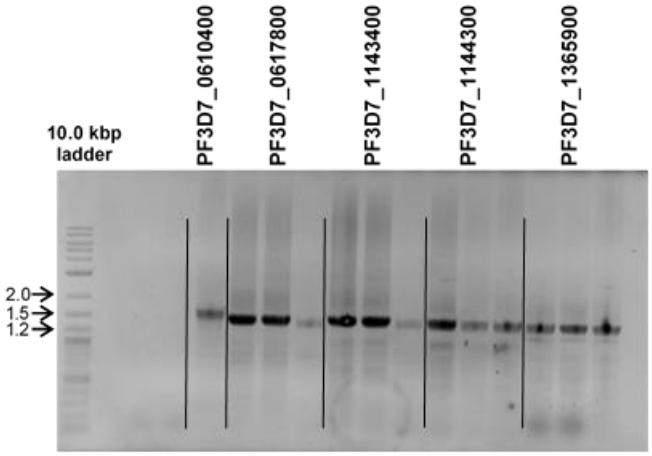

Figure S1: PCR amplification of promoter regions for the top constitutive genes.
Promoter regions were PCR amplified with genomic DNA from NF54 parasites using primers shown in Table 2.1. PCR conditions had an annealing temperature of 60°C. The expected promoter region band sizes were obtained for five constitutive markers: 1597 bp (PF3D7_0610400), 1463 bp (PF3D7_0617800), 1480 bp (PF3D7_1143400), 1454 bp (PF3D7_1144300) and 1428 bp (PF3D7_1365900). NEB quick-load purple 1 kb plus DNA ladder and DNA fragments were separated on a gel and visualised with ethidium bromide staining.

Figure S2 shows the *histone H3* promoter successfully being cloned into competent cells as confirmed with PCR screening.

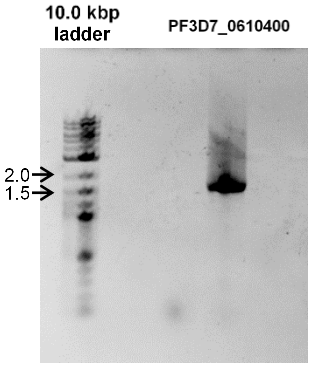

Figure S2: PCR screening of pASEX-5'*H3*-myc-CBG99-3'*nap*.
Screening of *histone H3* promoter region (PF3D7_0610400) cloned into pASEX plasmid by colony PCR using primers shown in Table 2.1. The expected promoter region band size was obtained 1597 bp. NEB quick-load purple 1 kb plus DNA ladder and DNA fragments were separated on a gel and visualised with ethidium bromide staining.

Figure S3 shows the entire gel for Figure 3.10 in the main text.

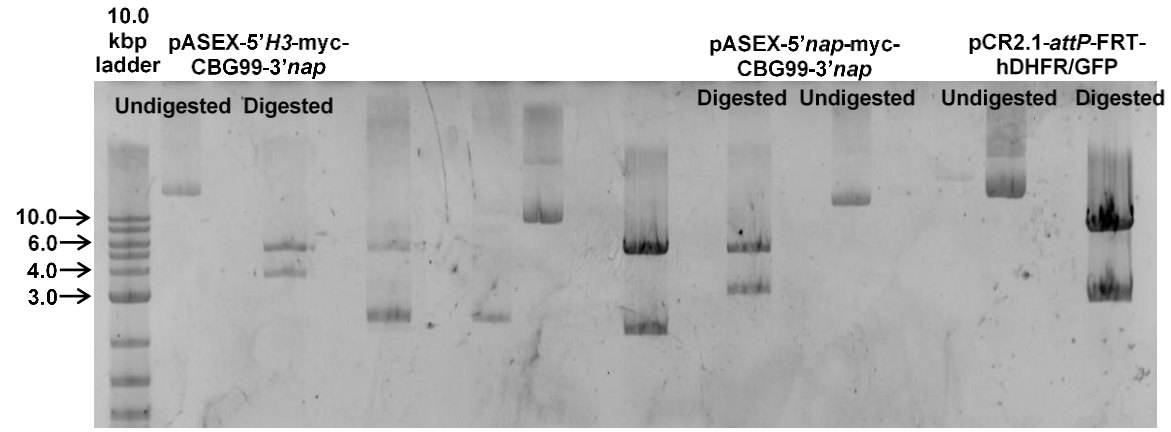

Figure S3: Restriction enzyme digestion of pASEX and pCR2.1-*attP*-FRT-hDHFR/GFP plasmids. *Xho*I and *Not*I restriction enzyme digestion of the pASEX-5'*H3*-myc-CBG99-3'*nap* (9113 bp), pASEX-5'*nap*-myc-CBG99-3'*nap* (8570 bp), and pCR2.1-*attP*-FRT-hDHFR/GFP (10241 bp) plasmids showed the expected band sizes. Undigested and digested plasmids can be seen on the gel. NEB quick-load purple 1 kb plus DNA ladder and DNA fragments were separated on a gel and visualised with ethidium bromide staining. Other bands were not used for this work.

Figure S4 shows the *histone H3* and *nap* promoter along with the reporter successfully being cloned into competent cells as confirmed with PCR screening.

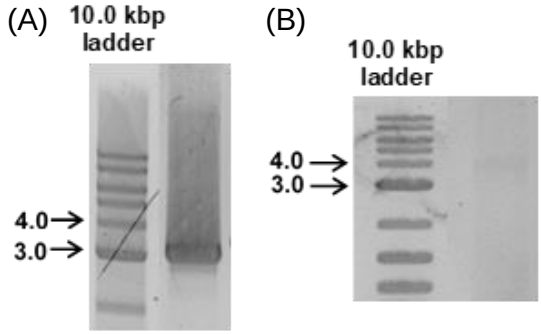

Figure S4: PCR screening of final pCR2.1-*attP*-FRT-hDHFR/GFP plasmid clones.
Screening of cassettes – (A) *nap* and (B) *histone H3* promoters with myc-tagged luciferase - cloned into pCR2.1-*attP* plasmid by colony PCR using promoter F1 and CBG R1 primers as shown in Table 2.2. The expected band sizes for the promoter and reporter region were obtained 3754 bp (*H3*) and 3214 bp (*nap*). NEB quick-load purple 1 kb plus DNA ladder and DNA fragments were separated on a gel and visualised with ethidium bromide staining.

Figure S5 shows the entire gel for Figure 3.11B in the main text.

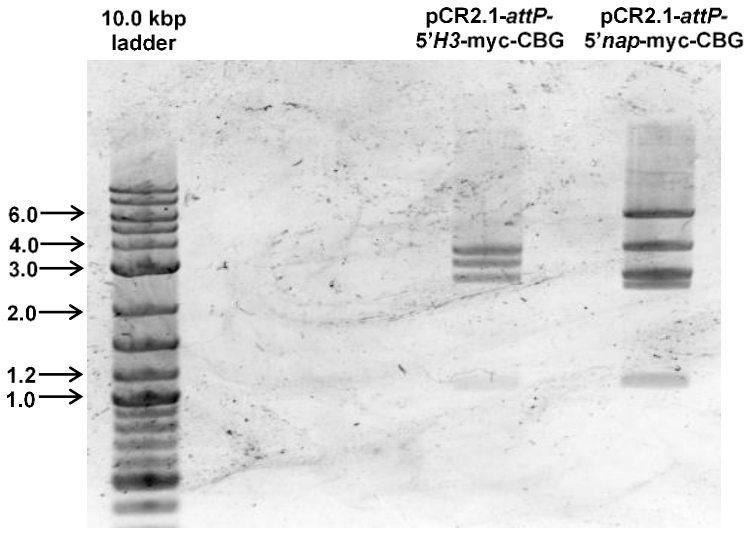

Figure S5: Restriction enzyme mapping of final pCR2.1-*attP*-FRT-hDHFR/GFP plasmid clones.
Restriction enzyme mapping with *Xho*I and *Spe*I of pCR2.1-*attP*-5'*H3*-myc-CBG showed expected DNA band sizes for complete digestion (3855, 3256, 2776, 1099 bp). However, pCR2.1-*attP*-5'*nap*-myc-CBG showed complete and partial digestion on the gel (6569, 3855, 2776, 2714, 1099 bp). NEB quick-load purple 1 kb plus DNA ladder and DNA fragments were separated on a gel and visualised with ethidium bromide staining.

Figure S6 shows the entire gel for Figure 3.13 in the main text.

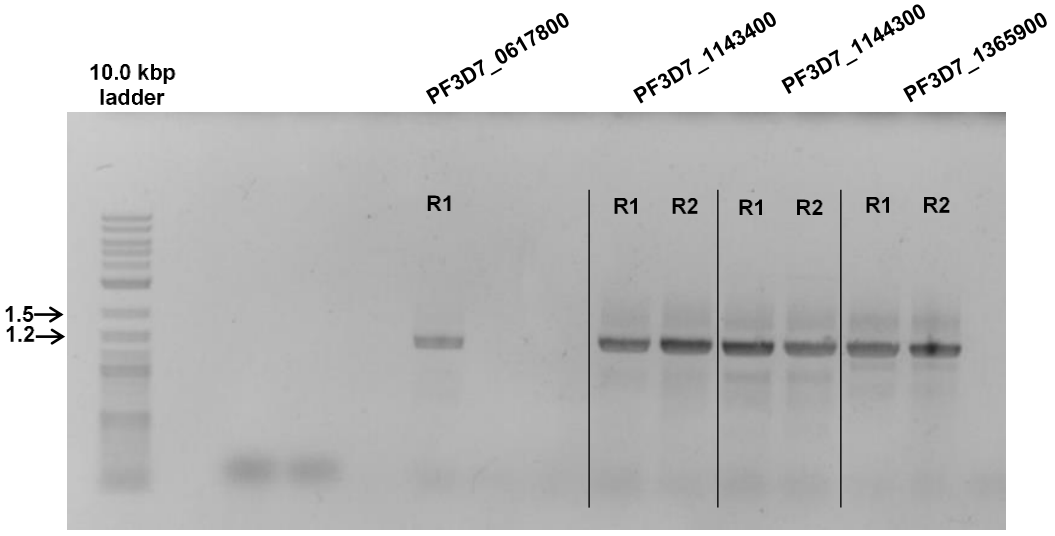

Figure S6: PCR screening of pGEM-T Easy vector clones.
Screening of promoter regions cloned into pGEM-T Easy vectors by colony PCR using primers shown in Table 2.1. The expected promoter region band sizes were obtained 1463 bp (PF3D7_0617800), 1480 bp (PF3D7_1143400), 1454 bp (PF3D7_1144300) and 1428 bp (PF3D7_1365900). (R indicates bacterial clone replicates). NEB quick-load purple 1 kb plus DNA ladder and DNA fragments were separated on a 1 % (w/v) agarose/TAE gel and visualised with ethidium bromide staining.

Figure S7 shows partial sequencing for the promoter region of pCR2.1-*attP*-5'*ubiq*-myc-CBG.

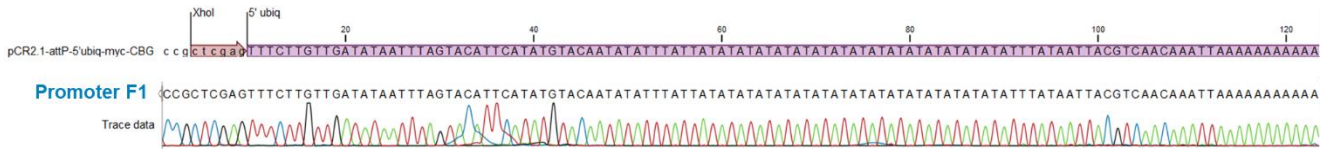

Figure S7: Sequencing of final pCR2.1-*attP*-5'*ubiq*-myc-CBG plasmid clone.
Sequencing results shows the *XhoI* restriction enzyme site and start of the 5' *ubiq* promoter region. The promoter F1 primer was used for sequencing, as seen in Table 2.2, aligned to the expected reference sequence.